UNIVERSITY OF CALGARY

Na^+-affinity and relation to transport kinetics of Na^+/Ca^{2+}-K^+ exchanger NCKX2

by

Haider F. Altimimi

A THESIS

SUBMITTED TO THE FACULTY OF GRADUATE STUDIES

IN PARTIAL FULFILMENT OF THE REQUIREMENTS FOR THE

DEGREE OF MASTER OF SCIENCE

DEPARTMENT OF NEUROSCIENCE

CALGARY, ALBERTA

October, 2008

UNIVERSITY OF CALGARY

FACULTY OF GRADUATE STUDIES

UNIVERSITY OF
CALGARY

Abstract

Na^+/Ca^{2+}-K^+ exchangers (NCKX) constitute an important family of plasma membrane Ca^{2+} transport proteins in animal cells; to date, however, relatively little is known of their molecular functional operation. This thesis describes the development of a fluorescence-based assay to measure Na^+-dependent changes in intracellular Ca^{2+}, through the use of the alkali cation ionophore gramicidin to control $[Na^+]_i$. The assay was used to scan through single amino acid substitution mutant constructs of human NCKX2 for shifts in Na^+-affinity, to determine which amino acids/regions of the molecule are involved in Na^+ transport/liganding. In the process, a kinetic regulatory feature, herein termed Na^+_i-dependent inactivation was discovered; this inactive state was produced upon prolonged (>40 s) exposure of NCKX2 to high intracellular Na^+ (>35 mM).

Preface

In accordance with the Copyright Permission Policy of the American Society for Biochemistry and Molecular Biology Journals, some of the data presented in this thesis have been published, and portions of figures were also adapted from:

Altimimi, H. F., and Schnetkamp, P. P. M. 2007. Na^+-dependent inactivation of the retinal cone/brain Na^+/Ca^{2+}-K^+ exchanger NCKX2. J. Biol. Chem. **282**: 3720-3729.

Acknowledgements

First and foremost, I would like to thank my supervisor Dr. Paul Schnetkamp for allowing me the opportunity to carry out my first officially (partly) independent post as scientific trainee in his laboratory. I greatly value his mentorship, not only in as far as the great wealth of scientific knowledge I have gained while under his guidance, but also for his direction, and willingness to share his experiences and advice on all matters scientific. From trials and tribulations of scientific research, to the political aspects involved in the career of a researcher, I've had the privilege of seeing first-hand what it's like to be in the driver's seat. If I had any doubts about my choice of pursuing a career in scientific research before embarking on this long and arduous journey, my experiences in Dr. Schnetkamp's lab have cemented my ambition and determination to reach for the goal of, hopefully in the not too distant future, becoming a full-fledged research scientist myself.

The work presented in this thesis would not have been possible without the excellent knowledge and expertise handed to me by Mr. Robert Szerencsei, and Dr. Kyeong-Jin Kang. In addition to them, several other present and former members of the Schnetkamp laboratory have also contributed to this work, notably for the molecular cloning of the namesake of this thesis – NCKX2, and the countless mutant constructs of NCKX2; to this end, I would like to specifically acknowledge the contributions of, and thank Mr. Robert (Bob) Winkfein.

I would like to extend my deep gratitude to the following University of Calgary professors: Dr. Robert (Bob) French, and Dr. Jonathan Lytton; both discerning, and positively critical scientists of my supervisory committee. I would also like to especially thank Dr. French, and Dr. Lytton for being more than willing to open up their laboratories to me for all of my past proposed scientific whims and (mis)adventures. Another very special thank you goes to Dr. William (Bill) Stell, whose continual support was instrumental in helping me make this achievement, and further my (as of yet) fledgling scientific career (and also for opening up his lab to me for a couple of past misadventures there!).

Last, but certainly not least, I would like to thank my family for their love and support.

I would also like to acknowledge the funding sources that made this work possible: operating grant that funded Dr. Schnetkamp's laboratory from the Canadian Institutes of Health Research, and graduate student scholarships from the Foundation Fighting Blindness – Canada, and the Natural Sciences and Engineering Research Council of Canada.

TABLE OF CONTENTS

List of Figures

List of Symbols, Abbreviations, and Nomenclature

ATP	adenosine triphosphate
ATP	adenosine triphosphatase gene
cDNA	complementary deoxyribonucleic acid
Ctrl	control
DMF	*N,N*-dimethylformamide
DMEM	Dulbecco's modified Eagle medium
DTT	dithiothreitol
EDTA	ethylenediaminetetraacetic acid
FCCP	carbonyl cyanide *p*-trifluoromethoxyphenylhydrazone
gram	gramicidin
HEDTA	*N*-(2-hydroxyethyl)ethylenediamine-*N,N′,N′*-triacetic acid
HEK293	human embryonic kidney 293 cells
HEPES	*N*-(2-hydroxyethyl)piperazine-*N′*-(2-ethanesulfonic acid)
mRNA	messenger ribonucleic acid
NCX	Na^+/Ca^{2+} exchanger
NCKX	Na^+/Ca^{2+}-K^+ exchanger
PMCA	plasma membrane Ca^{2+} adenosine triphosphatase
SD	standard deviation
SEM	standard error of the model
SERCA	sarco-endoplasmic reticulum Ca^{2+} adenosine triphosphatase
SLC	solute carrier gene
SPCA	secretory pathway Ca^{2+} adenosine triphosphatase
TAPS	*N*-[tris(hydroxymethyl)methyl]-3-aminopropanesulfonic acid
Tg	thapsigargin
TM	transmembrane spanning α-helix
wt	wild-type

CHAPTER ONE: INTRODUCTION

1. 1. Background

Calcium serves a ubiquitous intracellular signalling role in eukaryotes, controlling many functions from cell cycle and gene transcription, to fast events in animal cells such as neurotransmitter release in synaptic terminals of neurons, and excitation-contraction coupling in muscle tissue. A multitude of protein channels have thus evolved to mediate the movement of Ca^{2+} from the extracellular environment into the cytoplasm (or from intracellular membrane-bounded stores into the cytoplasm) where Ca^{2+} can carry out its functions. To be effective as a signalling molecule, the resting level of Ca^{2+} in the cytoplasm must be maintained at low concentrations – typically around 10^{-7} M. Upon influx of Ca^{2+} signals into the cytoplasm, and consequent elevation of local cytoplasmic $[Ca^{2+}]_i$, the Ca^{2+} must subsequently be returned to baseline level, either by extruding Ca^{2+} to the extracellular environment, or by sequestering Ca^{2+} into intracellular membrane-bounded stores – both processes requiring the uphill movement of Ca^{2+} against a concentration gradient of up to 10^4. For this purpose, several protein families have evolved to carry out the function of Ca^{2+} buffering, and eventual clearance from the cytoplasm, and hence are instrumental in shaping the spatial and temporal properties of cytoplasmic Ca^{2+} signals.

Ca^{2+} extrusion proteins of animal cells can be divided broadly into primary active transporters or ATP-coupled pumps, and secondary active transporters which do not depend directly on ATP, but rather utilize energy stored in existing ionic gradients – specifically Na^+ – to couple to the uphill counter-transport of Ca^{2+}. The former category of so called P-type ATPases includes the sarco-endoplasmic reticulum Ca^{2+} ATPases (SERCA; which in humans are products of three distinct genes *ATP2A1-3* (Prasad *et al*. 2004)), the plasma membrane Ca^{2+} ATPases (PMCA; which in humans are products of four distinct genes *ATP2B1-4* (Strehler and Zacharias 2001)), and the secretory pathway Ca^{2+} ATPases (SPCA; which in humans are products of two distinct genes *ATP2C1-2* (Xiang *et al*. 2005)). The other category of Ca^{2+} extrusion proteins in animals constitute two distinct

protein families of Na^+/Ca^{2+} exchangers: the Na^+/Ca^{2+} exchangers (NCX) which belong to the *SLC8* gene family are products of three distinct genes *SLC8A1-3* (Quednau *et al*. 2004), and the Na^+/Ca^{2+}-K^+ exchangers (NCKX) which belong to the *SLC24* gene family and are products of five distinct genes *SLC24A1-5* (Schnetkamp 2004); another putative Ca^{2+}/cation exchanger (denoted NCLX) exists in mammalian genomes, but is poorly characterized at present (Lytton 2007). In addition, mitochondria offer a membrane-bounded compartment that acts as an important cytoplasmic Ca^{2+} clearance organelle in animal cells, accomplished by way of a putative Ca^{2+} uniporter; however, mitochondrial Ca^{2+} transport mechanisms have not been identified at the molecular level (Duchen 2000). This thesis is a study of Na^+/Ca^{2+} exchangers, which focuses specifically on one member of the NCKX family of proteins.

1. 2. Na^+/Ca^{2+} exchangers

Na^+/Ca^{2+} exchange as a Ca^{2+} clearance mechanism was first identified in the plasma membrane of squid axons, as well as frog and mammalian cardiac muscle (Niedergerke 1963; Reuter and Seitz 1968; Baker *et al*. 1969). Since then, Na^+/Ca^{2+} exchange has been identified in a variety of tissues and cell types as a major plasma membrane Ca^{2+} extrusion mechanism, along with PMCA. The major difference between these two mechanisms, aside from Na^+/Ca^{2+} exchangers being absolutely dependent on $[Na^+]_o$ to extrude Ca^{2+} and PMCA being absolutely dependent on intracellular ATP, is that Na^+/Ca^{2+} exchangers have a relatively low affinity for Ca^{2+} – on the order of a few μM, while PMCA is sensitive to $[Ca^{2+}]_i$ in the nanomolar range – typically less than 0.5 μM (Carafoli 1991; Blaustein and Lederer 1999). Hence, it is generally posited that the role of PMCA is to fine-tune resting, and small changes in $[Ca^{2+}]_i$ to the typical resting level of ~100 nM, while Na^+/Ca^{2+} exchangers handle relatively larger fluxes of Ca^{2+}, such as the dynamic fluxes experienced by excitable tissue of muscle and nerve.

1. 3. Discovery of Na^+/Ca^{2+}-K^+ exchange

Towards the late 1980s, work on isolated vertebrate retinal rod outer segments, which were known to display prominent Na^+/Ca^{2+} exchange activity, culminated in the

demonstration of a unique feature of Na^+/Ca^{2+} exchange in this preparation, in that the putative Na^+/Ca^{2+} exchanger of vertebrate rod outer segments required K^+ to be co-transported along with Ca^{2+} in exchange for Na^+ (Cervetto *et al*. 1989; Schnetkamp *et al*. 1989). The exchanger of vertebrate rod outer segments was shown to mediate electrogenic transport of Ca^{2+} at a stoichiometry of 1 Ca^{2+} ion + 1 K^+ ion for every 4 Na^+ ions, contrasted with the electrogenic transport of 1 Ca^{2+} ion for every 3 Na^+ ions previously established for the Na^+/Ca^{2+} exchanger in cardiac sarcolemmal vesicles (Reeves and Hale 1984). Initially, it was postulated that the unique features of Na^+/Ca^{2+} exchange in vertebrate retinal rod outer segments was an adaptation to the ionic conditions of these cellular compartments. In the dark, the cyclic nucleotide-gated channels of vertebrate rod outer segments mediate a current of ~30 pA carried by Na^+ and Ca^{2+}, which results in a relatively depolarized membrane potential of ~-40 mV, an elevated resting $[Ca^{2+}]_i$ of ~0.5 μM, as well as elevated $[Na^+]_i$ (Sampath *et al*. 1998; Woodruff *et al*. 2002). Under such conditions, it would be expected that a Na^+/Ca^{2+} exchanger with a stoichiometry of 3 Na^+:1 Ca^{2+} may be compromised in clearing $[Ca^{2+}]_i$, while a Na^+/Ca^{2+} exchanger that additionally uses the energy stored in the outwardly directed K^+ gradient to extrude Ca^{2+} from the cytoplasm would be optimally suited for this particular environment (Schnetkamp 1995c). A later study suggested that in rat brain synaptic plasma membrane vesicles, up to 20% of the Na^+/Ca^{2+} exchange activity was in fact dependent on K^+, and others reported that the Na^+/Ca^{2+} exchanger of human platelets also transported K^+, suggesting that Na^+/Ca^{2+}-K^+ exchange may be more widespread than initially posited (Dahan *et al*. 1991; Kimura *et al*. 1993).

These observations of distinct Na^+/Ca^{2+} exchange processes were confirmed when the cardiac Na^+/Ca^{2+} exchanger of canine cardiac muscle was cloned, followed by cloning of the Na^+/Ca^{2+}-K^+ exchanger of bovine retina (Nicoll *et al*. 1990; Reiländer *et al*. 1992). The primary amino acid sequence derived from the cDNA of the cardiac Na^+/Ca^{2+} exchanger and the retinal rod outer segment Na^+/Ca^{2+}-K^+ exchanger revealed only limited sequence homology, within internal motifs of transmembrane spanning helices (TM; Fig. 1 B); these TM segments were later termed α-repeats 1 and 2 (Reiländer *et al*. 1992, Schwarz and Benzer 1997). Later cloning efforts culminated in the discovery of several paralogs for

Fig. 1. Sequence alignments of NCKX1-5 and NCX1. **A.** Amino acid sequences of human NCKX1-5 (NCBI Sequence Viewer accession numbers: NP_004718.1, NP_065077.1, NP_065740.2, NP_705934.1, NP_995322.1) were aligned using ClustalW2 from the European Bioinformatics Institute website – www.ebi.ac.uk; only the sequence alignment of the α_1 and α_2 regions are shown. The grey shading indicates predicted transmembrane α-helical segments. The position of critical acidic residues, Glu^{188}, and Asp^{548}, within the α_1 and α_2 repeats respectively are highlighted by large typeface. In addition, another acidic residue Asp^{575} found to define K^+-dependence of NCKX is also highlighted, along with another conserved amino acid investigated in this thesis – Asn^{572}. **B.** Amino acid sequence alignment of the α repeats of human NCKX2 as a representative of the *SLC24* gene family, and the subject of this thesis, with the α repeats of human NCX1 (NCBI Sequence Viewer accession number NP_066920.1) as a representative of the *SLC8* gene family.

Fig. 1.

A.

```
                                         TM2                              TM3
NCKX3          LEKICERLHLSEDVAGATFMAAGSSAPELFTSVIGVFITKGDVGVGTIVGSAVFNILCII 195
NCKX4          LEKICERLHLSEDVAGATFMAAGSSTPELFASVIGVFITHGDVGVGTIVGSAVFNILCII 121
NCKX5          LEIISESLGLSQDVAGTTFMAAGSSAPELVTAFLGVFITKGDIGISTILGSAIYNLLGIC 154
NCKX1          LGVITDKLQISEDVAGATFMAAGGSAPELFTSLIGVFISHSNVGIGTIVGSAVFNILFVI 540
NCKX2          LTVITEKLGISDDVAGATFMAAGGSAPELFTSLIGVFIAHSNVGIGTIVGSAVFNILFVI 220
               *  * : * :*:****:******.*:**.:.:.:****::.::*:.**:***::*:* :

                                      TM8                        TM9
NCKX3          IIGYTLGIPDVIMGITFLAAGTSVPDCMASLIVARQGMGDMAVSNSIGSNVFDILIGLGL 559
NCKX4          IIGYTLGIPDVIMGITFLAAGTSVPDCMASLIVARQGLGDMAVSNTIGSNVFDILVGLGV 472
NCKX5          ITGETLEIPDTVMGLTLLAAGTSIPDTIASVLVARKGKGDMAMSNIVGSNVFDMLC-LGI 416
NCKX1          QVGETIGISEEIMGLTILAAGTSIPDLITSVIVARKGLGDMAVSSSVGSNIFDITVGLPV 1020
NCKX2          QVGETIGISEEIMGLTILAAGTSIPDLITSVIVARKGLGDMAVSSSVGSNIFDITVGLPL 582
                 * *: *.: :**:*:******:** ::*::***:* ****:*. :***:**:   * :
```

B.

```
NCX1           132 ETVSNLTLMALGSSAPEILLSVIEVCGHNFTAGDLGPSTIVGSAAFNMFIII 183
NCKX2          172 DDVAGATFMAAGGSAPELFTSLIGVF---IAHSNVGIGTIVGSAVFNILFVI 220
                   : *:. *:** *.****:: *:* *    :: .::* .******.**::::*

NCX1           826 GCTIGLKDSVTAVVFVALGTSVPDTFASKVAATQDQYADASIGNVTGSNAVN   877
NCKX2          525 GETIGISEEIMGLTILAAGTSIPDLITSVIVARKG-LGDMAVSSSVGSNIFD   575
                   * ***:.:.: .:.::* ***:** ::* :.* :.  .* ::.. .*** .:
```

both canine cardiac Na^+/Ca^{2+} exchanger, and bovine retinal rod Na^+/Ca^{2+}-K^+ exchanger, giving rise to the *SLC8* and *SLC24* gene families respectively, now both classified as members of a larger superfamily of Ca^{2+}/cation exchanger genes (Li *et al*. 1994; Nicoll *et al*. 1996; Tsoi *et al*. 1998; Kraev *et al*. 2001; Li *et al*. 2002; Cai and Lytton 2004; Lamason *et al*. 2005).

1. 4. Animal tissue distribution of Na^+/Ca^{2+} exchangers, and physiological roles

The first discovered member of the *SLC8* gene family, NCX1 has relatively widespread tissue distribution, with cardiac muscle, kidney, and spleen displaying particularly strong expression at the mRNA level (Lee *et al*. 1994; Nicoll *et al*. 1996). NCX2 and NCX3 on the other hand are largely restricted to brain and skeletal muscle (Li *et al*. 1994; Nicoll *et al*. 1996). Transgenic embryonic knockout of NCX1 was lethal highlighting the importance of NCX1 for the development of the cardiovascular system (Wakimoto *et al*. 2000). NCX2 knockout mice proved to have altered Ca^{2+} clearance in hippocampal neurons shifting the frequency of long term potentiation in hippocampus to lower frequencies, and thereby enhancing performance in hippocampus-dependent learning and memory tasks (Jeon *et al*. 2003). NCX3 knockout mice had localized muscle fiber necrosis, defective transmission at the neuromuscular junction and fatigability of limb muscles (Sokolow *et al*. 2004).

NCKX proteins, on the other hand, are predominantly found in neuronal cells (Li and Lytton 2002; Lytton *et al*. 2002). NCKX1 is the only functionally proven Ca^{2+} extrusion mechanism in the plasma membrane of vertebrate rod outer segments, but mRNA transcripts have also been reported in megakaryocytes, and at low levels in brain (Schnetkamp *et al*. 1991a; Kim *et al*. 1998; Kimura *et al*. 1999; Pyrski *et al*. 2007). NCKX2 was cloned, and found only in brain, as well as in retinal ganglion cells and cone photoreceptors (Tsoi *et al*. 1998; Prinsen *et al*. 2000; Kim *et al*. 2003; Paillart *et al*. 2007). NCKX3 and NCKX4 are also both found in brain, but with lower levels of mRNA transcripts localized to various other smooth muscle tissues such as intestine, aorta, lung, and uterus (Kraev *et al*. 2001; Li *et al*. 2002; Dong *et al*. 2006). NCKX5 is localized to melanin rich tissues, namely skin and retinal pigment epithelium; the unique feature of

NCKX5 is that it was localized to internal membranes, and did not appear to ordinarily reach the plasma membrane (Lamason *et al*. 2005; Ginger *et al*. 2008). Interestingly, NCKX2 knockout mice displayed a phenotype different from NCX2 knockout mice, in that knockout of NCKX2 favoured long term depression in hippocampus, and resulted in deficits in specific motor learning and special memory tasks (Li *et al*. 2006). Mutant zebrafish, termed *golden*, that had hypopigmentation of skin and retinal pigment epithelium led to the initial characterization of NCKX5; later development of a mouse NCKX5 knockout corroborated that this isoform is mainly involved in retinal pigment epithelium pigmentation, at least in mice (Lamason *et al*. 2005, Vogel *et al*. 2008).

1. 5. Structural features

The most extensively studied NCKX protein structurally is NCKX2. At the primary structural level, NCKX2 is most closely related to NCKX1 (~60% amino acid identity), while NCKX3 and NCKX4 are each other's closest relatives (also ~60% amino acid identity); NCKX5 amino acid sequence lies somewhere in between the two pairs of NCKX1/NCKX2 and NCKX3/NCKX4 (Cai and Lytton 2004; Fig. 1 A). All NCKX isoforms are thought to share the following experimentally determined structural features of NCKX2: a cleavable TM signal peptide (for plasma membrane targeting) at the N-terminus, plus ten TM segments arranged in two clusters of five TM segments separated by a relatively large intracellular loop, and both N- and C-termini are exoplasmic (Kang and Schnetkamp 2003; Kinjo *et al*. 2003; Fig. 2). NCKX proteins additionally share a similar motif in their hydrophobic clusters, termed α-repeats 1 and 2, which are arranged in an anti-parallel orientation with respect to the plane of the membrane (Cai and Lytton 2004). Cysteine cross-linking experiments indicated that these α-repeats associate closely in the folded protein structure, forming a postulated binding pocket for the transported ions; those results also pointed to non-purely helical TM segments in the α-repeat regions (Kang *et al*. 2005a; Kinjo *et al*. 2005). In comparison, NCX proteins also share a similar overall topology with two clusters of TM segments separated by a large cytoplasmic loop, and a cleavable signal peptide at the N-terminus; in contrast, the two clusters of TM segments of

Fig. 2. Topological model of NCKX2. Predicted α-helical segments are numbered 1-11. Two sets of five transmembrane segments are separated by a large cytoplasmic loop, while both N- and C- termini are extracellular. The location of the highly conserved α repeats is highlighted in grey; α_1 spans transmembrane segments 2-3, and α_2 spans transmembrane segments 8-9. The predicted location of various amino acid residues investigated functionally in this thesis are indicated inside ovals.

Fig. 2.

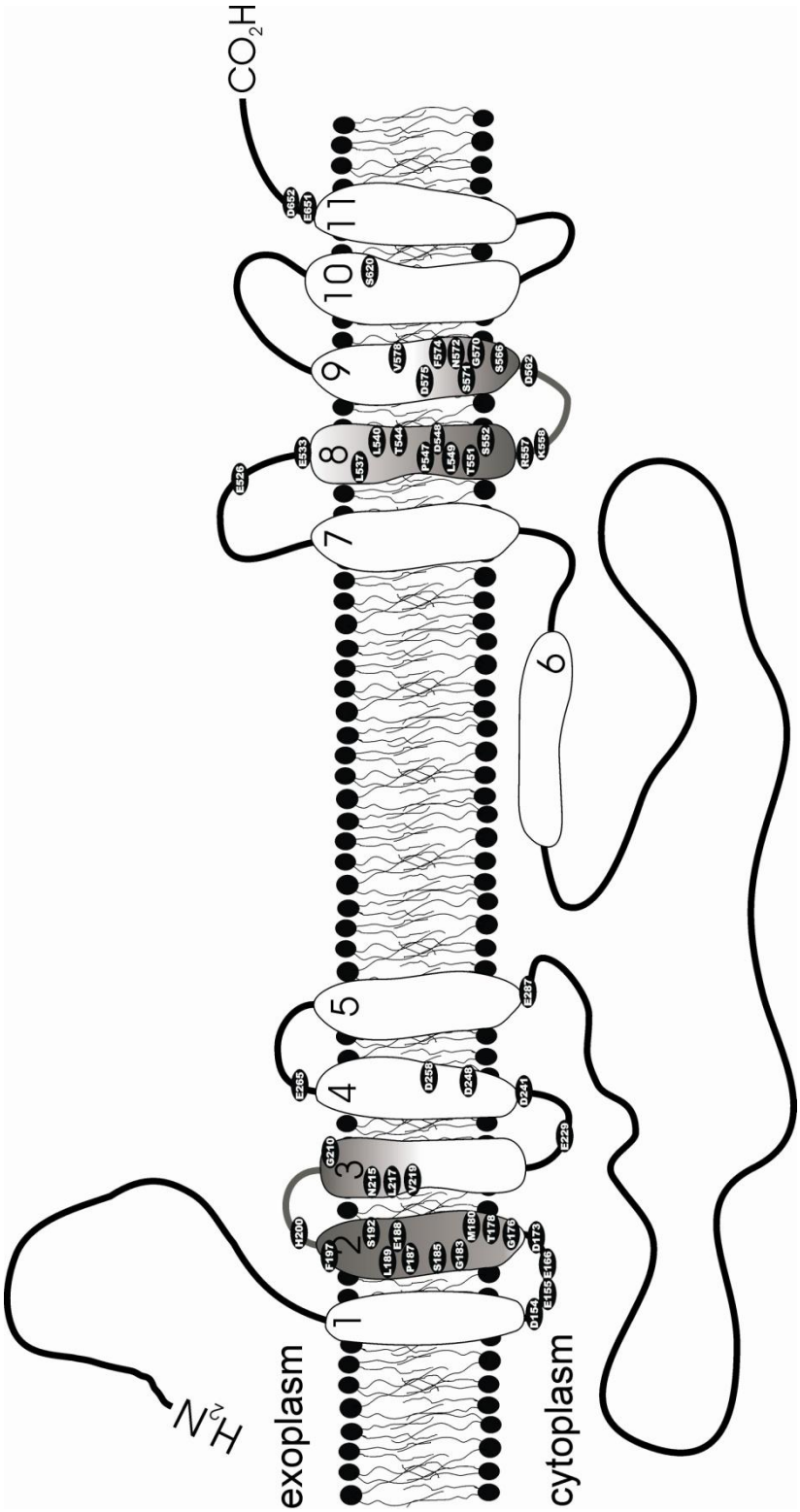

NCX are made up of five and four helices, resulting in a cytoplasmic C-terminus, and the α-repeat regions contain re-entrant P-loops (Nicoll *et al*. 1999; Iwamoto *et al*. 2000).

1. 6. Functional properties - operational model

The presumptive mode of transport of NCKX proteins is that which is accepted as the model for all other primary and secondary active transporters – the alternating access model (Jardetzky 1966). In short, the model proposes that the ion transporter contains one or a set of liganding site(s) that bind substrate on one side of the membrane, and subsequently undergoes a conformational change in transporting the substrate(s) so that the liganding site(s) faces the opposite side of the membrane. The conformational cycling involves gating steps, which prevent the substrate from being simultaneously exposed to both sides of the membrane, presumably with an intermediate step where the substrate is completely occluded within the membrane domain. It follows that substrate transport (ions in the case of NCKX) can be described by Michaelis-Menten kinetics, with an experimentally observable saturation of transport (V_{max}), and apparent substrate dissociation or Michaelis-Menten constant (K_m). Also, for many membrane transporters, different substrate species are transported by the same protein across membranes giving rise to so-called sym- or co-transporters, and anti- or counter-transporters (NCX and NCKX would fall in the latter grouping), and according to the model, the substrate species transported would display characteristic stoichiometric relationships. Across the numerous different membrane transporters, substrate fluxes (reflecting transport cycles) can vary immensely – from the order of 10^1 s^{-1} to 10^4 s^{-1}; some transporters (transporting substrate uphill against its concentration gradient) can mediate the activation of transport currents more rapidly than currents elicited by ion channels (which transport substrate downhill along its concentration gradient), for example the serotonin transporter in presynaptic nerve terminals (Bruns *et al*. 1993; West 1997). Also, in several transporters, experimentally determined stoichiometric determinations are not necessarily fixed, e,g, the cardiac Na^+/Ca^{2+} exchanger NCX1 has been assigned a transport stoichiometry of 4 Na^+ ions in exchange for 1 Ca^{2+} ion (contrasted with 3 Na^+:1 Ca^{2+}); while in another study, NCX1 was reported to display other transport "modes" of electroneutral 2 Na^+:1 Ca^{2+}, as well as net

Na^+ influx (Fujioka *et al*. 2000; Dong *et al*. 2002; Kang and Hilgemann 2004). Yet another example is the appearance of channel-like properties with the Na^+/K^+ ATPase of animal cells when treated with the marine toxin palytoxin, which competes with the ouabain binding site on the Na^+/K^+ ATPase to induce small unitary currents of a few pS (Habermann 1989; Artigas and Gadsby 2003; DeFelice and Goswami 2007). These observations, taken together, suggest that some secondary active transporters operate as channels, but with two separate gates occluding access to the two sides of the membrane. Hence, it follows that conformational changes in the protein need not be particularly large to accomplish substrate transport, which would explain the fast flux rates observed in some transporters. With regards to NCKX, the best evidence supporting the alternating access model for its operation are measurements of its ability to carry out $(Ca^{2+} + K^+):(Ca^{2+} + K^+)$, and $Na^+:Na^+$ self-exchange in bovine retinal rod outer segments (Schnetkamp 1989; Schnetkamp and Szerencsei 1991). A simplified schematic of the kinetic model of NCKX transport function is illustrated in Fig. 3.

1. 7. Functional properties - ionic affinities

NCKX proteins are bi-directional transporters, with the direction of Ca^{2+} transport dependent on both Na^+ and K^+ gradients across the membrane. For the remainder of this thesis dissertation, I will refer to the modes of transport as Ca^{2+} influx mode (often referred to in the literature as reverse mode) and Ca^{2+} extrusion mode (often referred to in the literature as forward mode). While physiologically, it is presumed that the main function of NCKX proteins is Ca^{2+} extrusion, from an experimental stand-point Ca^{2+} influx mode is the more readily and extensively studied using different techniques – examples in (Schnetkamp 1986; Schnetkamp *et al*. 1989; Schnetkamp *et al*. 1991b; Sheng *et al*. 2000; Dong *et al*. 2001; Szerencsei *et al*. 2001; Kang *et al*. 2005a; Visser *et al*. 2007). Therefore, for each experimentally governed Ca^{2+} transport mode, a set of apparent ion dissociation constants can be derived. Stoichiometric measurements converge on an exchange of 4 Na^+ ions for 1 Ca^{2+} ion + 1 K^+ ion (Schnetkamp *et al*. 1989; Dong *et al*. 2001; Szerencsei *et al*. 2001). Accordingly, there is a sigmoidal dependence (Hill coefficient between 2-3) of Ca^{2+} extrusion on external $[Na^+]$, with K_m values reported ranging between 30-50 mM Na^+

Fig. 3. Kinetic model of operation of NCKX. Simplified schematic of alternating access model for NCKX operation, with indicated stoichiometric relationships for transported ions: 4 Na^+:1 Ca^{2+} + 1 K^+. Direction of Ca^{2+} transport is reversible, depending on the gradients of Na^+ and K^+, as well as membrane potential; Ca^{2+} efflux mode is in the direction of the black arrows, while Ca^{2+} influx mode is in the direction of the grey arrows. This thesis investigates a novel kinetically inactive state, which is revealed upon prolonged exposure to high intracellular Na^+; broken arrows indicate likely pathway by which the inactive kinetic state is reached.

Fig. 3.

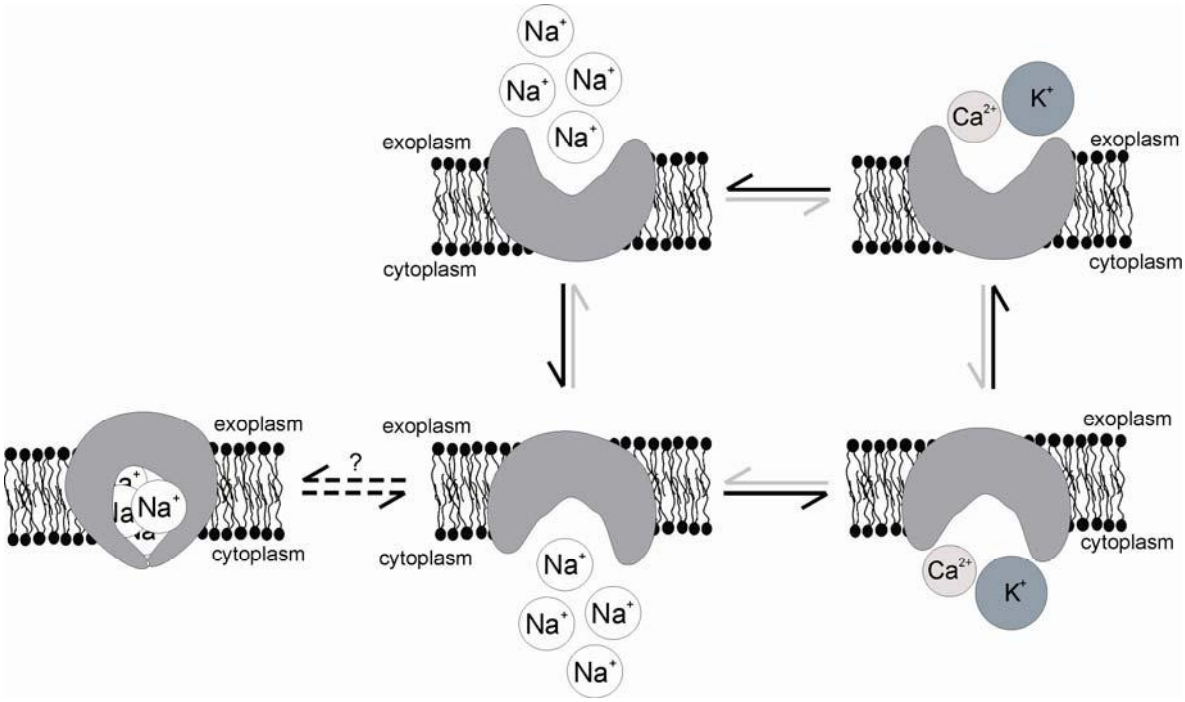
Na+
Na+
Na+
Na+
exoplasm
cytoplasm
Ca2+
K+
exoplasm
cytoplasm
exoplasm
Na+
cytoplasm
?
exoplasm
cytoplasm
Na+
Na+
Na+
Na+
exoplasm
cytoplasm
Ca2+
K+

(Schnetkamp 1991; Sheng *et al*. 2000). Ca^{2+} affinities have been measured for the exofacial configuration of NCKX (in the Ca^{2+} influx mode) and these values range between 1-3 μM (Sheng *et al*. 2000; Szerencsei *et al*. 2001; Kang *et al*. 2005a; Visser *et al*. 2007). K^+ affinities measured for the exofacial configuration of NCKX (in the Ca^{2+} influx mode) ranged widely, depending on the NCKX isoform tested and major cation constituent of the medium, with values reported between 1 mM to more than 30 mM (Szerencsei *et al*. 2000; Dong *et al*. 2001; Kang *et al*. 2005a; Visser *et al*. 2007). As for the cytoplasmic configuration of NCKX, The K_m for Ca^{2+} ranged between 0.5-2 μM, and values around 1.5 mM have been reported for transported K^+ (Lagnado *et al*. 1988; Schnetkamp *et al*. 1989; Schnetkamp 1991; Sheng *et al*. 2000). The only measurements, to date, of NCKX dependence on cytoplasmic Na^+ have reported a K_m between 30-40 mM in bovine retinal rod outer segments (no Hill coefficient was reported), while a relatively high K_m of 150 mM Na^+ (Hill coefficient 3.1) was reported for NCKX2 heterologously expressed in the High Five insect cell line (Schnetkamp *et al*. 1995; Winkfein *et al*. 2003). In comparison, NCX affinities measured for Ca^{2+} are lower than those of NCKX; examples of measurements of K_m for external Ca^{2+} (in mammalian cells) ranged between 100-300 μM, while for intracellular Ca^{2+} K_m values ranged between 0.6-10 μM; measurements of affinities of NCX proteins for intracellular Ca^{2+} are complicated by NCX requirement for regulatory Ca^{2+}, discussed below (Miura and Kimura 1989; Matsuoka and Hilgemann 1992; Linck *et al*. 1998; Iwamoto *et al*. 2000; Ottolia *et al*. 2005). On the other hand, affinities measured for extracellular Na^+ reported values for K_m between 43-118 mM, and for intracellular Na^+ K_m values ranged between 13-20 mM, with Hill coefficient values of around 2 (Miura and Kimura 1989; Matsuoka and Hilgemann 1992; Iwamoto *et al*. 2000; Ottolia *et al*. 2005).

1. 8. Functional properties - regulatory processes

Much more information is known about regulatory processes governing the operation of NCX than of NCKX. The large cytoplasmic loop of NCX proteins is integral for several regulatory processes; removal of the large cytosolic loop either by chymotrypsin treatment in giant excised patches, or by site directed mutagenesis of heterologously

expressed NCX1 removes several of the regulatory processes described below (Hilgemann *et al*. 1992a; Matsuoka *et al*. 1993). The large cytoplasmic loop of NCX contains two sites for binding Ca^{2+}, which is required to activate NCX activity in giant excised patches in the concentration range 0.2-0.6 μM; in the absence of regulatory intracellular Ca^{2+}, NCX1 enters into an inactive kinetic state (termed I_2 inactivation) (Hilgemann *et al*. 1992b; Matsuoka *et al*. 1995; Matsuoka *et al*. 1997). The large intracellular loop also contains an amino acid stretch termed exchanger inhibitory peptide where it was discovered that an exogenously applied oligopeptide with that same sequence inhibited NCX when applied to the cytoplasmic side (Li *et al*. 1991). In addition, the large cytoplasmic loop is instrumental in mediating Na^+_i-dependent inactivation (termed I_1 inactivation); this kinetic state results from application of high $[Na^+]_i$ on the order of ~100 mM, and manifests itself in giant excised patches as a decay (τ ~4 s) of NCX mediated outward peak currents to a steady-state current that is anywhere between 10-70% of peak current (Hilgemann *et al*. 1992a). ATP is also known to have stimulatory effects on NCX activity in giant excised patches, and this is due to increased production of phosphatidylinositol 4,5-bisphosphate – a direct lipid regulator of NCX activity, but ATP may also stimulate NCX activity through phosphorylation of NCX (Hilgemann *et al*. 1992b; Hilgemann and Ball 1996; Ruknudin *et al*. 2007). As for NCKX, the only functional regulatory processes described thus far are a process of Ca^{2+} extrusion inactivation in retinal rod outer segments, where it was found that Ca^{2+} loading mediated by NCKX1 was not completely reversible (this thesis re-examines this regulatory process), and a report of protein kinase C mediated phosphorylation and resultant enhancement of activity of NCKX2 heterologously expressed in HEK293 cells (Schnetkamp *et al*. 1991c; Schnetkamp and Szerencsei 1993; Schnetkamp 1995b; Lee *et al*. 2006).

1. 9. Thesis objectives, and hypothesis

In an effort to understand the molecular operation of NCKX, as in other transporters, it is pertinent to know which regions of the protein are involved in binding and/or transporting substrate. Toward this end, Dr. Schnetkamp's lab has generated a large number (> 150) of single amino acid substitution mutants of the short splice variant of

human NCKX2; these have recently been analyzed in assays designed to test for shifts in the apparent K_m values for Ca^{2+} and K^+ (Kang *et al*. 2005a; Kang *et al*. 2005b). The results indicated that two acidic amino acid residues that lie within the mid-plane of TM segments 2 and 8 are critical for defining the apparent affinities for Ca^{2+} and K^+, as mutation of either of these residues, Glu^{188} or Asp^{548}, resulted in 100-fold and 10-fold decreases in the apparent affinities for Ca^{2+} and K^+, respectively (Kang *et al*. 2005a; for sequence location and predicted topological location of these residues see Fig. 1 and Fig. 2). Another acidic residue predicted to lie in the mid-plane of TM 9, Asp^{575}, was found to define K^+-dependence of NCKX, as substituting this residue with either Asn or Cys resulted in Na^+/Ca^{2+} exchange activity that was independent of K^+; it is also worth noting that this residue is not conserved between members of NCKX proteins and NCX proteins – in the latter group, the amino acid that is in the equivalent position is Asn (Kang *et al*. 2005b; Fig. 1 B). The results obtained by Kang *et al*. (2005a) also indicated that in all cases tested, amino acid substitutions which resulted in shifts in apparent Ca^{2+}-affinity of NCKX, resulted in parallel shift in apparent K^+-affinity, corroborating the hypothesis that these ions share a common transport site (or set of transport sites), and their transport is directly coupled. Hence, one of the major aims of this thesis is to test whether these residues which have proven to be important for Ca^{2+} and K^+ liganding are also important for liganding the counter-transported ion Na^+. To accomplish this, the assay that had been used in the previous studies, must be adjusted so as to allow for measurement of the $[Na^+]$-dependence of NCKX activity, from which we can derive a quantitative measure of apparent Na^+-affinity of NCKX.

Another aim of this study derives from observations made during preliminary experimentation aimed at devising the assay to be used to define apparent Na^+-affinity of NCKX. The observation was that the Ca^{2+}-extrusion mode of NCKX was not operational under all assay conditions; specifically the clearance rate abruptly diminished upon exposure to high $[Na^+]_i$ as illustrated in Fig. 6 A and B. Such an observation had been reported previously in a study of NCKX *in situ* in isolated bovine rod outer segments, and had been suggested to be resultant of inactivation of the exchanger (Schnetkamp *et al*. 1991c; Schnetkamp and Szerencsei 1993; Schnetkamp 1995b). Hence, the other major aim

of this thesis was to examine this apparent inactivation process of NCKX and define the conditions under which it occurrs.

Therefore, the following thesis will address the general hypothesis:

"Exchanger function of NCKX is accomplished in accordance with the alternating access model."

This general hypothesis entails the more specific hypothesis that the same amino acid residues found to be critical for NCKX liganding of Ca^{2+} and K^{+}, will also prove to be critical in defining the apparent affinity of NCKX for Na^{+}.

Additionally, this thesis will address the hypothesis that NCKX displays an inactive kinetic state. Specifically, this inactive state is revealed when NCKX is exposed to high intracellular Na^{+}.

The major finding of this thesis with respect to inactivation of NCKX has been published (Altimimi and Schnetkamp 2007). The results of the development of the assay for assessing shifts in apparent affinity for Na^{+}, and its feasibility for scanning through the large number of single amino acid substitution constructs of NCKX2 is addressed in the DISCUSSION section.

CHAPTER TWO: MATERIALS AND METHODS

2. 1. Basic methodology

The experimental approach used to make measurements of Na^+/Ca^{2+} exchange using heterologous expression described herein is based on methods developed previously in Dr. Schnetkamp's laboratory (Cooper *et al*. 2000; Kang *et al*. 2005a). All chemical reagents used were from Sigma, unless otherwise indicated.

All cDNA constructs used were previously cloned in Dr. Schnetkamp's lab. The wild-type human NCKX2 cDNA construct used was the short-splice variant, which has a region of 17 amino acids spliced out from its large cytoplasmic loop, cloned into the mammalian expression vector pcDNA3.2, and with a Myc tag inserted near the N-terminus, from here on in designated as wild-type (wt) NCKX2 (Prinsen *et al*. 2000). All single-point amino acid substitution mutant cDNAs used were made in the wt NCKX2 cDNA background.

Transient transfections were always carried out on freshly thawed HEK293 cells. After a stock of HEK293 cells were thawed and reached confluency (cultured in 10 cm culture plates containing 10 ml of high glucose DMEM (GIBCO) supplemented with 10% fetal bovine serum (GIBCO), 100 units/ml Penicillin (GIBCO), 100 µg/ml Streptomycin (GIBCO), 2 mM L-glutamine (GIBCO), and 2.5 µg/ml Fungizone Amphotericin B (GIBCO) in a humidified 37 ºC 5% CO_2 incubator), they were sub-cultured to 10 cm culture plates for transient transfection using standard calcium phosphate DNA precipitation. One day following sub-culturing of the HEK293 cells, when the cells had reached ~50-70% confluency, to each 10 cm plate a 1 ml transfection mix was added; the transfection mix consisted of 0.5 ml 0.25 M $CaCl_2$ to which 15 µg of a given cDNA was added, and 0.5 ml of HEPES-buffered solution (in mM: 274 NaCl, 1.8 Na_2HPO_4, 50 HEPES, pH 7.07). The cells were then returned to the 37 ºC incubator for a period of 12 h, at which time point, the medium was replaced with fresh DMEM. The cells were then returned to the incubator for a further 24 h; in some cases the cells were transferred to a humidified 5% CO_2 incubator set to 28 ºC ~24 h post-transfection.

Cells were harvested for functional assaying 36-48 h post-transfection. The medium in each plate was decanted, and the cells were trypsinized by first washing each plate twice with 3 ml PBS, followed by the addition of 1.5 ml 0.05% Trypsin-EDTA (GIBCO). Approximately one minute following the addition of 0.05% Trypsin-EDTA, the cells were agitated by mechanical shaking of the plate to lift them, and immediately 2.5 ml of fresh DMEM added to the resultant cell suspension. The cell suspension from each plate was then individually transferred to separate 50 ml Falcon conical tubes (in cases where many measurements of the same protein construct were to be made, cell suspensions from more than one plate transfected with the same cDNA construct were pooled) and centrifuged at 300 *g* for 1 min to pellet the cells. Thereafter, the supernatant was decanted, and the pellet of cells washed with 5 ml of DMEM, followed by centrifugation at 300 *g* for 1 min. Thereafter the medium was decanted, and the cell pellet resuspended in 0.5 ml DMEM (without added fetal bovine serum). The cells were then loaded with the cell-permeable calcium indicator, fluo-3AM (Molecular Probes) to a suspension concentration of 2 μM (in 0.2% v/v final concentration of *N,N*-dimethylformamide (DMF)), for a period of 30 min. After fluo-3AM loading, the suspension of cells was centrifuged at 300 *g* for 1 min, the supernatant decanted, and the resultant pellet washed with 5 ml Li-EDTA (in mM: 150 LiCl, 20 HEPES, 6 D-glucose, 0.5 DTT, 0.25 sulfinpyrazone (in 0.25% v/v final concentration of DMF), 0.1 L-Arginine-EDTA, pH adjusted to 7.4 with ~8 mM L-Arginine). The medium was then decanted and the cells resuspended in a small volume (300-500 μl – depending on the number of experimental measurements to be carried out on that particular suspension of cells) of Li-EDTA and incubated for further 20-30 min at room temperature, before commencing functional measurements.

An experimental measurement was made by taking an aliquot from a given cell suspension (typically 50 μl of cell suspension containing ~10^5 cells), and placing the aliquot of cell suspension in a plastic cuvette, with a magnetic stir bar, containing 1950 μl of test medium – usually KCl-EDTA (in mM: 150 KCl, 20 HEPES, 6 D-glucose, 0.5 DTT, 0.25 sulfinpyrazone (in DMF), 0.1 L-Arginine-EDTA, pH adjusted to 7.4 with ~8 mM L-Arginine) so that the total volume in the cuvette is 2 ml. The cuvette was then placed in the cuvette holder of a Series 2 SLM spectrometer; the cuvette holder was warmed by a

circulating water jacket held at 25 ºC. Fluorescence emission of the cell suspension in the cuvette was monitored continuously, under constant stirring, at 530 nm (with excitation set at 480 nm), and the fluorescence data were integrated over 1.0 s time bins. Ionophore and pharmacological agents were added to the cuvette immediately after placing the cuvette in the spectrometer instrument. The ionophore used was the channel-forming alkali cation ionophore gramicidin (in 0.2% v/v final concentration of ethanol), which was added to a final cuvette concentration of 2 μM. Empirical observations made in the lab indicated that for effective formation of the gramicidin alkali cation clamp in HEK293 cells, an incubation period of at least one min was required following the addition of gramicidin. Effective clamp formation was judged in preliminary experiments, by examining the rates of initial fluorescence increase upon addition of different [Na^+] to the cuvette; in all cases the rate of fluorescence increase was instantaneous upon addition of Na^+ to the cuvette, provided that gramicidin was applied to the HEK293 cells for at least one minute prior to Na^+ addition. Also, in many experiments, thapsigargin (Tg) was added to the cells to a final cuvette concentration of 0.4 μM (in 0.2% v/v final concentration of DMF) – this was to inhibit SERCA and eliminate Ca^{2+} sequestration into the endoplasmic reticulum. Since Tg treatment results in transient cytoplasmic Ca^{2+} elevation, reflecting the release of Ca^{2+} from the leaky ER compartment, and this transient typically lasts between 2-3 min, Na^+/Ca^{2+} exchange measurements were always made at least 3 min following gramicidin and other drug treatments.

Na^+/Ca^{2+} exchange was measured in the Ca^{2+} influx mode by the addition of Ca^{2+} to the cuvette, followed by the addition of Na^+. The addition of 350 μM Ca^{2+} from a 250 mM stock of $CaCl_2$ to the cuvette achieved a final free Ca^{2+} concentration of 250 μM (note that the cuvette KCl-EDTA medium contained 100 μM EDTA). This Ca^{2+} addition resulted in an instantaneous increase in fluorescence (within 1 s, which is the time required for the addition of a salt solution to be mixed thoroughly with the cuvette medium; Fig. 4). This increase in fluorescence signified the saturation of de-esterified fluo-3 that had leaked from the fluo-3 loaded cell suspension in the cuvette; this fluorescence level remained constant throughout the data recording period (Fig. 4 illustrates a short 30 s duration of Ca^{2+} addition), and is also seen in mock-, or non-transfected HEK293 cells, likewise loaded with

fluo-3AM and placed in suspension. The next addition to the cuvette was NaCl, which resulted in the rapid increase in fluorescence only in NCKX-transfected HEK293 cells treated with gramicidin. Fluorescence from fluo-3 loaded wt NCKX2-transfected HEK293 typically reached a plateau peak within 10 s. In some experiments, we examined the Ca^{2+} extrusion mode by the addition of EDTA to the cuvette at a time point subsequent to the addition of Na^{+}; the EDTA was added (from a 100 mM stock solution with pH adjusted to 7.4 with L-Arginine) to a final cuvette concentration of 1 mM, sufficient to chelate the 250 μM free Ca^{2+} in the cuvette medium, thereby reversing the Ca^{2+} gradient for the cells that were Ca^{2+} loaded. The fluorescence rapidly decreased to a baseline plateau (within 10 s); however, note that the initial period (of ~1 s) of the rapid fluorescence decrease upon addition of EDTA was not entirely due to release of Ca^{2+} from the cells mediated by the exchanger, but rather signified chelation of Ca^{2+} from the leaked fluo-3 present in the cuvette medium (Fig. 4).

2. 2. Notes on variations in assay methodology

The assay conditions and solutions described above were employed for the bulk of the experiments described in this thesis, and were employed after an initial period of preliminary experimentation which was employed to produce the results illustrated in Fig. 5. For the experiments illustrated in Fig. 5, the initial assay conditions differed as follows: The fluo-3 loaded transfected HEK cells were resuspended in a medium of buffered 150 mM NaCl, 1.5 mM $CaCl_2$ (same composition as solutions described above, except without addition of EDTA, or DTT). This resuspension solution was later changed to 150 mM Li-EDTA buffer because we observed that for some constructs (notably D548E which has a substantially increased affinity for Na^{+}, see Fig. 5 D, and Fig. 12) there appeared to be $[Ca^{2+}]_i$ run up after addition of Ca^{2+}, but before addition of Na^{+}; this was later attributed to the carry over of Na^{+} from the buffered 150 mM NaCl, 1.5 mM $CaCl_2$ solution to the cuvette medium, and was eliminated by replacing the 150 mM NaCl, 1.5 mM $CaCl_2$ solution with buffered 150 mM Li-EDTA solution. KB-R7943 which is an isothiourea derivative used to inhibit Na^{+}/Ca^{2+} exchangers of the NCX family was employed during our initial experiments and screening of NCKX2 mutant constructs for shifts in Na^{+}-affinity

Fig. 4. Basic functional Na^+/Ca^{2+} exchange measurement. HEK293 cells transiently transfected with wild-type NCKX2 were harvested and loaded in suspension with cell-permeable fluo-3AM. The HEK293 cell suspension was then washed with 150 mM LiCl/100 μM EDTA buffer (for composition of solutions see MATERIALS AND METHODS) and resuspended in the same medium. An aliquot of 50 μl of the concentrated HEK293 cell suspension was then added to a cuvette with magnetic stir bar, which contained 1950 μl of 150 mM KCl/100 μM EDTA buffer, and placed in a thermostatted (25 ºC) cuvette holder of an SLM AMINCO Series 2 Spectrometer. Fluorescence (emission 530 nm, excitation 480 nm) was monitored continuously under constant stirring. At the time points indicated by the upward pointing arrows, the following additions were made: Tg, 0.4 μM thapsigargin (in 0.2% v/v final concentration of *N,N*-dimethylformamide (DMF)); gram, 2 μM gramicidin S (in 0.2% v/v final concentration of ethanol); KB-R, 10 μM KB-R7943 (in 0.2% v/v final concentration of DMF; note that KB-R7943 was only added to the experiment illustrated here, and those illustrated in Fig. 5, but was not included in subsequent experimentation illustrated in Fig. 6 – Fig. 14, see text for details). To initiate Ca^{2+} influx mode of NCKX2, at the 200 s time point, 350 μM $CaCl_2$ was added, resulting in 250 μM free [Ca^{2+}] in the cuvette. Thirty seconds following the addition of $CaCl_2$, NaCl was added (from a concentrated 5 M stock) to a final cuvette concentration of 75 mM. To initiate the Ca^{2+} extrusion mode of NCKX2, at the downward pointing arrow, 1 mM EDTA was added to the cuvette to chelate external Ca^{2+}. At the upward pointing arrow labelled sap, 0.02% v/v saponin was added to the cuvette to permeabilize the fluo-3 loaded HEK293 cells, after which 2 mM $CaCl_2$ was added to saturate all fluo-3 in the suspension. The fluorescence step observed upon first addition of $CaCl_2$ (labelled "ext") signified Ca^{2+} binding to fluo-3 leaked from the cell suspension; this value was subtracted from all subsequent fluorescence values during data analysis, and in cases where 1 mM EDTA was added to the cuvette, the same value was added to fluorescence values subsequent to EDTA addition (see MATERIALS AND METHODS Data analysis for details).

Fig. 4 legend continued on page 24

Fig. 4.

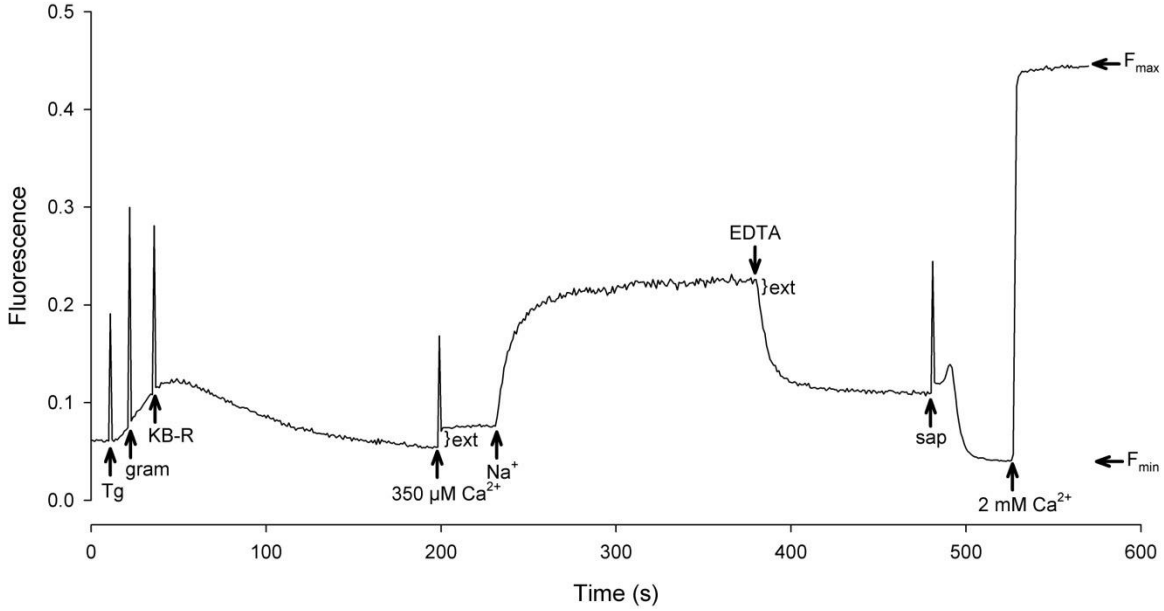
0.5
0.4
0.3
0.2
0.1
0.0
Fluorescence
0
100
200
300
400
500
600
Time (s)
Tg
gram
KB-R
350 µM Ca2+
}ext
Na+
EDTA
}ext
sap
2 mM Ca2+
Fmax
Fmin

Fig. 4 (legend continued).

The F_{min} and F_{max} represent minimal and maximal fluorescence values for each experiment; only F_{max} was routinely obtained, which was used to normalize fluorescence values recorded for the respective experimental measurement. The spikes seen in the trace with some of the additions (e.g. Tg, gram, and KB-R) were caused by light scattering from lowering the pipette tip into the path of the light source.

(Fig. 4 and Fig. 5) to avoid possible contamination of our $[Ca^{2+}]_i$ measurements with $[Ca^{2+}]_i$ rise due to endogenous Na^+/Ca^{2+} exchange activity (Iwamoto *et al*. 1996). However, we affirmed that HEK293 cells do not express any endogenous Na^+/Ca^{2+} exchange activity, and the use of KB-R7943 was later eliminated in all subsequent experimentation.

2. 3. Data analysis

For the purpose of data analysis, the value of fluorescence increase recorded upon addition of Ca^{2+} at the beginning of the experimental recording, was later added to all fluorescence values recorded after the addition of EDTA to the cuvette (see "}ext" label in Fig. 4). As a means of normalizing the experimental recording (to control for variables such as amount of fluo-3 loaded cells present in the cuvette, and extent of fluo-3 loading), at the end of each experimental trace, saponin was added to 0.02% v/v final cuvette concentration, so as to release fluo-3 molecules trapped inside the cells, and obtain a value of F_{max} for each respective trace/experimental recording by the addition of saturating $CaCl_2$ (typically 2 mM). Note that in cases where 1 mM EDTA was added to the cuvette, the addition of saponin resulted in loss of fluorescence due to the excess EDTA in the cuvette medium – this fluorescence level corresponded to F_{min} (Fig. 4). The F_{min} value, however, was not routinely obtained for each experimental recording; but all data presented in this thesis were always normalized with respect to the F_{max} value for each experimental recording trace, and are henceforth termed normalized fluorescence.

To obtain a $[Na^+]$-NCKX activity relationship to measure the affinity of wild-type NCKX2 and mutant constructs for Na^+, we used initial rates of rise in $[Ca^{2+}]_i$ as a measure of NCKX2 activity. This was accomplished by fitting a least squares linear regression to the data points corresponding to the longest initial linear rate of rise in fliuorescence for each experimental measurement/trace. These rates were then plotted against $[Na^+]$, and the rates normalized with respect to the highest $[Na^+]$ tested, or the $[Na^+]$ that produced the highest rate of initial rise in fluorescence. Graphing of data was made using SigmaPlot 2001 for Windows version 7.0; the software was also used to fit the data with three parameter least squares regression models of Hill plots. The resultant K_m parameter was

taken as an estimate of the affinity of wild-type, or single amino acid substitution construct of NCKX2 construct for $[Na^+]_i$.

CHAPTER THREE: RESULTS

Dr. Schnetkamp's lab had previously characterized NCKX activity extensively using fluorescence based free $[Ca^{2+}]_i$ measurement of Na^+/Ca^{2+} exchange in assays of ensemble preparations of *in situ* NCKX1 from bovine rod outer segments, as well as NCKX2 heterologously expressed in HEK293 cells (examples in (Schnetkamp *et al*. 1991b; Kang *et al*. 2005a)). This assay was recently used to scan through a number of single-point amino acid substitution mutants of NCKX2 for relative shifts in the apparent K_m values for transported Ca^{2+}, and K^+. One of the main aims of this thesis was to adapt this assay, so as to provide an efficient means of assaying through the large number of NCKX2 single residue substitution mutants for shifts in the apparent K_m for Na^+.

3. 1. Assaying for Na^+/Ca^{2+} exchange using gramicidin to control $[Na^+]_i$

As described in MATERIALS AND METHODS, the assay was based on the use of the channel-forming alkali cation ionophore gramicidin to clamp Na^+ concentration across the plasma membrane, and thereby we were able to obtain a quantitative measure of the affinity of NCKX2 for Na^+ by comparing the capacity of different Na^+ concentrations in driving Ca^{2+} transport across the membrane. Each measurement entailed taking an aliquot from a suspension of fluo-3 loaded cells (the suspension typically contained all HEK293 cells harvested from one 10 cm culture plate, transiently transfected with a test cDNA construct), and placing the aliquot in a cuvette containing 150 mM KCl/100 μM EDTA medium, followed by the addition of 2 μM gramicidin and 0.4 μM Tg. Three minutes following the addition of gramicidin, the first addition was always Ca^{2+}; this is to saturate the small amount of fluo-3 that inevitably leaked from the cells into the cuvette medium. Thirty seconds following the addition of Ca^{2+} (the lag period was to ensure that no extraneous intracellular free Ca^{2+} run-up was observed) NaCl, from a concentrated 5 M stock, was added to the cuvette. At the end of the experimental trace, saponin was added in the presence of saturating Ca^{2+}, and the F_{max} value thus obtained was used to normalize the fluorescence values of that respective experimental trace (Fig. 4). A series of NaCl concentrations were tested by taking individual aliquots from the original suspension, and

testing them in separate cuvettes for each measurement. Thus, we constructed a family of Na^+-dependence traces for each construct as illustrated in Fig. 5. The individual traces were very stereotypical, with a rapid phase of fluorescence increase to some plateau value, typically for NCKX2 constructs that had wild-type levels of activity the initial rise phase was less than 10 s. This proved to be a very reliable and efficient method to obtain reproducible Na^+-dependence curve families for the more than 100 single-amino acid substitution mutants of NCKX2 tested. For our initial screening, we chose a small number of different Na^+ concentrations to test (in mM: 10, 20, 35, 75; 0 traces were obtained by the addition of Ca^{2+} alone, without subsequent addition of Na^+). By visually comparing the family of Na^+-dependence curves of the different mutants to that of wt NCKX2, specifically, by examining the progression of the curves from low to high [Na^+], we were able to effectively evaluate which constructs showed significant deviations from the pattern of Na^+-dependence curves of wt NCKX2 (Fig. 5). This was achieved despite some constructs having far lower levels of activity than that of wt NCKX2. Next we sought to investigate the Ca^{2+} extrusion mode of NCKX2.

3. 2. Examining NCKX2-mediated Ca^{2+} extrusion

While the assay devised herein essentially measures the capacity of NCKX2 to mediate Ca^{2+} influx into HEK293 cells, we were interested in also examining the other mode of transport of NCKX2 – Ca^{2+} extrusion mode. Given that in each experimental measurement, we produced HEK293 cells that were loaded with Ca^{2+} by way of NCKX2 using the single gradient – the Ca^{2+} gradient resultant from experimentally added 250 μM Ca^{2+} to the cuvette (both Na^+ and K^+ gradients are in principle irrelevant due to the use of gramicidin), it follows that if that gradient was reversed at a time point when $[Ca^{2+}]_i$ had reached a steady-state plateau (by chelating $[Ca^{2+}]_o$), we should observe Ca^{2+} clearance through NCKX2. Thus, for all experimental traces plotted in Fig. 6., 1 mM EDTA was added to the cuvette at the time point indicated (150 s following the induction of Ca^{2+} influx by the addition of the various [Na^+]). In most cases, as expected, the free $[Ca^{2+}]_i$ was rapidly cleared, presumably through NCKX. In fact, the clearance rates were markedly

more rapid than the initial phase of Ca^{2+} influx through NCKX. Also note that free $[Ca^{2+}]_i$ during the clearance phase reached initial baseline free $[Ca^{2+}]_i$ at the beginning of the trace, or closely approached baseline within ~20 s. However, for the highest Na^+ concentration tested (75 mM), and consequently the highest $[Ca^{2+}]_i$, there was an initial very rapid Ca^{2+} clearance of ~5 s duration, followed by an abrupt halt in $[Ca^{2+}]_i$ clearance at a plateau that is significantly elevated from baseline (see Fig. 6 A and B). It was expected that the initial phase of Ca^{2+} clearance would be more rapid the higher the $[Na^+]$ in the cuvette was (just as the initial $[Ca^{2+}]_i$ rise phase was more rapid with higher $[Na^+]$); the abrupt diminishment of the $[Ca^{2+}]_i$ clearance rate was unexpected. This result was intriguing, in that it was reminiscent of results obtained previously with assays of NCKX1 in isolated rod outer segments, where NCKX1 was used to load rod outer segments with Ca^{2+}, but Ca^{2+} fluxes were not completely reversible as NCKX1 appeared to inactivate and hence became ineffective in clearing $[Ca^{2+}]_i$ back to baseline levels (Schnetkamp *et al*. 1991c; Schnetkamp and Szerencsei 1993; Schnetkamp 1995b). Note that in Fig. 6 A, the NCKX2 transfected HEK293 cells had not been treated with Tg; in the middle panel, the same measurements were carried out on NCKX2 transfected HEK293 cells that had been pretreated with 0.4 μM Tg (at the same time as gramicidin). In this case, elimination of SERCA as a $[Ca^{2+}]_i$ sequestration mechanism revealed a correlation between higher $[Na^+]$ and progression towards higher plateau values reached after engaging the Ca^{2+}-extrusion mode of NCKX. We next addressed whether we had effectively isolated heterologously expressed NCKX2 activity in HEK293 cells thus far, by examining the role of mitochondria.

3. 3. NCKX2-mediated Ca^{2+} extrusion inactivates upon exposure to high $[Na^+]_i$

The observable difference between $[Ca^{2+}]_i$ clearance of NCKX2 transfected HEK293 cells that had been treated with Tg versus non-treated, led to the question of whether some other cellular Ca^{2+} handling mechanism may be contributing to our free $[Ca^{2+}]_i$ measurements. Hence, we tested the effects of FCCP, which is a proton ionophore that is commonly used to collapse the proton gradient across membranes, especially the inner mitochondrial membrane which maintains a large proton gradient and a resultant

Fig. 5. Scanning of NCKX2 single amino acid substitution mutants for shifts in apparent Na^+-affinity. **A-E.** Representative data of wild-type NCKX2-mediated Na^+-induced rises in free $[Ca^{2+}]_i$, and some substitution mutants of relatively conserved NCKX amino acids. For each panel, a single suspension of HEK293 cells transiently transfected with wild-type NCKX2 (top left panel) or the indicated amino acid substitution construct, was assayed as described in MATERIALS AND METHODS and legend of Fig. 4; the assay medium was 150 mM KCl/100 μM EDTA buffer, with 350 μM Ca^{2+} added 30 s prior to Na^+ addition. The family of traces illustrated for each construct were compiled from the individual measurements for each indicated Na^+ concentration; the 0 mM Na^+ trace was measured in the absence of added Na^+ (after the addition of 250 μM free Ca^{2+} alone). The HEK293 cells, in addition to 2 μM gramicidin, were treated with 0.4 μM thapsigargin and 10 μM KB-R7943. Constructs indicated by * were additionally treated with 2 μM carbonyl cyanide *p*-trifluoromethoxyphenylhydrazone (FCCP). All free $[Ca^{2+}]_i$ measurements were made with fluo-3.

Fig. 5 A.

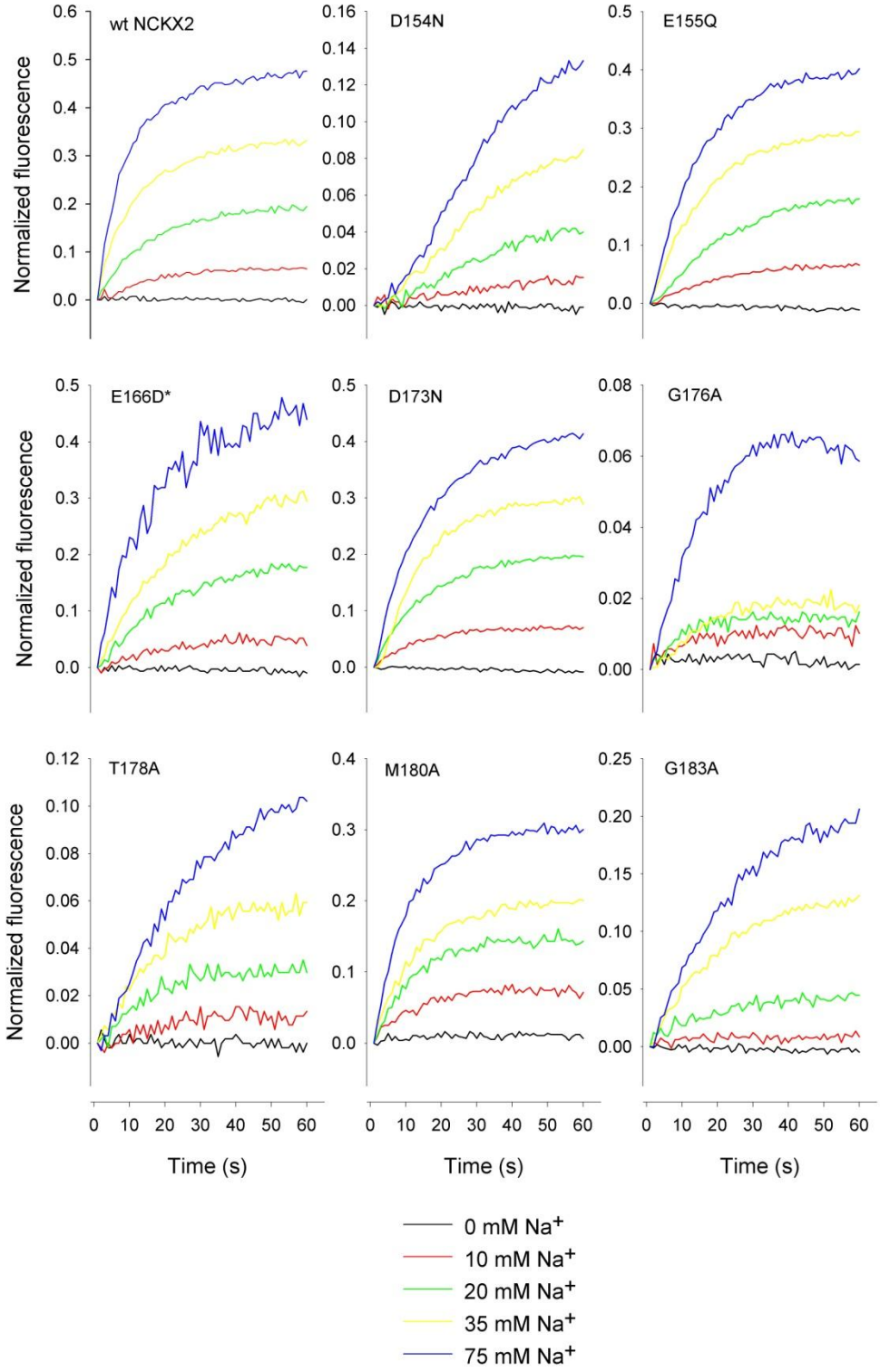
wt NCKX2
D154N
E155Q
E166D*
D173N
G176A
T178A
M180A
G183A
Normalized fluorescence
Time (s)
0 mM Na+
10 mM Na+
20 mM Na+
35 mM Na+
75 mM Na+

Fig. 5 B.

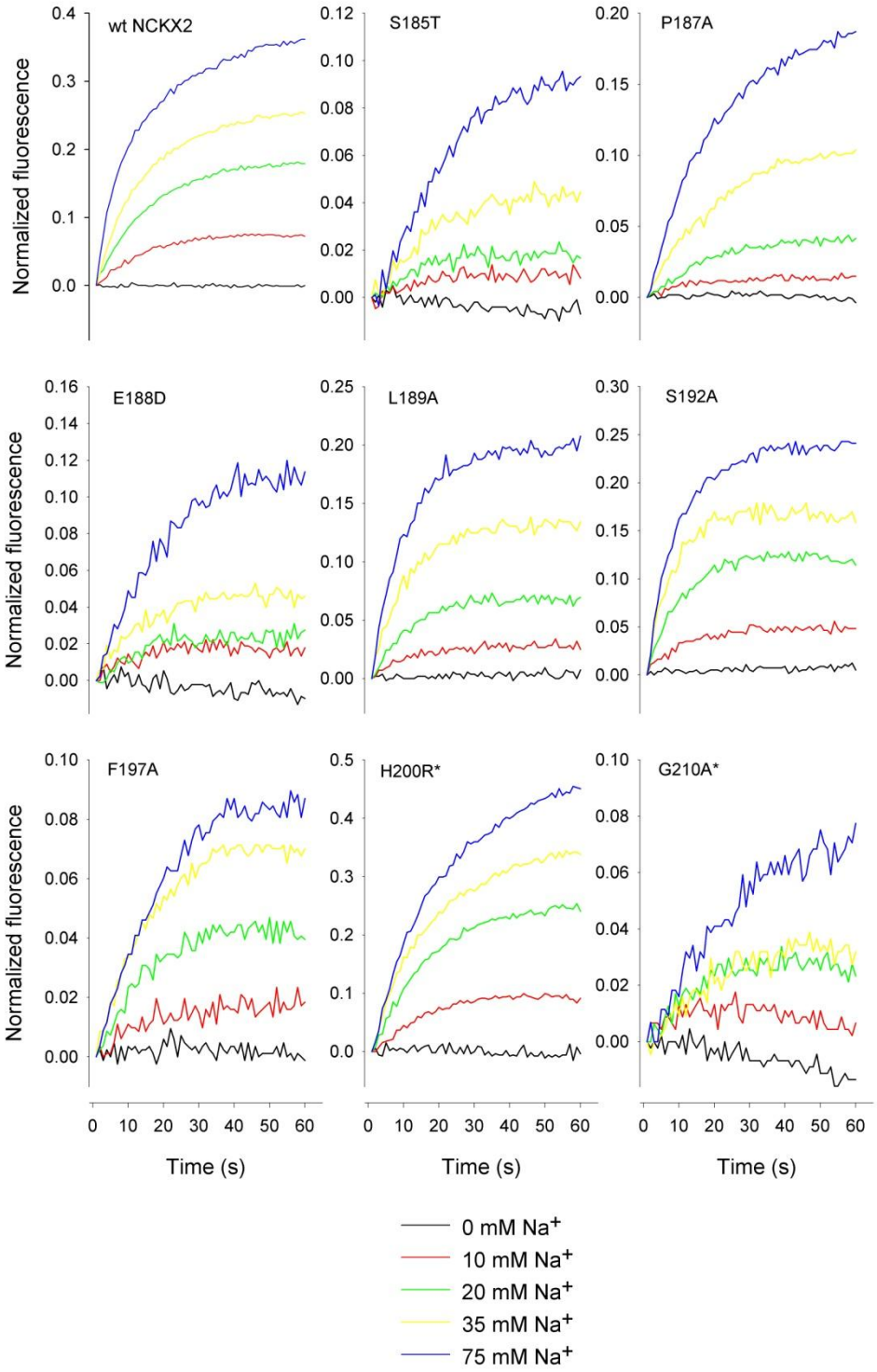
wt NCKX2
S185T
P187A
E188D
L189A
S192A
F197A
H200R*
G210A*
Normalized fluorescence
Time (s)
0 mM Na+
10 mM Na+
20 mM Na+
35 mM Na+
75 mM Na+

Fig. 5 C.

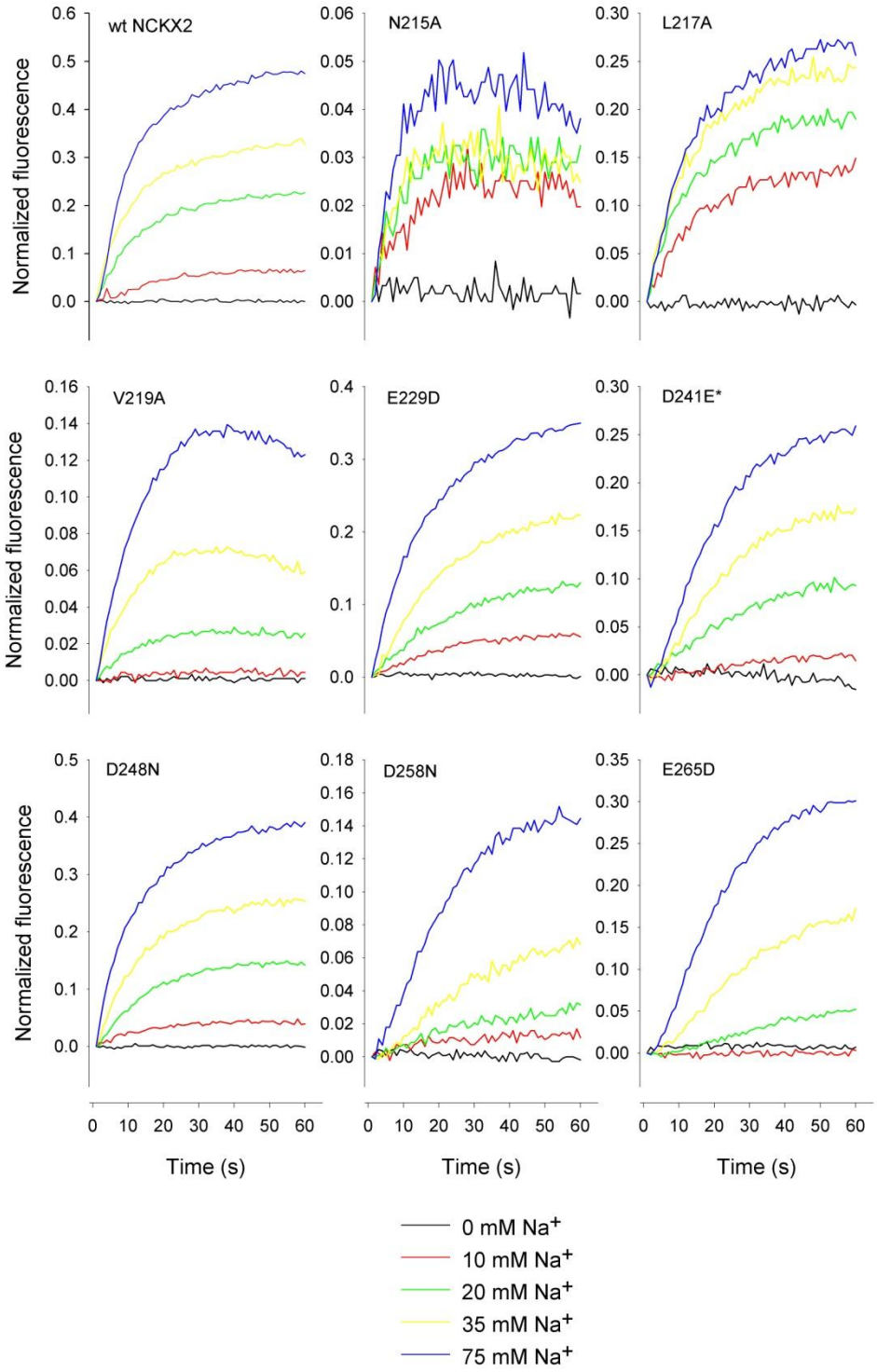
wt NCKX2
N215A
L217A
V219A
E229D
D241E*
D248N
D258N
E265D
Normalized fluorescence
Time (s)
0 mM Na+
10 mM Na+
20 mM Na+
35 mM Na+
75 mM Na+

Fig. 5 D.

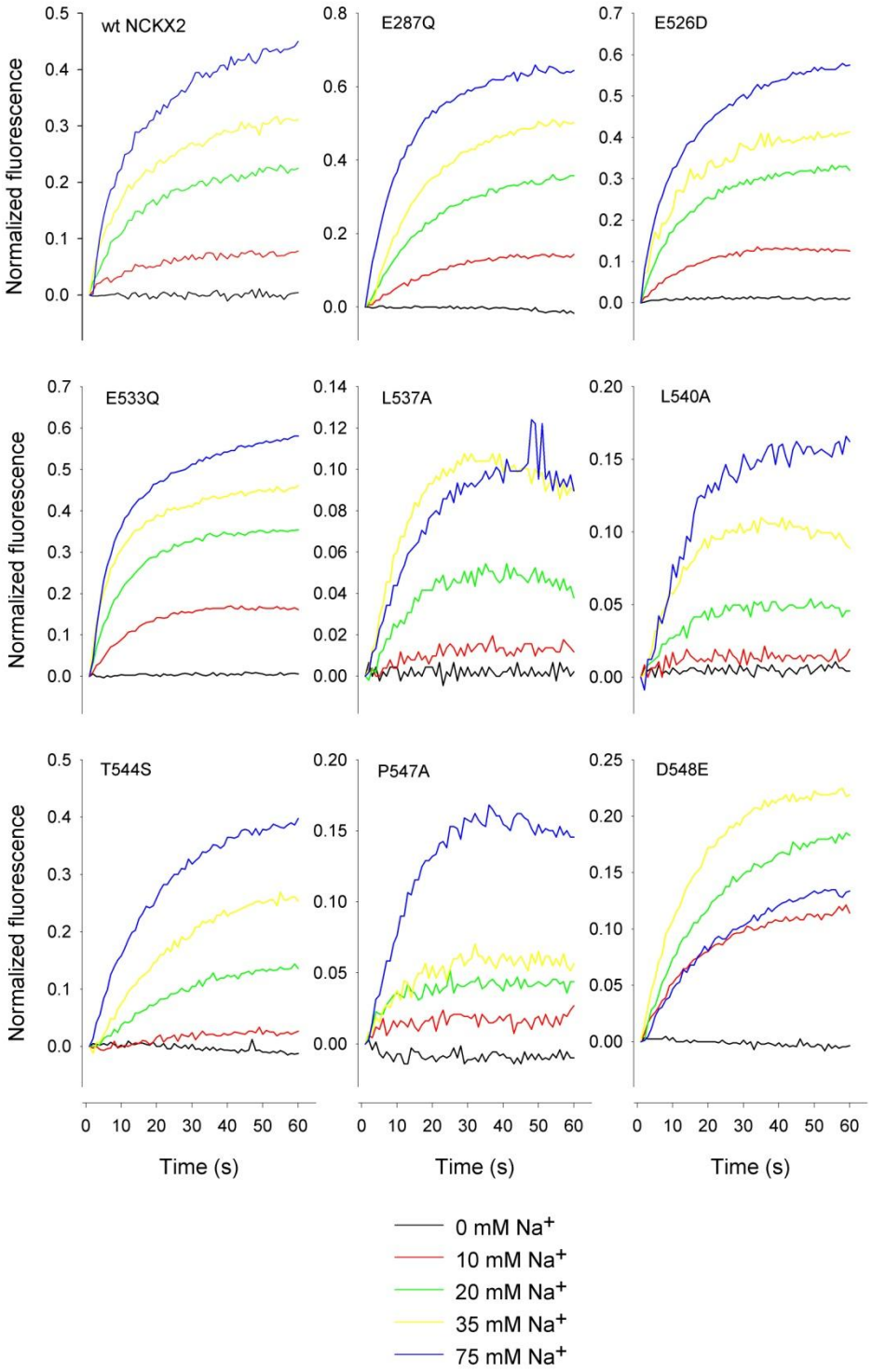
wt NCKX2
E287Q
E526D
E533Q
L537A
L540A
T544S
P547A
D548E
Normalized fluorescence
Time (s)
0 mM Na+
10 mM Na+
20 mM Na+
35 mM Na+
75 mM Na+

Fig. 5 E.

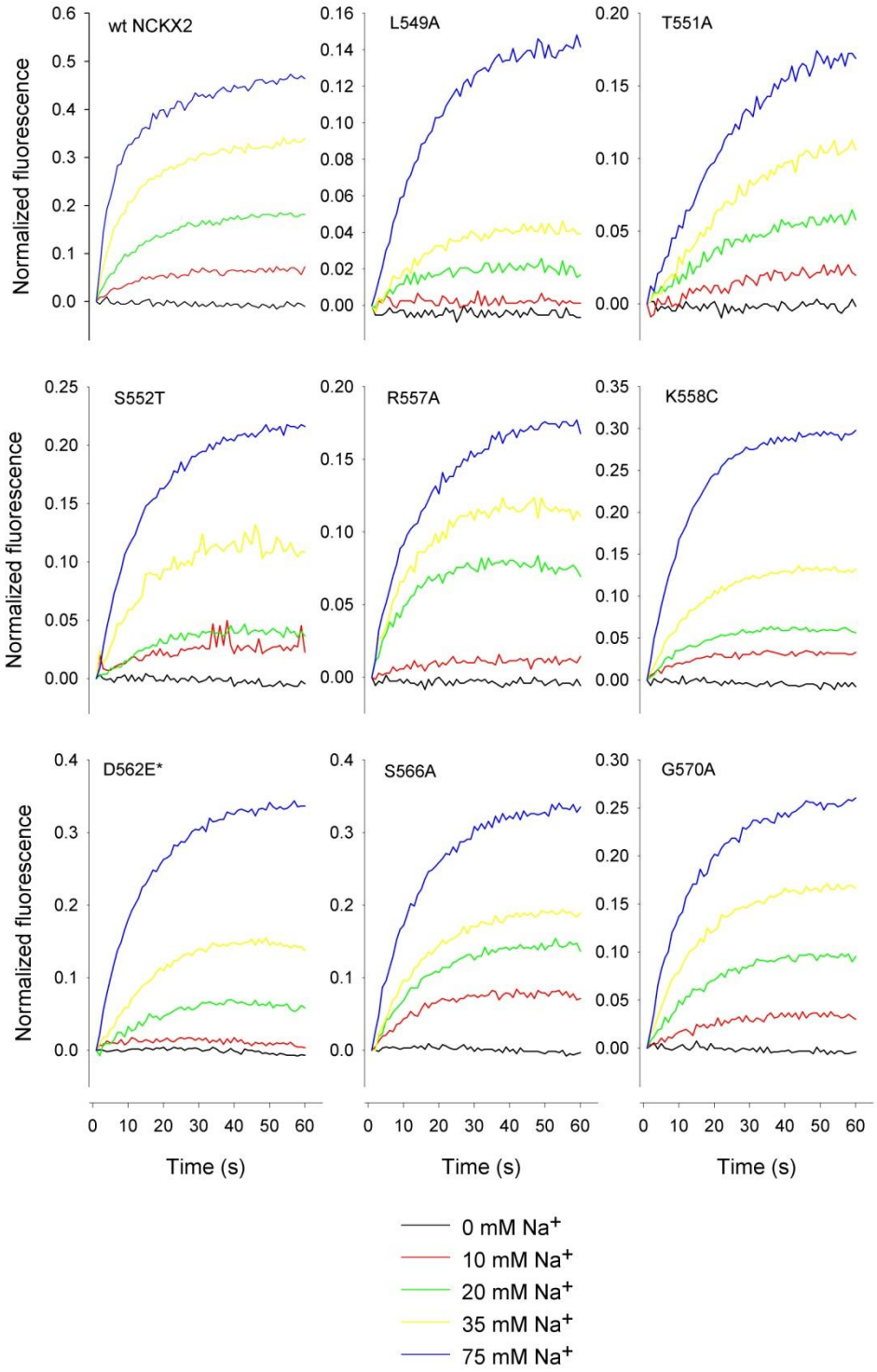
wt NCKX2
L549A
T551A
S552T
R557A
K558C
D562E*
S566A
G570A
Normalized fluorescence
Time (s)
0 mM Na+
10 mM Na+
20 mM Na+
35 mM Na+
75 mM Na+

Fig. 5 F.

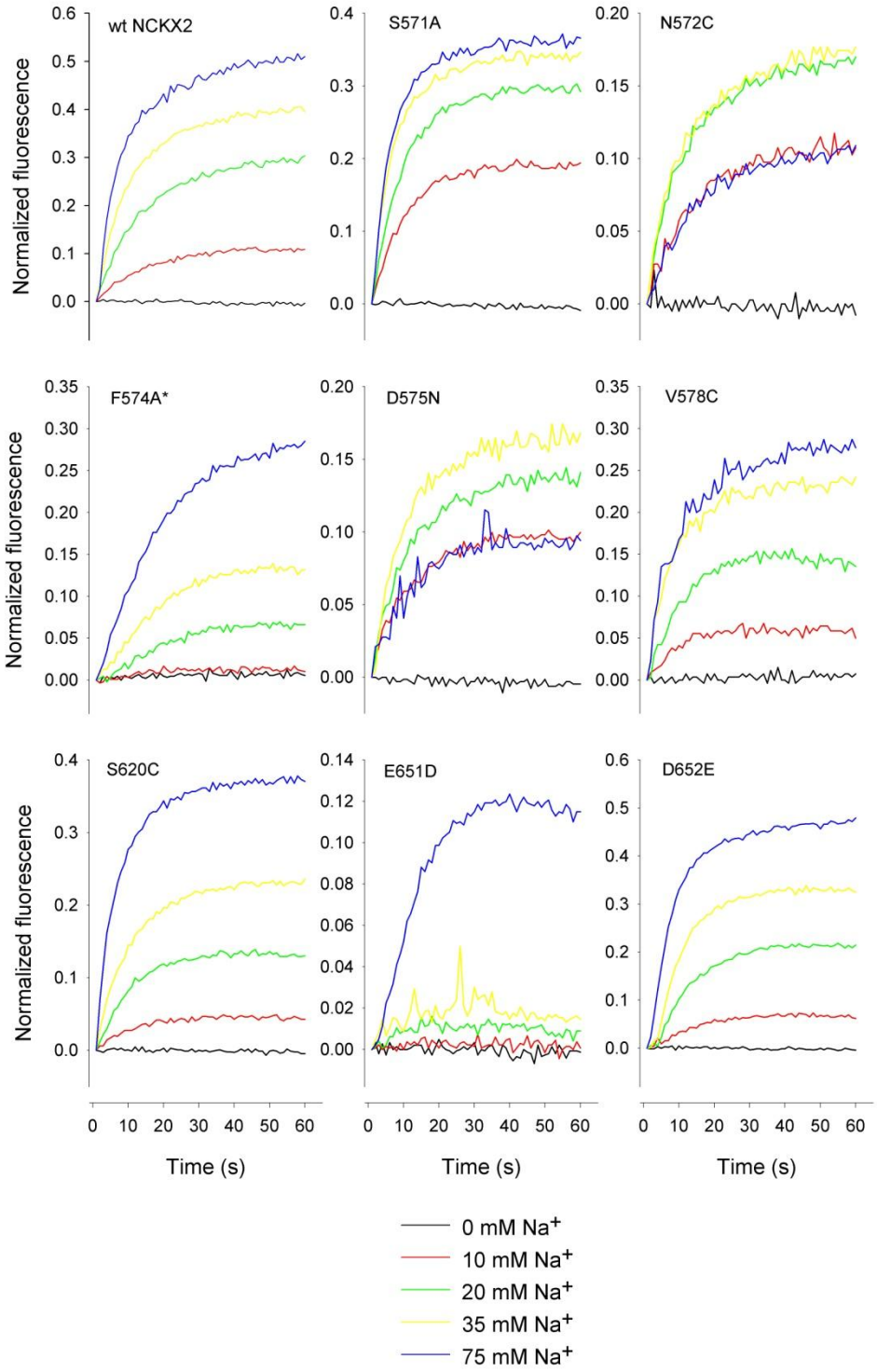
wt NCKX2
S571A
N572C
F574A*
D575N
V578C
S620C
E651D
D652E
Normalized fluorescence
Time (s)
0 mM Na+
10 mM Na+
20 mM Na+
35 mM Na+
75 mM Na+

inside-negative potential, in turn necessary for the Ca^{2+}-uniporter of mitochondria to accumulate Ca^{2+} from the cytoplasm. When NCKX2 transfected HEK293 cells were additionally pretreated with 2 μM FCCP (at the same time as gramicidin and Tg), the initial NCKX2-mediated $[Ca^{2+}]_i$ rise appeared to be significantly higher for each $[Na^+]$ tested. More strikingly, at the time point when the Ca^{2+} gradient was reversed with cuvette addition of EDTA to engage $[Ca^{2+}]_i$ extrusion through NCKX2, it appeared that with $[Na^+]$ up to 35 mM, $[Ca^{2+}]_i$ was cleared effectively back to baseline (note, however, the apparent slowing of the $[Ca^{2+}]_i$ clearance rate in the case of the 35 mM Na^+ trace), except in the case of 75 mM Na^+. In the measurement where 75 mM Na^+ was used to load the NCKX2 transfected HEK293 cells with Ca^{2+}, the kinetics of $[Ca^{2+}]_i$ clearance were markedly different, in that the trace appeared as a slow drift towards baseline, as opposed to displaying a short phase of rapid Ca^{2+} efflux followed by an abrupt decrease in clearance rate as in Fig. 6 A or B. In fact, in many cases, the $[Ca^{2+}]_i$ levels did not reach baseline even after more than 2 min of fluorescence recording subsequent to EDTA addition (see examples in Fig. 9). The results obtained with NCKX2 transfected HEK293 cells that were treated with FCCP suggested that mitochondria were a potentially interfering mechanism in our free $[Ca^{2+}]_i$ measurements. Mitochondria are known to be a major intracellular Ca^{2+} clearance mechanism, especially when $[Ca^{2+}]_i$ reaches relatively high levels in the μM range (David and Barrett 2000; Kim *et al*. 2005). Another question that this observation raised was whether the $[Ca^{2+}]_i$ probe we were using – fluo-3, was being saturated by what appeared to be high levels of NCKX2-mediated $[Ca^{2+}]_i$ loading in cells pretreated with FCCP? This was evident when examining the difference in kinetics of both the initial rise phase of $[Ca^{2+}]_i$, and more so the $[Ca^{2+}]_i$ clearance phase.

3. 4. NCKX2-mediated Ca^{2+} fluxes are large, necessitating the use of low affinity Ca^{2+} probe

To address the question of $[Ca^{2+}]_i$ probe saturation, we used fluo-4FFAM (Molecular Probes), another cell-permeable $[Ca^{2+}]_i$ probe derived from the parent fluo-3 molecule. The K_m values for Ca^{2+} of fluo-3 and fluo-4FF as reported by Molecular Probes are 0.325 μM and 9.7 μM respectively. A suspension of NCKX2 transfected HEK293 cells

Fig. 6. Examination of Ca^{2+} extrusion mode of NCKX2, and relation to $[Na^{+}]$ and cellular Ca^{2+} handling mechanisms. **A.** fluo-3 loaded NCKX2 transfected HEK293 cells were assayed for Na^{+}-affinity, and Ca^{2+} extrusion mode examined as described in MATERIALS AND METHODS and legend of Fig. 4, except without addition of thapsigargin (Tg). NCKX2 Ca^{2+} influx mode was initiated by addition of the indicated Na^{+} at the upward pointing arrow, in 150 mM KCl buffer with 250 μM free Ca^{2+}. NCKX2 Ca^{2+} extrusion mode was initiated by the addition of 1 mM EDTA at the downward pointing arrow. **B.** Same conditions as in **A**, but with addition of 0.4 μM Tg. **C.** Same conditions as in **A**, but with addition of 0.4 μM Tg, and 2 μM FCCP. Results obtained in **A-C** were representative of three other separate experiments.

Fig. 6.

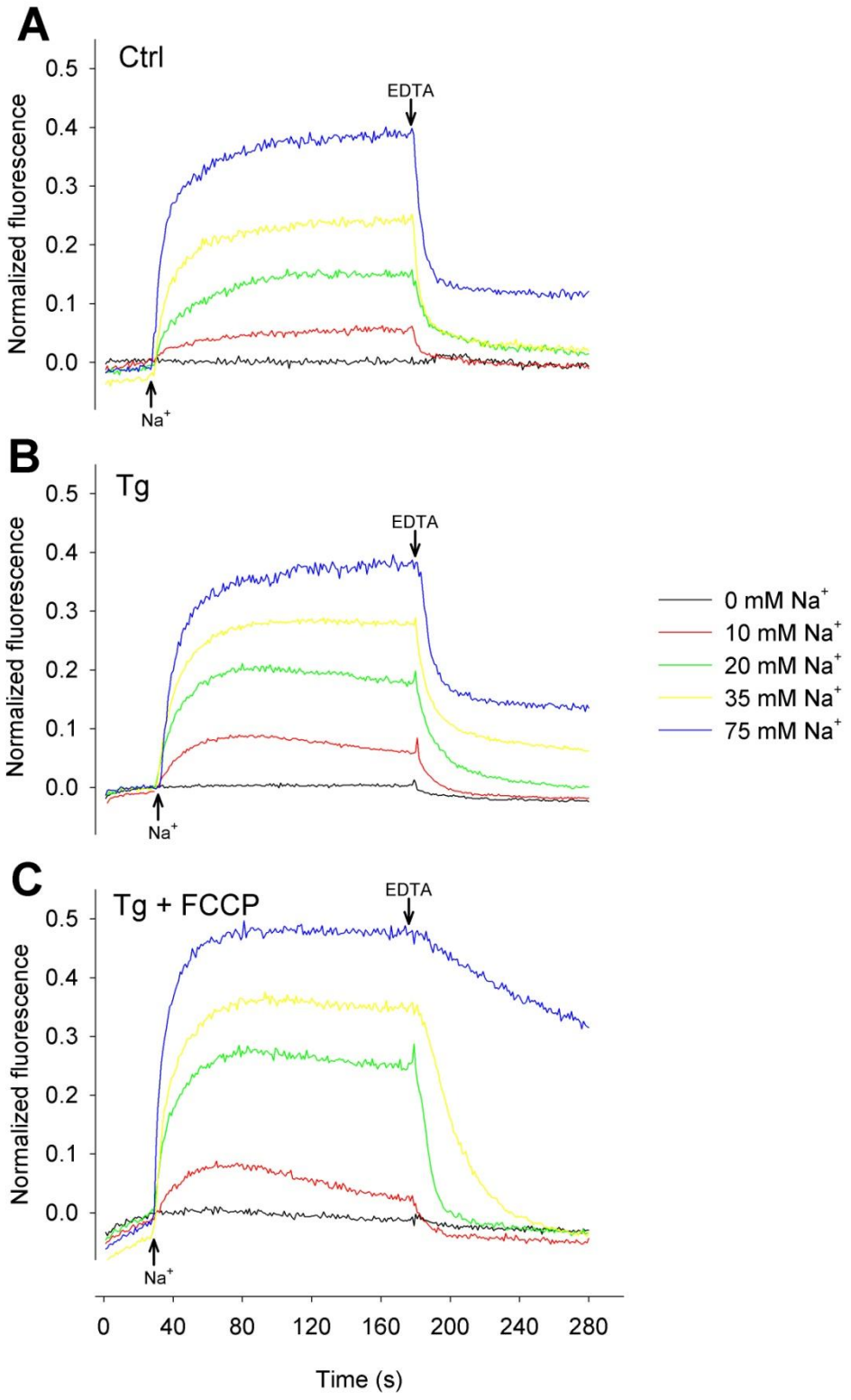
A
Ctrl
EDTA
Normalized fluorescence
0.5
0.4
0.3
0.2
0.1
0.0
Na+
B
Tg
EDTA
Normalized fluorescence
0.5
0.4
0.3
0.2
0.1
0.0
Na+
C
Tg + FCCP
EDTA
Normalized fluorescence
0.5
0.4
0.3
0.2
0.1
0.0
Na+
0
40
80
120
160
200
240
280
Time (s)
0 mM Na+
10 mM Na+
20 mM Na+
35 mM Na+
75 mM Na+

was split into two portions, each loaded separately, one with 2 μM fluo-3, the other with 2 μM fluo-4FF. The experimental measurements shown in Fig. 7 A compare $[Ca^{2+}]_i$ rise and clearance through NCKX2 tranfected HEK293 cells loaded with the high affinity Ca^{2+} probe fluo-3, and the low affinity probe fluo-4FF, using identical ionic conditions (250 μM free Ca^{2+} in the cuvette, and Na^+/Ca^{2+} exchange engaged by the addition of 75 mM Na^+ in KCl-EDTA medium). Notice the slower initial rate of $[Ca^{2+}]_i$ rise in fluo-4FF loaded cells, and the subsequent faster clearance as compared to fluo-3 loaded cells. The bottom panel (Fig. 7 B) illustrates more clearly that the fluo-3 Ca^{2+} probe is amenable to saturation under these assay conditions; in this experiment, free $[Ca^{2+}]_o$ added to the cuvette was only 10 μM (buffered by adding a mixture of 1 mM HEDTA and 8 mM CaHEDTA to the cuvette). In this case, $[Ca^{2+}]_i$ clearance was rapid even after applying 75 mM Na^+; this will be addressed further in experiments discussed below. Note that in the measurements illustrated in Fig. 7, the NCKX2 transfected HEK293 cells were pretreated with both 0.4 μM Tg and 2 μM FCCP. All subsequent measurements were made with fluo-4FF, unless otherwise indicated.

3. 5. Interplay between NCKX2 and Ca^{2+} handling mechanisms endogenous to HEK293 cells

With a more suitable tool to measure the large changes in free $[Ca^{2+}]_i$, we next attempted to more thoroughly examine and quantify the contribution of the various endogenous Ca^{2+} handling mechanisms of HEK293 cells to free $[Ca^{2+}]_i$ rise mediated by NCKX2. Fig. 8 illustrates measurements made from the same suspension of NCKX2 transfected HEK293 cells, tested with 250 μM $[Ca^{2+}]_o$ and 75 mM Na^+. The conditions compared were: Ctrl, where the HEK293 cells were only treated with gramicidin; Tg, cells were additionally treated with 0.4 μM Tg to inhibit SERCA; pH 8.8, the test medium in the cuvette was of the same composition as KCl-EDTA – but the buffer used was TAPS to maintain pH at 8.8 to reduce Ca^{2+} clearance through PMCA; FCCP, cells were additionally treated with 2 μM FCCP to inhibit mitochondrial Ca^{2+} accumulation. The treatment that had the greatest effect on free $[Ca^{2+}]_i$ changes was FCCP, indicating that for the levels of free $[Ca^{2+}]_i$ changes mediated by NCKX2, mitochondria were the major competing Ca^{2+}

clearance mechanism. Elevation of the pH of the medium to pH 8.8, one of the proven methods for reducing PMCA activity since it requires extracellular H^+ in extruding intracellular Ca^{2+}, also increased the magnitude of $[Ca^{2+}]_i$ changes, suggesting that perhaps PMCA may be another effective competitor for clearance of $[Ca^{2+}]_i$ (Chen *et al*. 2003; Wennemuth *et al*. 2003; Duman *et al*. 2008). However, the result with elevated medium pH must be regarded with prudence; although the manipulation is expected to decrease PMCA activity to ~20% of PMCA activity at pH 7.4, the increase in medium pH is also expected to simultaneously increase the activity of NCKX2; thus it is difficult to judge whether the increase in free $[Ca^{2+}]_i$ levels attained in the pH 8.8 medium are a result of disabling the Ca^{2+} clearance capability of PMCA, or simply an enhancement of $[Ca^{2+}]_i$ elevation mediated by NCKX2 (Schnetkamp 1995a; Xu *et al*. 2000). Therefore, we chose not to carry out our assay in high pH media, especially considering that with the use of gramicidin that would lead to strong alkalinization of the cytoplasm. In Fig. 8 B, the extent to which the competing Ca^{2+} clearance mechanisms contribute to the rise phase of free $[Ca^{2+}]_i$ was quantified by measurement of the steady-state free $[Ca^{2+}]_i$ plateau attained with 250 μM free $[Ca^{2+}]_o$ and the addition of 75 mM Na^+. Although cells pretreated with Tg exhibited higher plateau levels of free $[Ca^{2+}]_i$, the result was not statistically significant from the plateau of free $[Ca^{2+}]_i$ attained with cells not treated with Tg ($P>0.05$, student's t-test). On the other hand, cells pretreated with both FCCP and Tg exhibited significantly elevated free $[Ca^{2+}]_i$ ($P<0.05$, student's t-test) from non-treated cells, and hence all subsequent measurements were carried out on cells pretreated with both Tg and FCCP (unless otherwise indicated).

3. 6. Examining the time-course of the development of NCKX2 Na^+_i-dependent inactivation

Even with the use of the low affinity Ca^{2+} probe fluo-4FF, it became evident that Ca^{2+} fluxes mediated by NCKX2 were not completely reversible – at least under certain conditions. The results from Fig. 6 C, although measured with high affinity fluo-3, indicated that when $[Na^+]$ in the medium was high (75 mM), NCKX2 became ineffective in clearing the Ca^{2+} load from HEK293 cells; this is also evident when measured with fluo-

Fig. 7. Comparison of NCKX2-mediated free $[Ca^{2+}]_i$ fluxes when measured with fluo-3 and fluo-4FF. NCKX2 transfected HEK293 cells were loaded with the indicated Ca^{2+} probe (black trace, fluo-3; grey trace, fluo-4FF), and assayed as described in legend of Fig. 4 – cells, in addition to 2 μM gramicidin treatment, were additionally treated with 0.4 μM Tg, and 2 μM FCCP. **A.** 75 mM Na^+ was added to cuvette containing 150 mM KCl buffer in the presence of 250 μM free $[Ca^{2+}]_o$. **B.** 75 mM Na^+ was added to cuvette containing 150 mM KCl buffer in the presence of 10 μM free $[Ca^{2+}]_o$ (buffered by the addition of 1 mM *N*-(2-hydroxyethyl)ethylenediaminetriacetic acid (HEDTA) and 8 mM CaHEDTA). Portions of this figure were adapted from Altimimi and Schnetkamp (2007).

Fig. 7.

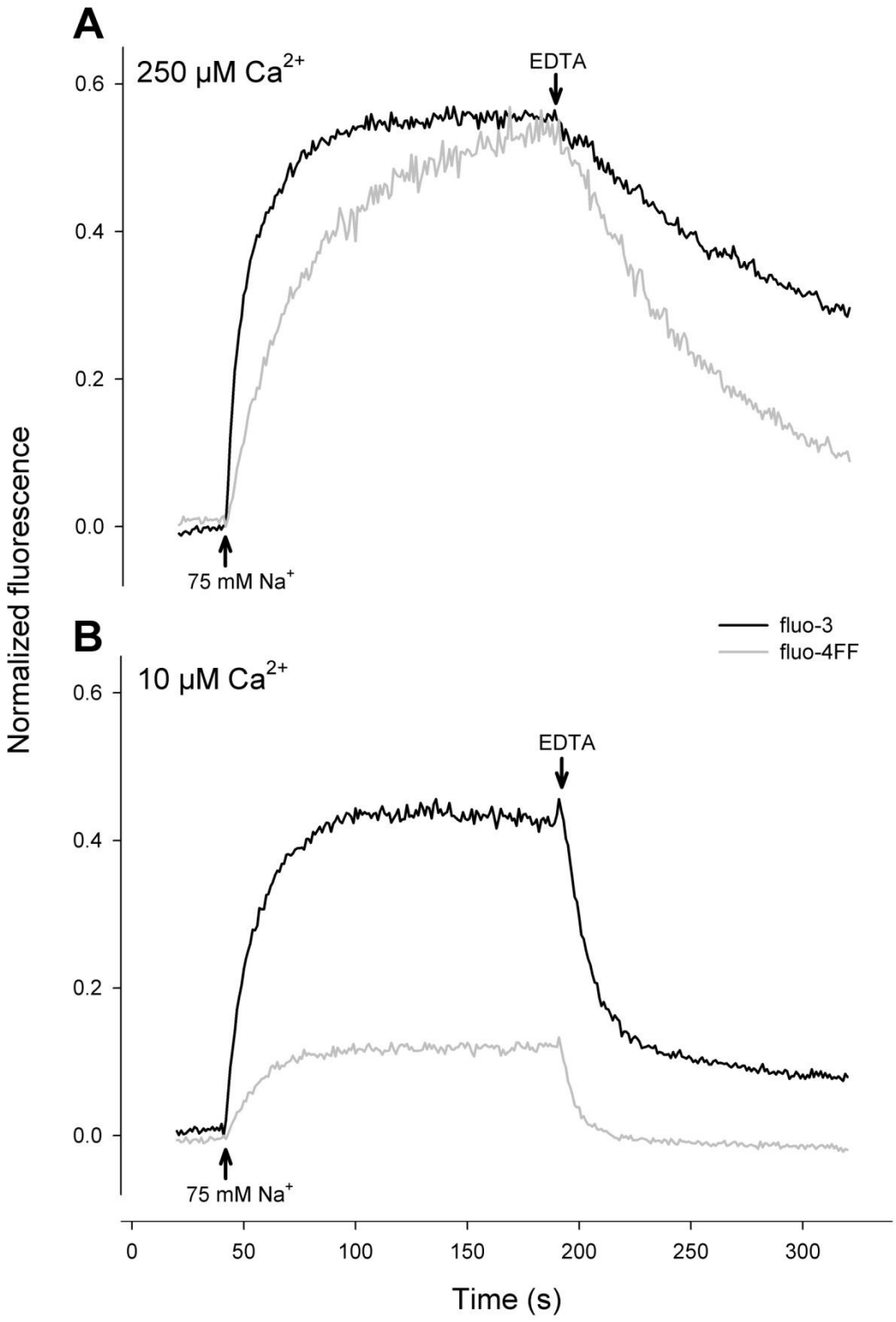
A
250 μM Ca2+
EDTA
0.6
0.4
0.2
0.0
75 mM Na+
B
10 μM Ca2+
EDTA
0.6
0.4
0.2
0.0
75 mM Na+
fluo-3
fluo-4FF
Normalized fluorescence
0
50
100
150
200
250
300
Time (s)

Fig. 8. Influence of cellular Ca^{2+} handling mechanisms on NCKX2-mediated changes in free $[Ca^{2+}]_i$. **A.** NCKX2 transfected HEK293 cells were assayed as described in legend of Fig. 4 – cells, aside from 2 μM gramicidin treatment, were: Ctrl, not additionally treated with other pharmacological agents; Tg, additionally treated with 0.4 μM Tg; pH 8.8, placed in 150 mM KCl/100 μM EDTA buffer medium adjusted to pH 8.8 (buffered with 3-[tris(hydroxymethyl)methyl]aminopropanesulfonic acid (TAPS)); FCCP, additionally treated with 2 μM FCCP. The upward pointing arrow indicates addition of 75 mM Na^+ (30 s subsequent to addition of 250 μM free $[Ca^{2+}]_o$), and the downward pointing arrow indicates addition of 1 mM EDTA. Data illustrated are representative of three other experiments. **B.** Summary data of effects of the additional treatments of either 0.4 μM Tg alone (Tg) or the combination of 0.4 μM Tg and 2 μM FCCP (Tg + FCCP) on $[Ca^{2+}]_i$ levels (compared at time point of 60 s after addition of Na^+) attained with NCKX2 transfected HEK293 cells after the addition of 75 mM Na^+ in the presence of 250 μM $[Ca^{2+}]_o$, compared to NCKX2 transfected HEK293 cells treated with gramicidin alone (Ctrl). Free Ca^{2+} measurements were made with fluo-4FF. Data are the means of the number of measurements indicated by parentheses above each bar, plus SD. * Indicates significantly greater than Ctrl ($P < 0.05$, student's t-test).

Portions of this figure were adapted from Altimimi and Schnetkamp (2007).

Fig. 8.

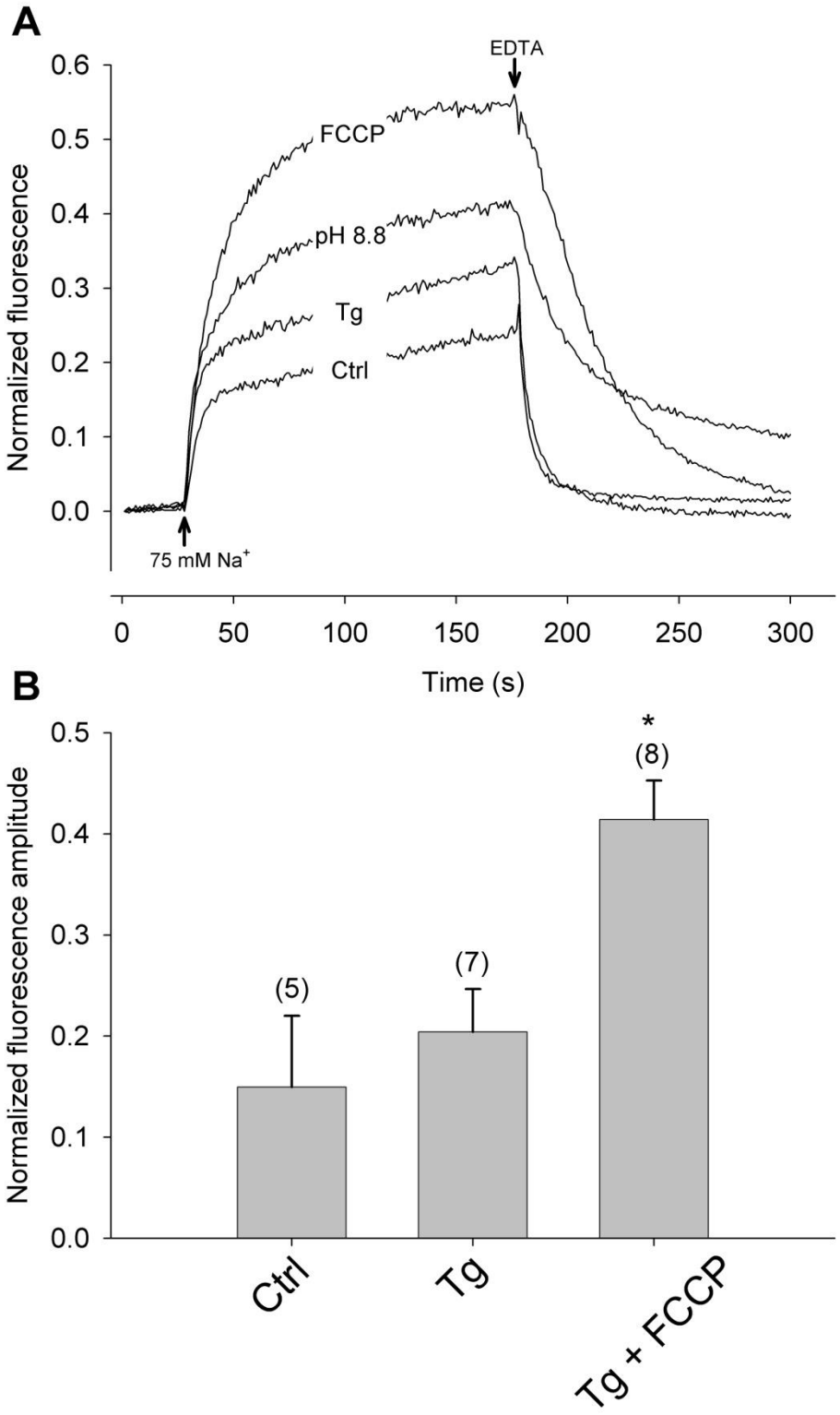
A
EDTA
FCCP
pH 8.8
Tg
Ctrl
75 mM Na+
Normalized fluorescence
0.0
0.1
0.2
0.3
0.4
0.5
0.6
0
50
100
150
200
250
300
Time (s)
B
Normalized fluorescence amplitude
0.0
0.1
0.2
0.3
0.4
0.5
(5)
(7)
*
(8)
Ctrl
Tg
Tg + FCCP

4FF as in Fig. 7 A, where again the cells were loaded with Ca^{2+} via NCKX2 by the addition of 75 mM Na^+. These results could be interpreted to reflect a true inactive kinetic state of NCKX2 under such ionic conditions, but an alternative explanation could be competitive inhibition. The use of gramicidin to clamp Na^+ concentrations across the membrane was a necessity, so as to obtain a concentration-response relationship in gauging the affinity of NCKX2 for Na^+ (the Na^+ acting on the cytoplasmic ion binding sites of the exchanger to drive Ca^{2+} influx). However, when the Ca^{2+} gradient is reversed by the addition of 1 mM EDTA to the cuvette, it is possible that the cytoplasmic configuration liganding sites were ineffective in binding and transporting intracellular Ca^{2+} because of the high $[Na^+]_i$ used to drive Ca^{2+} influx in the first place, i.e. there are potentially competitive interactions between Na^+ and Ca^{2+}. To begin to address this question, the experiments in Fig. 9 were carried out to examine the time-course of the development of NCKX2 inactivation. In Fig. 9 A, NCKX2 transfected HEK293 cells were loaded with Ca^{2+} by adding 250 μM free Ca^{2+} to the cuvette, followed by the addition of 75 mM Na^+. In separate experimental measurements, the time from Na^+ addition (Ca^{2+} loading) to EDTA addition was varied. In the trace where EDTA was added at the 180 s time point (150 s following Na^+ addition), Ca^{2+} clearance was slow (as shown in previous figures, e.g. Fig. 6 C, and 7 A). However when EDTA was added at earlier time points, the Ca^{2+} clearance rates were much more rapid; in fact, very little inactivation was apparent when EDTA was added 20 s or 40 s following Na^+ addition. This clear time-dependence of inactivation argues against competition between Na^+ and Ca^{2+} as the sole factor in what otherwise may be interpreted as the "apparent" inactivation of NCKX2. This is because competitive interactions would not be expected to be time-dependent; the same concentration of Na^+ was present for the trace where EDTA was added at 20 s or 150 s following Na^+ addition, but the clearance rates were markedly different. Although, arguably the $[Ca^{2+}]_i$ at the different time points discussed may be different, such that in experimental traces where Ca^{2+} was loaded into the cells for prolonged periods of time, much higher actual $[Ca^{2+}]_i$ levels were reached that was not registered by fluo-4FF because it might have become saturated at such high $[Ca^{2+}]_i$ levels. The results in Fig. 9 C however dispute this last argument; these two experimental traces were carried out with another Molecular Probes Ca^{2+} fluorophore (fluo-5N) with an even lower affinity for Ca^{2+} than that of fluo-4FF – 90 μM as reported by Molecular

Probes. Note that the amplitude of the $[Ca^{2+}]_i$ plateau in the two traces of Fig. 9 C are the same, and there is no run-up with the trace where Ca^{2+} was loaded for a longer period of time before the addition of EDTA, also note the different ordinate scales of normalized fluorescence between Fig. 9 A and C indicating that the changes in free $[Ca^{2+}]_i$ registered with fluo-5N were considerably lower. Yet, when 1 mM EDTA was added, nevertheless, there was a difference in the rate of Ca^{2+} clearance, with the rate being slower when Ca^{2+} loading (or Na^+ exposure) was prolonged (illustrated more clearly in the inset of Fig. 9 C, where the prolonged $[Ca^{2+}]_i$ loading trace was protracted to coincide the time points of EDTA addition).

As indicated by Fig. 6 C, NCKX2 inactivation only occurred with the highest $[Na^+]$ tested (75 mM), whereas there was no apparent inactivation with 20 mM Na^+, and perhaps only slight with 35 mM Na^+. Therefore, we used these lower concentrations as controls to investigate the time-dependence of inactivation. Fig. 9 B illustrates the same set of measurements as illustrated in Fig. 9 A, except Ca^{2+} loading was achieved by the addition of 35 mM Na^+. On the fluo-4FF normalized scale, the amplitude of free $[Ca^{2+}]_i$ reached with the addition of 35 mM Na^+ was 60-70% of that reached with 75 mM Na^+, yet, in most measurements, there did not appear to be appreciable inactivation, as judged by a decrease in the slope of $[Ca^{2+}]_i$ extrusion as the time to EDTA addition was prolonged. There does appear to be some slowing of the $[Ca^{2+}]_i$ extrusion rate with the experimental trace in which the NCKX2 transfected HEK293 cells were exposed to 35 mM Na^+ for 300 s; however, the extrusion rate is nevertheless much more rapid when compared to the equivalent experimental trace in Fig. 9 A. Similar results were obtained when these measurements were made with 20 mM Na^+ (Altimimi and Schnetkamp 2007).

Since our results suggested that NCKX2 mediated continuous Ca^{2+} influx under the conditions of our assay, and that mitochondria were the major Ca^{2+} sequestration mechanism, we evaluated the changes in the mitochondrial Ca^{2+} pool. The expectation was that the longer the NCKX2 transfected HEK293 cells were maintained under conditions that promote NCKX2-mediated Ca^{2+} influx, the larger the mitochondrial Ca^{2+} pool would become. Fig. 9 D illustrates a set of measurements made from one suspension of NCKX2 transfected HEK293 cells, which were treated identically to cells in Fig. 9 A, except FCCP

Fig. 9. Time course of development of NCKX2 inactivation. **A.** fluo-4FF loaded NCKX2 transfected HEK293 cells were treated as in legend of Fig. 4 – cells, aside from 2 μM gramicidin treatment, were additionally treated with 0.4 μM Tg, and 2 μM FCCP. NCKX2 Ca^{2+} influx mode was initiated at the upward pointing arrow by addition of 75 mM Na^+ to cuvette containing 150 mM KCl buffer in the presence of 250 μM free $[Ca^{2+}]_o$. NCKX2 Ca^{2+} extrusion was initiated by the addition of 1 mM EDTA at various time points thereafter, indicated by the downward pointing arrow; traces were from separate cuvettes, overlaid for illustration. Data are representative of three other experiments. **B.** Same experimental conditions as in **A**, but with addition of 35 mM Na^+ (in place of 75 mM Na^+). Data are representative of three other experiments. **C.** fluo-5N loaded NCKX2 transfected HEK293 cells were treated as in **A**. The inset highlights the time-dependent difference in Ca^{2+} extrusion kinetics by juxtaposing the two traces at time of 1 mM EDTA addition (the interleaving normalized fluorescence measurements of the longer trace were deleted). **D.** fluo-4FF loaded NCKX2 transfected HEK293 cells were treated as in **A**, except without prior treatment with FCCP. 2 μM FCCP was added 10 s following the initiation of Ca^{2+} extrusion mode of NCKX2 (by the addition of 1 mM EDTA), as indicated by the upward pointing arrowheads. Data are representative of three other experiments.
Portions of this figure were adapted from Altimimi and Schnetkamp (2007).

Fig. 9.

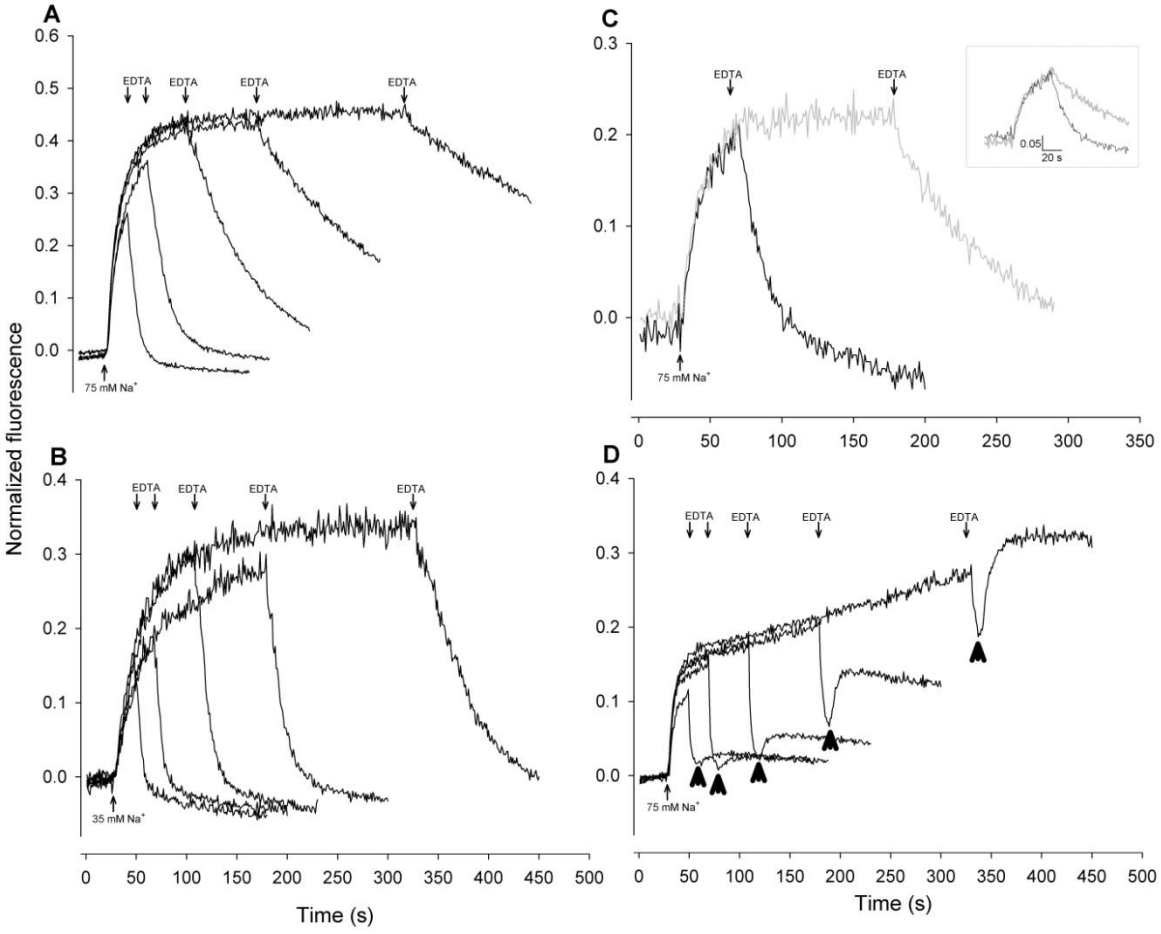
A
B
C
D
EDTA
75 mM Na+
35 mM Na+
0.05
20 s
Normalized fluorescence
Time (s)

was not added at the same time as gramicidin and Tg. Ten seconds following the time point when 1 mM EDTA was added to each cuvette, 2 μM FCCP was added on the trace so as to collapse the inner mitochondrial membrane potential and allow the accumulated Ca^{2+} to leak back to the cytosol. Indeed, it proved that the Ca^{2+} release induced by the addition of FCCP became larger, as the time that NCKX2 was allowed to load the cells with Ca^{2+} was extended.

3. 7. NCKX2 Na^{+}_{i}-dependent inactivation requires saturating $[Ca^{2+}]_o$, but not high $[Ca^{2+}]_i$

The results discussed thus far indicate that the NCKX2 inactivation process required prolonged exposure (> 40 s) of the cytoplasmic configuration of the exchanger to high Na^+ (> 35 mM). However, in all measurements illustrated thus far, high $[Na^+]$ was always coupled to large increase in $[Ca^{2+}]_i$ mediated by NCKX2. We sought to devise some measurements that would allow us to separate the two effects – the high intracellular Na^+ from high intracellular Ca^{2+}. The experiment illustrated in Fig. 10 A illustrates two measurements made from the same suspension of fluo-3 loaded NCKX2 transfected HEK293 cells. In one experimental trace, an aliquot of the cells was placed in a cuvette containing KCl-EDTA (the standard cuvette medium used in all our experiments) and the cells were loaded with Ca^{2+} by the addition of 250 μM free Ca^{2+} to the cuvette, followed by 20 mM NaCl (as per protocol established, the cells had been pretreated with 2 μM gramicidin, 2 μM FCCP, and 0.4 μM Tg). After 150 s of exposure to 20 mM Na^+, EDTA was added to chelate external Ca^{2+} in the cuvette, and reverse the Ca^{2+} gradient to promote $[Ca^{2+}]_i$ extrusion through NCKX2. As illustrated previously in Fig. 6 C, this concentration of Na^+ – 20 mM – was not sufficient to produce inactivation, and NCKX2 was competent in rapidly clearing that $[Ca^{2+}]_i$ load. Another aliquot from the same suspension of cells was placed in a separate cuvette which contained 150 NaCl-EDTA medium (the same composition as KCl-EDTA or Li-EDTA, but with 150 mM NaCl iso-osmotically replacing KCl or LiCl). The cells were likewise pretreated with 2 μM gramicidin, 2 μM FCCP, and 0.4 μM Tg. In this case, however, Ca^{2+} loading was induced by the addition of 250 μM free Ca^{2+} to the cuvette (the same concentration of free Ca^{2+} used previously) followed by

the addition of 3 mM KCl – the final substrate ion required to initiate Na^+/Ca^{2+} exchange through NCKX2. Ca^{2+} loading in the case where the assay was carried out in NaCl-EDTA medium with addition of 250 μM $CaCl_2$, and 3 mM KCl reached $[Ca^{2+}]_i$ plateau ~2/3 the magnitude of the $[Ca^{2+}]_i$ plateau attained in KCl-EDTA medium. Nevertheless, when EDTA was added to the 150 mM NaCl-EDTA cuvette after 150 s of Ca^{2+} loading, NCKX2 was inactivated; it appeared there was a very short (2-3 s) phase of rapid Ca^{2+} clearance that subsequently and very abruptly subsided to a dramatically reduced rate of $[Ca^{2+}]_i$ clearance. This experiment illustrates that the condition of high Na^+ (150 mM in this case) was sufficient to produce inactivation, and that high $[Ca^{2+}]_i$ was not necessary, since $[Ca^{2+}]_i$ in the experiment carried out in NaCl-EDTA medium was lower than in the experiment carried out in KCl-EDTA.

To investigate the relationship between NCKX2 inactivation and $[Ca^{2+}]_o$, two measurements were made from the same suspension of NCKX2 transfected HEK293 cells, but with Ca^{2+} loading induced by the addition of different $[Ca^{2+}]_o$ to the cuvette (NaCl addition was kept the same at 75 mM; Fig. 10 B). In the case where 250 μM free $[Ca^{2+}]_o$ was added to the cuvette, followed by 75 mM NaCl, NCKX2 appeared to have inactivated when Ca^{2+} extrusion mode was engaged by the addition of EDTA to the cuvette 150 s following Ca^{2+} loading (as established previously in experiments illustrated in Fig. 6 C, 7A, 9). However, when less free $[Ca^{2+}]_o$ was added to the cuvette (10 μM buffered by HEDTA), there was no apparent inactivation when Ca^{2+} extrusion mode of NCKX2 was engaged by the addition of EDTA to the cuvette medium. Note that in the case where $[Ca^{2+}]_o$ was 10 μM, there was far less $[Ca^{2+}]_i$ driven into the cells via NCKX2; this would have potentially resulted in stronger competition by intracellular Na^+ versus intracellular Ca^{2+} as NCKX2 was extruding the $[Ca^{2+}]_i$ load. But the surprising result was that NCKX2 was competent in rapidly clearing the relatively small intracellular load of Ca^{2+} (despite exposure of the cytoplasmic configuration Ca^{2+} transport sites of NCKX2 to 75 mM Na^+). This result was particularly intriguing because, firstly, it again argues against competitive inhibition being the cause of our observations of diminished $[Ca^{2+}]_i$ clearance. Secondly, this result was somewhat reminiscent of results reported for Na^+-dependent inactivation of cardiac NCX1; inactivation in the case of NCX1, not only required exposure to high

Fig. 10. NCKX2 Na^+_i-dependent inactivation does not require high $[Ca^{2+}]_i$, but requires high $[Ca^{2+}]_o$. **A.** fluo-3 loaded NCKX2 transfected HEK293 cells were treated as in legend of Fig. 4 – cells, aside from 2 μM gramicidin treatment, were additionally treated with 0.4 μM Tg, and 2 μM FCCP. In one cuvette containing 150 mM KCl buffer, NCKX2-mediated Ca^{2+} influx was initiated by the addition of 20 mM Na^+ (upward pointing arrow) in the presence of 250 μM free $[Ca^{2+}]_o$ (grey trace). In the other cuvette containing 150 mM NaCl buffer (same composition as 150 mM KCl buffer, but with NaCl iso-osmotically replacing KCl – see text), NCKX2-mediated Ca^{2+} influx was initiated by the addition of 3 mM K^+ (upward pointing arrow) in the presence of 250 μM free $[Ca^{2+}]_o$ (black trace). NCKX2-mediated Ca^{2+} extrusion, was initiated by the addition of 1 mM EDTA to both cuvettes. **B.** fluo-4FF loaded NCKX2 transfected HEK293 cells were treated as in legend of Fig. 4 – cells, aside from 2 μM gramicidin treatment, were additionally treated with 0.4 μM Tg, and 2 μM FCCP. NCKX2-mediated Ca^{2+} influx was initiated at the upward pointing arrow by the addition of 75 mM Na^+ in a cuvette containing 150 mM KCl buffer with free $[Ca^{2+}]_o$ buffered to: 250 μM (black trace), or 10 μM (grey trace). NCKX2 mediated Ca^{2+} extrusion was initiated by the addition of EDTA to the cuvette at the downward pointing arrow (1 mM EDTA was added to the cuvette with 250 μM free $[Ca^{2+}]_o$; 5 mM EDTA was added to the cuvette with 10 μM free $[Ca^{2+}]_o$ since it contained a total of 8 mM Ca^{2+} buffered with HEDTA – see text for details). Inset juxtaposes the same traces, but with normalized fluorescence values obtained in experiment carried out in 10 μM free $[Ca^{2+}]_o$ scaled up to equate the $[Ca^{2+}]_i$ plateaus obtained in both traces, to highlight the difference in Ca^{2+} extrusion kinetics.

Portions of this figure were adapted from Altimimi and Schnetkamp (2007).

Fig. 10.

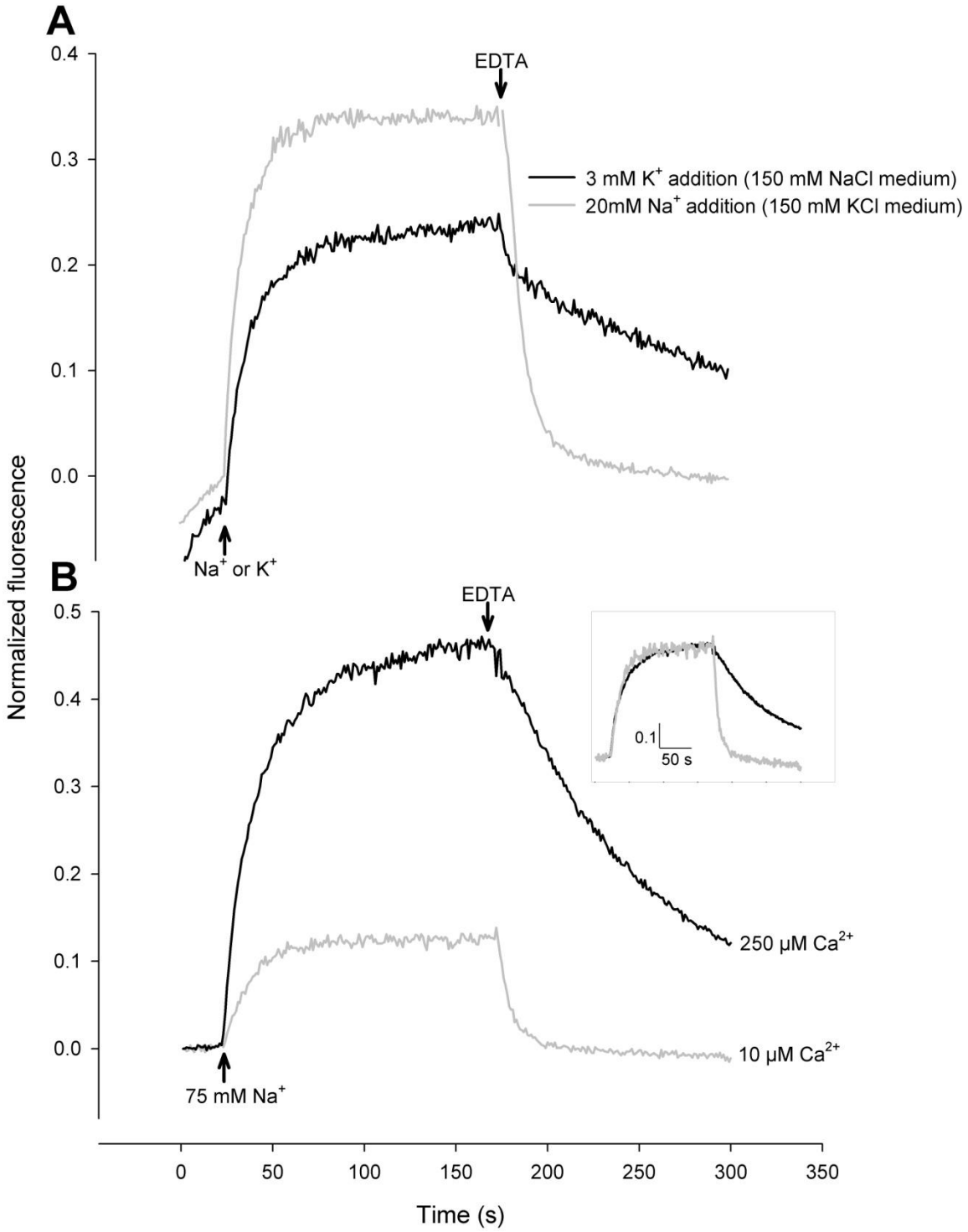
A
B
EDTA
3 mM K+ addition (150 mM NaCl medium)
20mM Na+ addition (150 mM KCl medium)
Na+ or K+
EDTA
0.1
50 s
250 μM Ca2+
10 μM Ca2+
75 mM Na+
Normalized fluorescence
Time (s)
0.0
0.1
0.2
0.3
0.4
0.5
0
50
100
150
200
250
300
350

$[Na^{2+}]_i$, but also to high $[Ca^{2+}]_o$ – discussed further below in the DISCUSSION section (Hilgemann *et al*. 1992a).

3. 8. Relief of Na^+_i-dependent inactivation of NCKX2

We next asked whether this Na^+-dependent inactivation process in NCKX2 is reversible, i.e. after the cytoplasmic configuration of NCKX2 had been exposed to high intracellular Na^+ for a prolonged period of time, and then subsequently the intracellular Na^+ was removed (or decreased) can NCKX2 recover its activity? To this end, we employed the same protocol used in previous experiments to load NCKX2 transfected HEK293 cells with Ca^{2+} using high $[Na^+]$ in the cuvette; except the assay volume was 0.5 ml KCl-EDTA medium (compared to the typical volume of 2 ml). The doses of gramicidin, FCCP, and Tg added to the cuvette were the same as those added to 2 ml volume, since the number of cells in the 0.5 ml cuvette was the same. After inducing Ca^{2+} influx through NCKX2 by the addition of 250 μM free Ca^{2+} to the cuvette, followed by 100 mM Na^+, the cells were maintained (with constant stirring) for a period of either 40 s, or 150 s, at which time point the cuvette was placed into the cuvette holder of the spectrorometer, and the assay medium in the cuvette diluted to a total volume of 2 ml with either 150 mM KCl-EDTA, or 150 mM NaCl-EDTA media (with EDTA elevated to 1 mM to chelate the 250 μM $[Ca^{2+}]$ in the cuvette), and engage the Ca^{2+} extrusion mode of NCKX2. Fig. 11 illustrates the results of these experiments using both the high affinity Ca^{2+} probe fluo-3 (Fig. 11 A), and the lower Ca^{2+} affinity fluo-4FF (Fig. 11 B). When the cells were loaded with Ca^{2+} for a period of 40 s, and then the medium was diluted with 150 mM KCl-EDTA (reducing $[Na^+]$ in the cuvette from 100 mM to 25 mM), $[Ca^{2+}]_i$ was cleared from the cells rapidly. However, when the loading was prolonged to 150 s before dilution of the cuvette medium, the $[Ca^{2+}]_i$ clearance was biphasic, with an initial slow period of clearance over the first 2 min, followed by a slight acceleration of the rate of $[Ca^{2+}]_i$ clearance, eventually approaching the baseline reached with the cuvette whose medium was diluted with KCl-EDTA only 40 s following Ca^{2+} loading. On the other hand, when the cuvette medium was diluted with NaCl-EDTA 150 s after Ca^{2+} loading (effectively maintaining $[Na^+]$ at > 100 mM, and diluting $[K^+]$ from 150 mM to 37.5 mM) NCKX2 inactivation was maintained, and at no

point in our recording did we observe rapid $[Ca^{2+}]_i$ extrusion, even with the low affinity Ca^{2+} probe fluo-4FF (Fig. 11 B). Also shown in Fig. 11 B is an experimental trace where cuvette medium was diluted with NaCl-EDTA 40 s after induction of Ca^{2+} loading. When the dilution with NaCl-EDTA was made after 40 s, there was an initial rapid phase of $[Ca^{2+}]_i$ extrusion which lasted approximately 10 s, followed by a diminished rate of $[Ca^{2+}]_i$ clearance; at the end of the recording, $[Ca^{2+}]_i$ was elevated in comparison to the level attained in cuvettes where the dilution medium was KCl-EDTA. These experiments corroborate the time-dependence of NCKX2 Na^+-dependent inactivation, in that full inactivation required exposure to high intracellular Na^+ for periods longer than 40 s to become prominent, and that Na^+_i-dependent inactivation can be relieved in a time-dependent manner by the reduction of $[Na^+]_i$. We next examined the $[Na^+]_i$ requirements for development of Na^+_i-dependent inactivation in NCKX2 mutants with altered Na^+-affinity.

3. 9. Na^+_i-dependent inactivation requires saturation of cytoplasmic configuration of NCKX2 with intracellular Na^+

To further validate that the inactivation of NCKX2 was related to intracellular Na^+, and since our earlier screening of single amino acid substitution mutants revealed some constructs with potentially altered affinities for intracellular Na^+, we asked whether some of these mutants would also display inactivation? Two constructs, tested in our earlier screen, in particular displayed an apparent increase in affinity for intracellular Na^+: Asp^{548}, and Asn^{572} (Fig. 5 D and F). The Asp^{548} residue had been analyzed previously for shifts in affinities for Ca^{2+} and K^+, and was found to have a shift to apparent affinities that were ~100-fold and ~10-fold lower than those of wild-type NCKX2 for extracellular Ca^{2+} and K^+ respectively (Kang *et al*. 2005a). The Asp^{548} residue is predicted to be in the α_2 repeat TM segment 8, and along with another acidic residue in the α_1 repeat – Glu^{188} – are thought to be critical for Na^+/Ca^{2+} exchangers as they are conserved in all NCKX isoforms, and have equivalents in the α repeats of NCX (see Fig. 1). The other residue, Asn^{572} has not been studied in detail previously, except for a comparison to wild-type NCKX2 of the level of activity this residue exhibits when substituted with either an alanine or a cysteine; Asn^{572} is

Fig. 11. Relief of Na^+_i-dependent inactivation of NCKX2. **A.** fluo-3 loaded NCKX2 transfected HEK293 cells were treated as in legend of Fig. 4 – cells, aside from 2 μM gramicidin treatment, were additionally treated with 0.4 μM Tg, and 2 μM FCCP. Aliquots of the HEK293 cells were placed in cuvettes containing 0.5 ml 150 mM KCl buffer, and NCKX2-mediated Ca^{2+} influx initiated by the addition of 100 mM Na^+ in the presence of 250 μM free $[Ca^{2+}]_o$. To initiate NCKX2-mediated Ca^{2+} extrusion, at time zero, the 0.5 ml cuvette medium was diluted 4-fold to 2 ml total with: 150 mM KCl buffer containing 1 mM EDTA (40 s following Na^+ addition/Ca^{2+} loading, black trace); 150 mM NaCl buffer containing 1 mM EDTA (150 s following Na^+ addition/Ca^{2+} loading, red trace); 150 mM KCl buffer containing 1 mM EDTA (150 s following Na^+ addition/Ca^{2+} loading, green trace). Data are representative of three other experiments. **B.** fluo-4FF loaded NCKX2 transfected HEK293 cells were treated as in **A.** One additional trace is illustrated, in which the cuvette medium was diluted 4-fold with 150 mM NaCl buffer (40 s following Na^+ addition/Ca^{2+} loading, blue trace). Data are representative of three other experiments. Portions of this figure were adapted from Altimimi and Schnetkamp (2007).

Fig. 11.

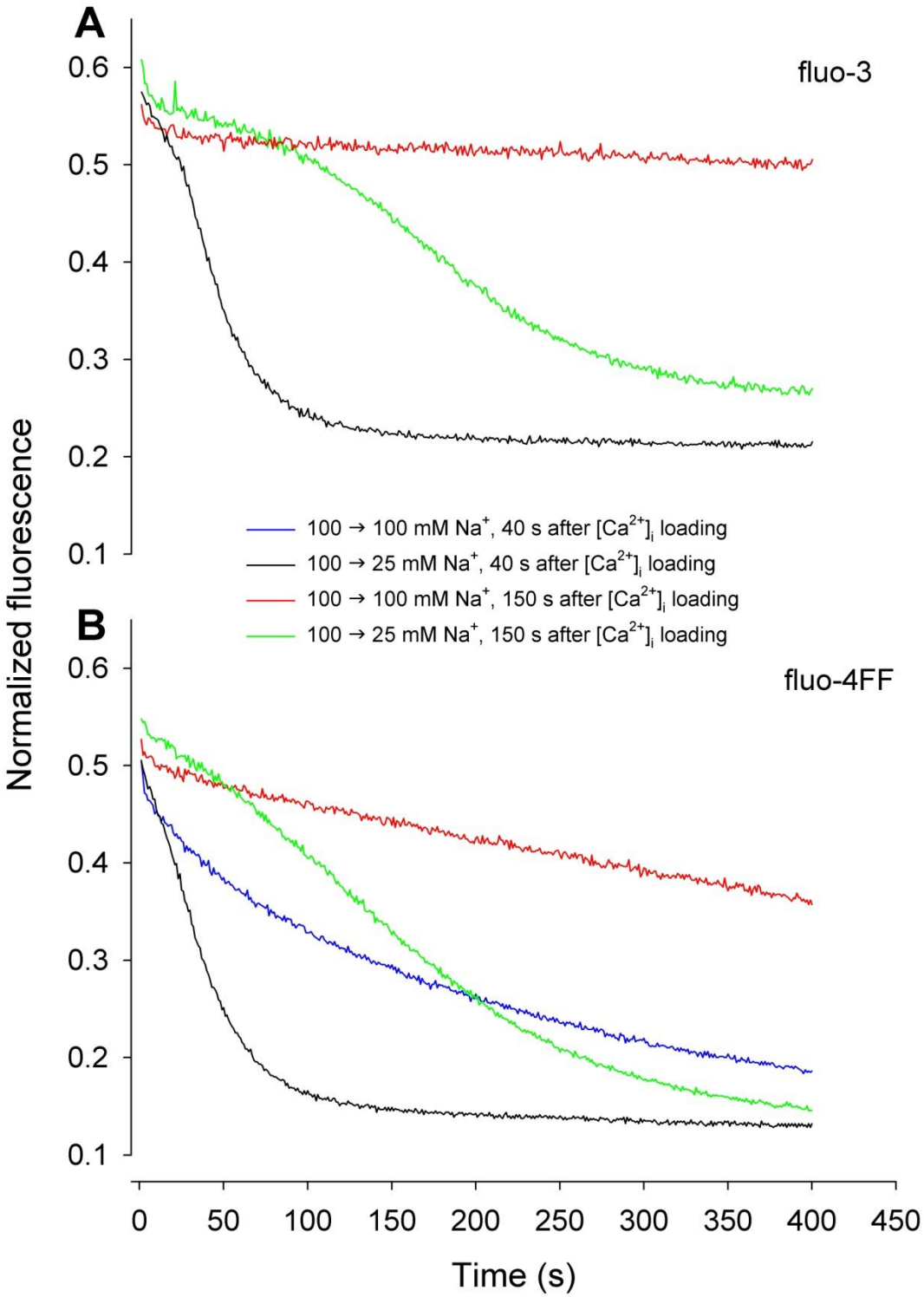
A
fluo-3
B
fluo-4FF
Normalized fluorescence
0.6
0.5
0.4
0.3
0.2
0.1
100 → 100 mM Na+, 40 s after [Ca2+]i loading
100 → 25 mM Na+, 40 s after [Ca2+]i loading
100 → 100 mM Na+, 150 s after [Ca2+]i loading
100 → 25 mM Na+, 150 s after [Ca2+]i loading
0
50
100
150
200
250
300
350
400
450
Time (s)

also conserved in all isoforms of NCKX, and is also conserved in the equivalent position in NCX isoforms (Winkfein *et al*. 2003; Fig. 1).

To confirm indications from our earlier screening of an increased apparent affinity for intracellular Na^+ for both Asp^{548} and Asn^{572}, we carried out a number of measurements of Ca^{2+} influx mode on each construct, as well as wild-type NCKX2, essentially as described in MATERIALS AND METHODS, except using the low affinity Ca^{2+} probe fluo-4FF. Fig. 12 A-C illustrate exemplar families of traces for each of wild-type human NCKX2, and the single amino acid substitution mutants Asp^{548}, and Asn^{572}. To evaluate apparent affinities for intracellular Na^+, the initial rate of $[Ca^{2+}]_i$ rise was plotted as a function of $[Na^+]$ (Fig. 12 D-F). Note that for both Asp^{548}, and Asn^{572} the initial rates of $[Ca^{2+}]_i$ rise increased when $[Na^+]$ was increased up to ~75 mM, but then the rate of $[Ca^{2+}]_i$ rise for both mutants was less with the highest $[Na^+]$ tested – 150 mM. This was in itself indicative of increased affinity for intracellular Na^+; the very high $[Na^+]$ becomes effective in competing with Ca^{2+} for the exofacial configuration binding pocket. This is based on the assumption, as previously shown, that the apparent affinities for transported ions measured for NCKX2 are symmetrical, i.e. reflect the apparent affinity of the ion transport sites whether in the cytoplasmic or exofacial configuration (Schnetkamp 1991; Schnetkamp *et al*. 1989; Schnetkamp *et al*. 1995). To plot a mathematical relationship (Hill plot) describing the relationship of the rate of $[Ca^{2+}]_i$ rise to $[Na^+]$, each of the three independent measurements for each construct were normalized with respect to the $[Na^+]$ giving the highest initial rate of $[Ca^{2+}]_i$ rise – that was 150 mM for wild-type NCKX2, and 45 mM for both Asp^{548} and Asn^{572}; this was to control for variations due to expression levels among the experiments. The measurements were then averaged for each construct, and the means were used to construct the plots in Fig. 12 G-I, and to fit least-squares regression Hill functions. The Hill plot function of the normalized rate of $[Ca^{2+}]_i$ rise for wild-type NCKX2 gave a K_m of 50 mM Na^+ (± standard error of the model (SEM) of 1.6 mM), and Hill coefficient of 2.6. For D548E those values were K_m of 18 mM Na^+ (± SEM of 0.8 mM), and Hill coefficient of 3.2, while for N572C those values were K_m of 20 mM Na^+ (± SEM of 2.4 mM), and Hill coefficient of 2.8.

Next, the Ca^{2+} extrusion mode of these constructs was examined; considering that the process of inactivation in wild-type NCKX2 was dependent on intracellular Na^+, we hypothesized that both D548E and N572C would display enhanced inactivation, since they exhibited an increased affinity, with respect to wild-type NCKX2, for intracellular Na^+. The typical protocol for examining Ca^{2+} extrusion mode was employed with HEK293 cells transiently transfected with wild-type NCKX2, D548E, or N572C. After the addition of 250 μM free Ca^{2+} to the cuvette, Ca^{2+} loading was induced by the addition of 35 mM Na^+, and after 150 s, 1 mM EDTA was added to the cuvette to chelate external Ca^{2+}. As illustrated in Fig. 13 A, and in accordance with earlier results (Fig. 6 C, and 9 B), 35 mM Na^+ was not sufficient to produce strong inactivation in wild-type NCKX2. However, D548E, which by the addition of 35 mM Na^+ elevated free $[Ca^{2+}]_i$ in HEK293 cells to the same amplitude as wild-type NCKX2 transfected HEK293 cells, was inactivated and did not extrude $[Ca^{2+}]_i$ rapidly. Likewise, N572C which had a lower rate of maximal activity than either wild-type NCKX2, or D548E was also inactivated by the relatively low Na^+ concentration used (D548E operates at ~40% of the rate of wt NCKX2 V_{max}, and N572C at ~18%, see Fig 12 D-F; in terms of the amplitudes of maximal $[Ca^{2+}]_i$ attained, D548E and N572C operate at 80% and 40% of the level of wt NCKX2, see Fig. 12 A-C). Also note that with N572C, $[Ca^{2+}]_i$ amplitude attained was relatively modest, and yet N572C was incompetent in clearing that $[Ca^{2+}]_i$ load. For comparison, another acidic residue substitute mutant of wt NCKX2 is also shown in Fig. 13 A. This residue Glu^{166} is predicted to lie in the cytoplasmic linker between TM1 and TM2, and is N-terminal to the α_1 repeat (Fig. 2), and is conserved among NCKX isoforms (the exception is NCKX1 where Asp replaces Glu in the equivalent position, Fig. 1). E166D did not display a clearly altered apparent Na^+-affinity (see Fig. 5 A). When examining Ca^{2+} extrusion with E166D, it did not display strong inactivation; this despite Ca^{2+} loading being induced with the relatively high $[Na^+]$ of 75 mM, to elevate $[Ca^{2+}]_i$ to a level comparable to $[Ca^{2+}]_i$ attained with wild-type NCKX2 transfected HEK293 cells (Fig. 13 A).

We also examined the time-course of inactivation of the D548E substitution mutant. As in the experiment described for examining the time-course of wild-type NCKX2 inactivation (Fig. 9), D548E transfected HEK293 cells were loaded with Ca^{2+} by the

Fig. 12. Na^+-affinity of wild-type NCKX2, and single amino acid substitutions D548E, and N572C. **A-C.** Representative traces of experiments to measure apparent affinity of NCKX2 for Na^+. fluo-4FF loaded NCKX2 (or indicated mutant) transfected HEK293 cells were treated as in legend of Fig. 4 – cells, aside from 2 μM gramicidin treatment, were additionally treated with 0.4 μM Tg, and 2 μM FCCP. Representative traces for Na^+_i-induced changes in free $[Ca^{2+}]_i$ are illustrated; at time zero, the indicated $[Na^+]$ was added to cells placed in 150 mM KCl buffer in the presence of 250 μM $[Ca^{2+}]_o$. The legend in **B** also applies to the traces illustrated in **C**. **D-F.** Initial rates derived from measurements of Na^+_i-induced rises in free $[Ca^{2+}]_i$. Each different symbol represents measurements made from a single experiment (from a separate transfection). Note the decline in rates at the highest $[Na^+]$ tested with D548E (panel **E**) and N572C (panel **F**), also seen in the 150 mM Na^+ traces illustrated in panels **B** and **C** respectively. **G-I.** Estimation of apparent affinity of NCKX2 for Na^+_i. Each of the initial rate of rise in $[Ca^{2+}]_i$ measurements in panels **D-F** were normalized with respect to the initial rate value corresponding to V_{max} (V_{max} for wt NCKX2 was taken at 150 mM Na^+, while for D548E and N572C V_{max} was taken at 45 mM Na^+). The mean data are plotted along with error bars indicating standard deviation (SD) about the mean. The line of best fit in each panel was a least squares regression of the means to a three parameter Hill equation (made using SigmaPlot 2001 for Windows Version 7.0). The Hill equation parameters for each panel were as follows: **G**, wt NCKX2 – V_{max}=1.07, Hill coefficient=2.6, K_m=50 mM Na^+ (± standard error of the model (SEM) of 2 mM Na^+); **H**, D548E – V_{max}=1.04, Hill coefficient=3.2, K_m=18 mM Na^+ (± SEM of 1 mM Na^+); **I**, N572C – V_{max}=1.07, Hill coefficient=2.8, K_m=20 mM Na^+ (± SEM of 2 mM Na^+). n=3 measurements (illustrated in panels **D-F**) for the mean data of each panel. Portions of this figure were adapted from Altimimi and Schnetkamp (2007).

Fig. 12.

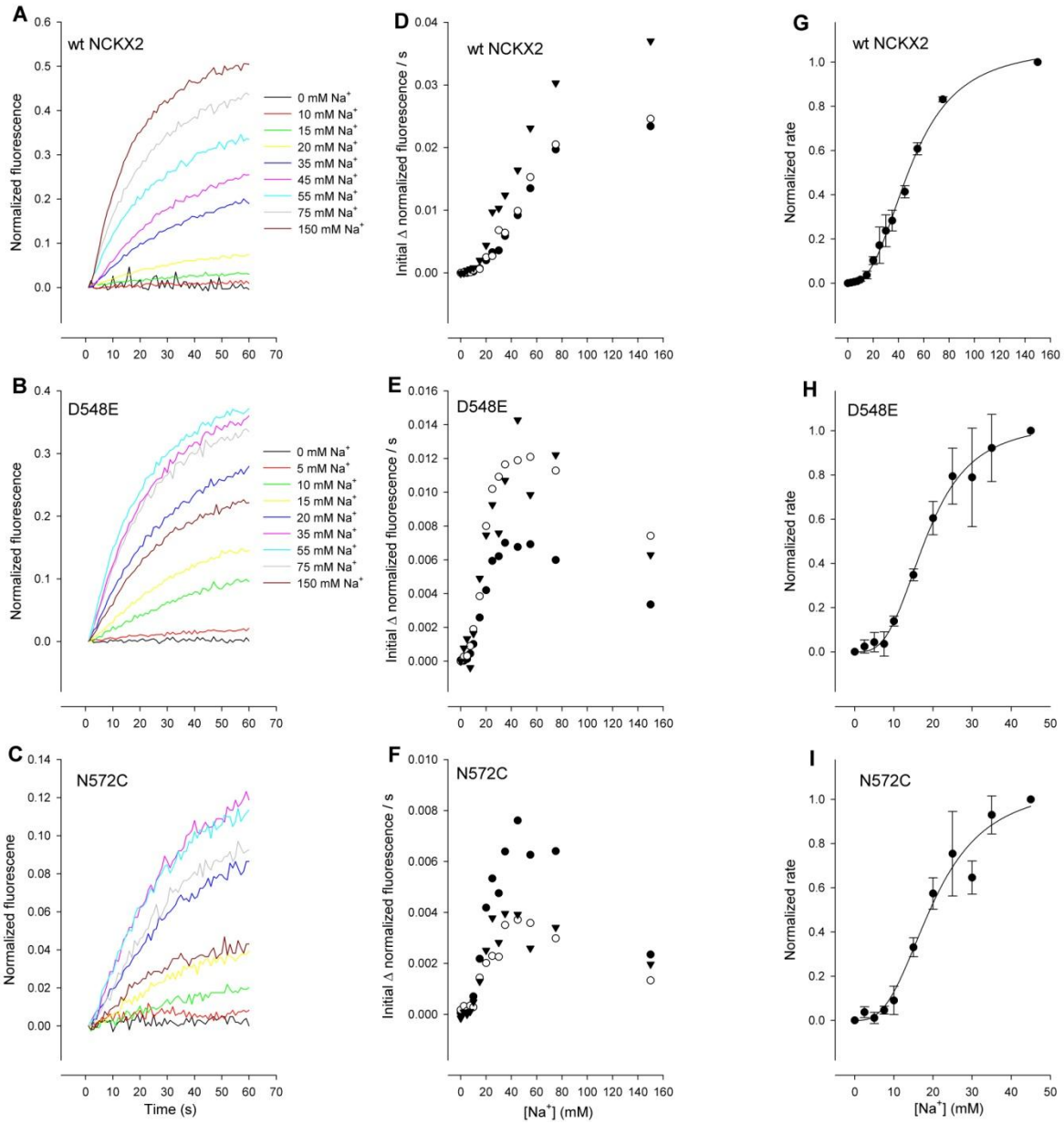
A
wt NCKX2
Normalized fluorescence
0 mM Na+
10 mM Na+
15 mM Na+
20 mM Na+
35 mM Na+
45 mM Na+
55 mM Na+
75 mM Na+
150 mM Na+
D
wt NCKX2
Initial Δ normalized fluorescence / s
G
wt NCKX2
Normalized rate
B
D548E
Normalized fluorescence
0 mM Na+
5 mM Na+
10 mM Na+
15 mM Na+
20 mM Na+
35 mM Na+
55 mM Na+
75 mM Na+
150 mM Na+
E
D548E
Initial Δ normalized fluorescence / s
H
D548E
Normalized rate
C
N572C
Normalized fluorescene
Time (s)
F
N572C
Initial Δ normalized fluorescence / s
[Na+] (mM)
I
N572C
Normalized rate
[Na+] (mM)

Fig. 13. Comparison of Ca^{2+} extrusion kinetics of wild-type NCKX2 and single amino acid substitutions D548E, and N572C. **A.** fluo-4FF loaded wild-type NCKX2, or indicated mutant construct, transfected HEK293 cells were treated as in legend of Fig. 4 – cells, aside from 2 μM gramicidin treatment, were additionally treated with 0.4 μM Tg, and 2 μM FCCP. NCKX2 Ca^{2+} influx mode was initiated at the upward pointing arrow by addition of 35 mM Na^+ (75 mM Na^+ in the case of E166D) to cuvette containing 150 mM KCl buffer in the presence of 250 μM free $[Ca^{2+}]_o$. NCKX2 Ca^{2+} extrusion was initiated by the addition of 1 mM EDTA at the downward pointing arrow. Trace illustrated for wild-type NCKX2 is representative of five other measurements; trace illustrated for D548E is representative of two other measurements. * 75 mM Na^+ was added to E166D transfected HEK293 cells. **B.** fluo-4FF loaded D548E transfected HEK293 cells were treated as in legend of Fig. 4 – cells, aside from 2 μM gramicidin treatment, were additionally treated with 0.4 μM Tg, and 2 μM FCCP. Ca^{2+} influx mode was initiated at the upward pointing arrow by addition of 35 mM Na^+ to cuvette containing 150 mM KCl buffer in the presence of 250 μM free $[Ca^{2+}]_o$. Ca^{2+} extrusion was initiated by the addition of 1 mM EDTA at the downward pointing arrow; two traces from separate cuvettes are overlaid for illustration. The inset juxtaposes the Ca^{2+} extrusion from the two traces illustrated in the main panel to highlight the difference in Ca^{2+} extrusion kinetics at the two different time points of EDTA addition.

Portions of this figure were adapted from Altimimi and Schnetkamp (2007).

Fig. 13.

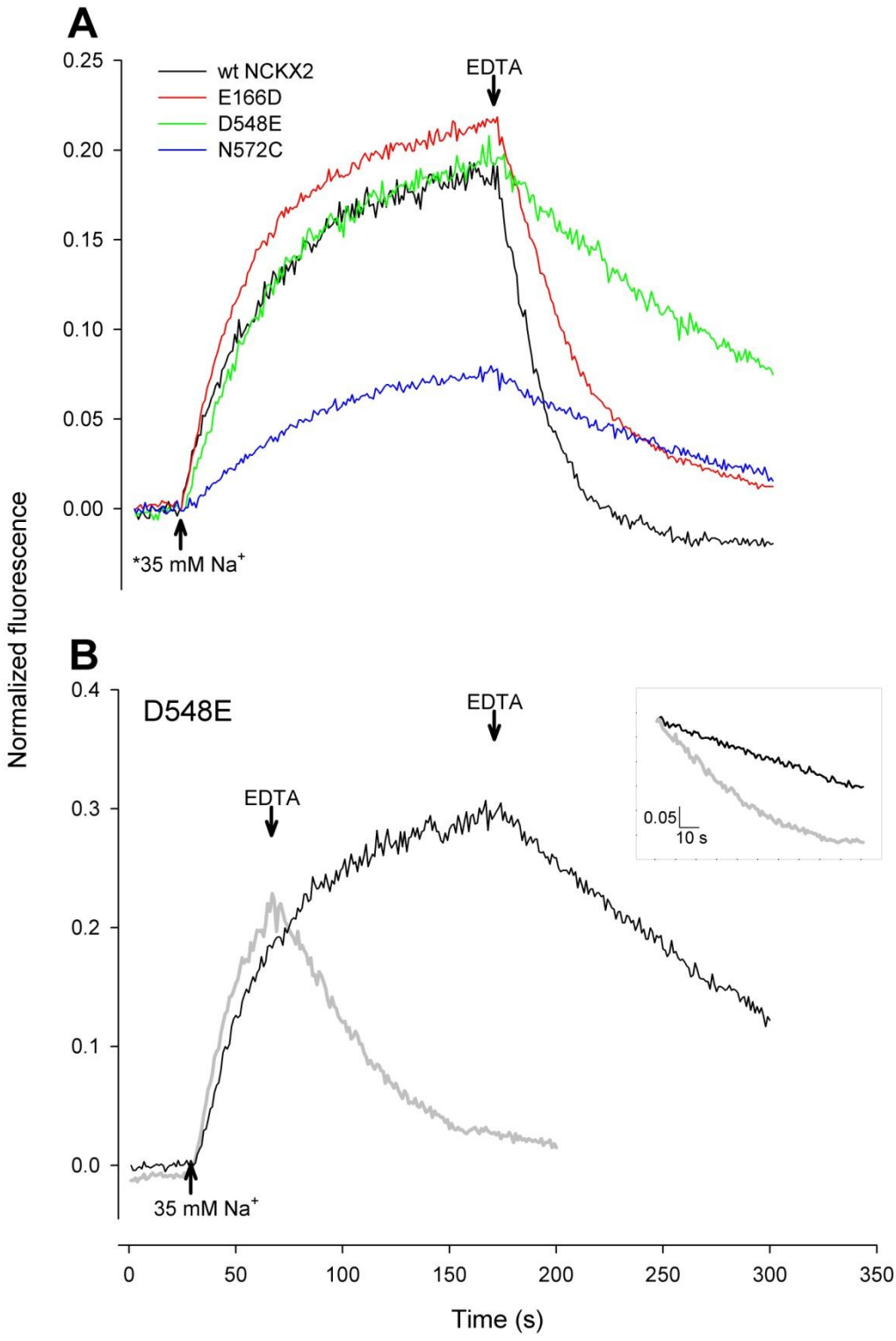
A
wt NCKX2
E166D
D548E
N572C
EDTA
*35 mM Na+
B
D548E
EDTA
EDTA
0.05
10 s
35 mM Na+
Normalized fluorescence
Time (s)
0.25
0.20
0.15
0.10
0.05
0.00
0.4
0.3
0.2
0.1
0.0
0
50
100
150
200
250
300
350

addition of 35 mM Na^+ (concentration sufficient to produce strong inactivation with this construct – see Fig. 13 A), and $[Ca^{2+}]_i$ clearance was examined at two time points following Ca^{2+} loading. When 1 mM EDTA was added 150 s following the addition of Na^+, there appeared to be strong inactivation, as illustrated in Fig. 13 A, but when 1 mM EDTA was added at an earlier time point (40 s following Na^+ addition), inactivation was less prominent (Fig. 13 B; the inset highlights the difference more clearly by juxtaposing the $[Ca^{2+}]_i$ clearance phases of both experimental traces at the same level and time point). The difference in kinetics with time also illustrates that the slow $[Ca^{2+}]_i$ extrusion rate of D548E was not the result of a mutant protein that was altogether compromised in $[Ca^{2+}]_i$ extrusion. Finally, we addressed the validity of the assay developed herein, and results reported for Na^+-affinity, by repeating our measurements with different $[Ca^{2+}]_o$.

3. 10. Relative shifts in affinity for Na^+ for mutant NCKX2 constructs are maintained irrespective of $[Ca^{2+}]_o$

Since it has been reported that D548E has a reduced affinity for Ca^{2+} (~100-fold increase in K_m measured for $[Ca^{2+}]_o$ in the Ca^{2+} influx mode), it was pertinent to assess whether the apparent affinities derived herein for $[Na^+]_i$ for D548E were valid, given that the free $[Ca^{2+}]$ used to make our measurements was 250 μM – potentially low since the K_m of D548E for $[Ca^{2+}]_o$ is around 100 μM (Kang *et al*. 2005a). The same issue might apply for our measurements of K_m for $[Na^+]_i$ for wild-type NCKX2 (i.e. using the gramicidin protocol, 250 μM $[Ca^{2+}]_o$ might not be sufficient to saturate the exofacial configuration Ca^{2+} binding site of NCKX2), so to validate our previous experiments, we carried out further measurements of Na^+-affinity using the same protocol, but with 2 mM Ca^{2+} added to the cuvette (rather than 250 μM used in previous experiments). We also made two improvements in our protocol for measuring rates of changes in free $[Ca^{2+}]_i$: firstly, the temporal resolution of our measurements was improved by using data integration window of 200 ms (as opposed to 1.0 s used in all previous experiments and figures). Secondly, we made simultaneous use of the two intracellular free Ca^{2+} probes with the most useful Ca^{2+}-affinity range – fluo-4 and fluo-4FF (fluo-4 was also from Molecular Probes, and has similar Ca^{2+} binding affinity (~0.34 μM) to fluo-3 used in our earlier experiments, but with

improved spectral properties). This was carried out by splitting a suspension of HEK293 cells transiently transfected with a given cDNA construct into two separate suspensions, and loading one with 2 μM fluo-4, and the other with 2 μM fluo-4FF. The impetus for making simultaneous measurements with fluo-4 and fluo-4FF was to be able to cover a wider dynamic range of free $[Ca^{2+}]_i$ measurements, since many of the single amino acid substitution constructs to be assayed for shifts in Na^+-dependence have a markedly reduced V_{max} (see Fig. 5). Fig. 14 A illustrates exemplar traces of free $[Ca^{2+}]_i$ measurements made from the same original suspension of wild-type transfected HEK293 cells; note that with fluo-4, the rates of free $[Ca^{2+}]_i$ measurements were approaching saturation with the addition of 35 mM Na^+, whereas the rate of free $[Ca^{2+}]_i$ rise induced by the same $[Na^+]$ recorded with fluo-4FF appeared to be near the lower end of the dynamic range of fluo-4FF. To integrate these measurements, the rates of free $[Ca^{2+}]_i$ rise calculated for each trace were represented as a fraction of the rate for one common $[Na^+]$ tested with both fluo-4 and fluo-4FF loaded NCKX2 transfected HEK293 cells from the same original suspension; as with previous data analysis, these rates were then subtracted from the rate obtained in zero $[Na^+]$ (Ca^{2+} addition alone), and normalized with respect to the $[Na^+]$ giving the highest V_{max} (200 mM Na^+ in this case). Fig. 14 B illustrates initial rates from a number of different experimental measurements made with wild-type NCKX2 transfected HEK293 cells when assayed with 250 μM Ca^{2+} in the cuvette (Fig. 14 B left panel) and with 2 mM Ca^{2+} in the cuvette (Fig. 14 B right panel); note that only initial rates recorded with the low affinity Ca^{2+} probe fluo-4FF are presented, and these may be compared with rates obtained in previous experiments illustrated in Fig 12 D. When the integrated free $[Ca^{2+}]_i$ rise rates obtained with the $Na^+{}_i$-dependence assay in 2 mM Ca^{2+} were averaged, and a Hill plot fitted to the means, a K_m value of 90 mM Na^+ (± SEM of 17 mM) was obtained (Hill coefficient 1.7, Fig. 14 C left panel); this value was different from that obtained from our earlier measurements made with 250 μM free Ca^{2+} in the cuvette (Fig. 12 G). The modified protocol was used to make Na^+-affinity measurements of wild-type NCKX2 again with 250 μM free Ca^{2+} in the cuvette (Fig. 14 B and D left panels) and the K_m thus derived coincided with our earlier estimates of K_m for intracellular Na^+; the Hill plot shown in Fig. 14 D left panel, gave a K_m of 56 mM Na^+ (± SEM of 3 mM), and Hill coefficient 2.9. The initial

Fig. 14. Comparison of the Na^+-affinity of wild-type NCKX2, and the low Na^+-affinity mutant L549A, at 250 μM $[Ca^{2+}]_o$ or 2 mM $[Ca^{2+}]_o$. **A.** Exemplar traces of wild-type NCKX2 transfected HEK293 cells from a single suspension, split into two suspensions and loaded separately with fluo-4 (left panel) and fluo-4FF (right panel) in 150 mM LiCl/100 μM EDTA buffer. Aliquots of the suspension of HEK293 cells were placed in cuvettes containing 150 mM KCl/100 μM EDTA buffer, and 2 μM gramicidin and 2 μM FCCP added to the cells in the cuvette 3 min prior to addition of 350 μM $CaCl_2$ (for a final free $[Ca^{2+}]_o$ of 250 μM). At time zero, the indicated $[Na^+]$ was added to the cuvette. **B.** Computed initial rates of rise in free $[Ca^{2+}]_i$ measured with fluo-4FF loaded, wild-type NCKX2 transfected HEK293 cells plotted as a function of $[Na^+]$. In the left panel the assay was carried out in the presence of 250 μM free $[Ca^{2+}]_o$, while in the right panel the assay was carried out in the presence of 2 mM free $[Ca^{2+}]_o$. Each of the different symbols used reflect results obtained from one experiment (or transfection); four separate measurements are illustrated for 250 μM free $[Ca^{2+}]_o$, and three are illustrated for 2 mM free $[Ca^{2+}]_o$. **C.** *left panel*, means (n=5) of the initial rates (normalized with respect to the initial rate obtained at the highest $[Na^+]$ tested – 200 mM), computed as in **B**, were plotted as a function of $[Na^+]$ for wild-type NCKX2 transfected HEK293 cells assayed in the presence of 2 mM free $[Ca^{2+}]_o$ (black circles; error bars indicate SD about the mean). The black line is a least squares regression of a Hill function yielding V_{max}=1.23, Hill coefficient=1.7, K_m=90 mM Na^+ (± SEM of 17 mM Na^+). D548E (white circles) and N572C (black triangles) transfected HEK293 cells were assayed likewise in the presence of 2 mM $[Ca^{2+}]_o$; the initial rates measured for those constructs were normalized to the initial rate obtained at 55 mM Na^+ (D548E) or 75 mM Na^+ (N572C). The data for both D548E and N572C were near overlapping; notice that for both constructs the normalized rate at the highest $[Na^+]$ tested – 150 mM – was substantially lower than the normalized rates at 55-75 mM Na^+ (the symbol for D548E normalized rate at 150 mM Na^+ is highlighted by the arrow; the normalized rate for N572C overlapped this same value). The data for D548E and N572C were fitted with Hill plots (grey trace for D548E, and dotted black trace for N572C) yielding V_{max}=1.01, Hill coefficient=2.9, K_m=23 mM Na^+ (± SEM of 2 mM Na^+) for

Fig. 14 legend continued on page 68

Fig. 14.

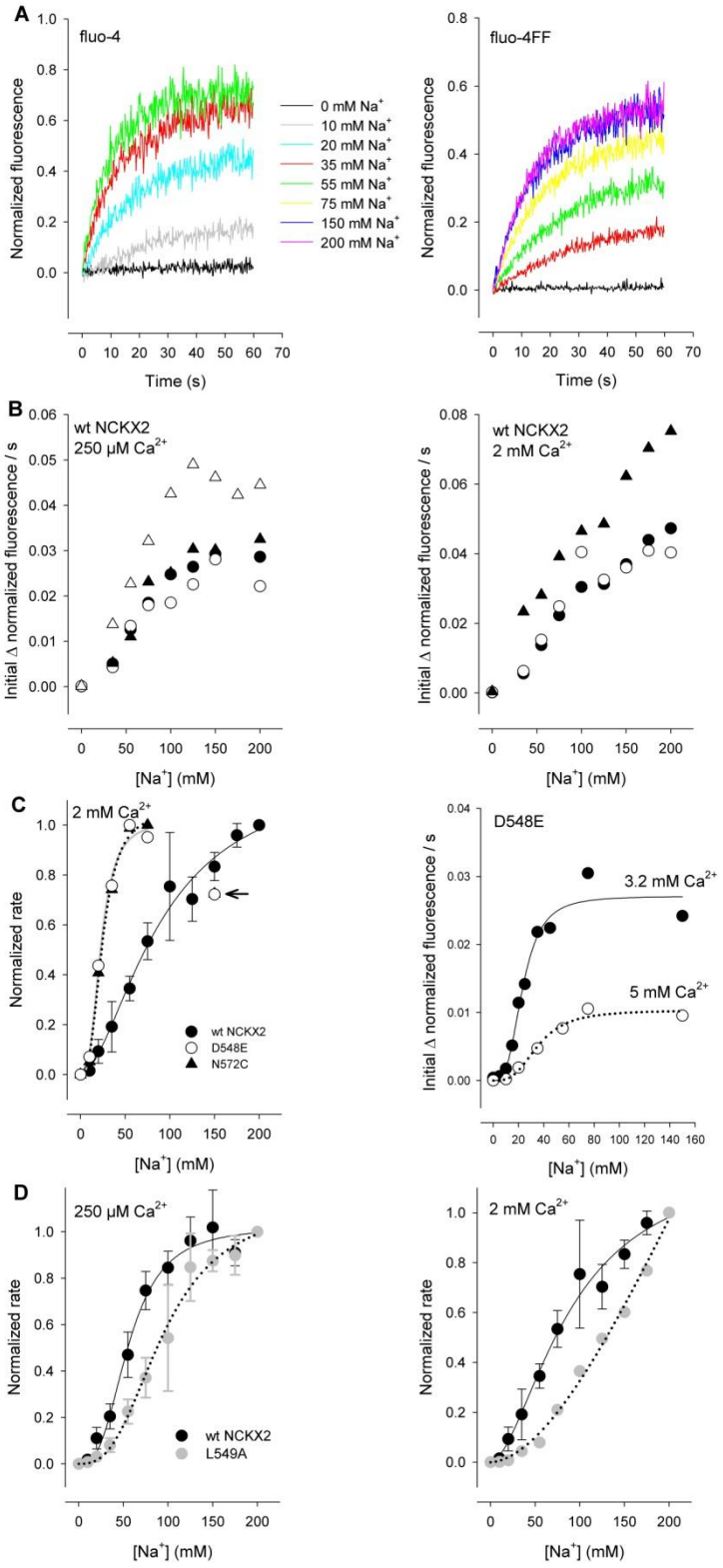
A
fluo-4
fluo-4FF
Normalized fluorescence
Time (s)
0 mM Na+
10 mM Na+
20 mM Na+
35 mM Na+
55 mM Na+
75 mM Na+
150 mM Na+
200 mM Na+
B
wt NCKX2
250 µM Ca2+
2 mM Ca2+
Initial Δ normalized fluorescence / s
[Na+] (mM)
C
2 mM Ca2+
Normalized rate
wt NCKX2
D548E
N572C
D548E
3.2 mM Ca2+
5 mM Ca2+
D
250 µM Ca2+
2 mM Ca2+
wt NCKX2
L549A

Fig. 14 (legend continued).

D548E, and V_{max}=1.06, Hill coefficient=2.8, K_m=24 mM Na^+ (± SEM of 1 mM Na^+) for N572C. *right panel*, D548E transfected HEK293 cells were assayed as in left panel, but in the presence of 3.2 mM $[Ca^{2+}]_o$ (black circles), or 5 mM $[Ca^{2+}]_o$ (white circles); notice in this panel, data were expressed as initial rates of change in normalized fluorescence and were not normalized with respect to apparent V_{max}. The data were fitted with Hill plots yielding Hill coefficient=3.1, K_m= 23 mM Na^+ (± SEM of 2 mM Na^+) for 3.2 mM $[Ca^{2+}]_o$ (black trace), and Hill coefficient=3.1, K_m=36 mM Na^+ (± SEM of 4 mM Na^+) for 5 mM $[Ca^{2+}]_o$ (dotted trace). **D.** *left panel*, means of the initial rates (normalized with respect to the initial rate obtained at the highest $[Na^+]$ tested – 200 mM), computed as in **B**, were plotted as a function of $[Na^+]$ for wild-type NCKX2 (black circles; n=5) and L549A (grey circles; n=3) transfected HEK293 cells assayed in the presence of 250 μM free $[Ca^{2+}]_o$; error bars indicate SD about the mean. Hill plots were fitted to the means yielding V_{max}=1.02, Hill coefficient=2.9, K_m=56 mM Na^+ (± SEM of 3 mM Na^+) for wild-type NCKX2 (black trace), and V_{max}=1.12, Hill coefficient=2.7, K_m=95 mM Na^+ (± SEM of 8 mM Na^+) for L549A (dotted trace). *right panel*, normalized rates for wild-type NCKX2 transfected HEK293 cells assayed in the presence of 2 mM $[Ca^{2+}]_o$ (same data as in **B** left panel, compared to normalized rate for L549A transfected HEK293 cells assayed in the presence of 2 mM $[Ca^{2+}]_o$. The black trace is the fitted Hill function to the means of the data for wild-type NCKX2 (see legend above for **B** for fitted Hill equation parameters), and dotted trace is Hill function fitted to data obtained for L549A (V_{max}=5.8, Hill coefficient=1.8, K_m=493 mM Na^+).

Portions of this figure were adapted from Altimimi and Schnetkamp (2007).

rate of free $[Ca^{2+}]_i$ rise data points measured with 2 mM $[Ca^{2+}]_o$ do not appear to reach saturation (V_{max}); the least squares regression used to produce the Hill plot predicted a value of 1.23 for V_{max} in the case of the data obtained with 2 mM $[Ca^{2+}]_o$ (compare with V_{max} predictions of 1.07 and 1.02 for data in Fig 12 G and Fig 14 D left panel respectively). The apparent right-ward shift (towards higher $[Na^+]$) in the K_m for $[Na^+]$ with increased $[Ca^{2+}]_o$ may be interpreted as an indication of possible competitive interactions between Na^+ and Ca^{2+} at the exofacial configuration of NCKX2, hence the value for K_m obtained previously was resultant of using too low $[Ca^{2+}]_o$ to overcome Na^+/Ca^{2+} competition – but see DISCUSSION section below for further discussion of the results. Nevertheless, when both D548E or N572C were assayed in the presence of 2 mM $[Ca^{2+}]_o$, the data and least-squares regression fits were the same as those obtained previously with 250 μM free $[Ca^{2+}]_o$, and certainly the relation with respect to wild-type NCKX2 remained the same – with D548E and N572C displaying substantially lower K_m values for Na^+ (Fig. 14 C left panel). Also note that even when D548E and N572C were assayed in the presence of 2 mM $[Ca^{2+}]_o$, the highest $[Na^+]$ tested (150 mM) resulted in an initial rate of free $[Ca^{2+}]_i$ rise that was lower than the initial rates obtained with 55-75 mM Na^+ (V_{max}), replicating the results obtained previously (see Fig. 12 E and F). D548E and N572C were well fit by Hill plots (including data points up to 75 mM Na^+, but not data point at 150 mM Na^+) giving K_m values of ~24 mM Na^+, and Hill coefficients of ~2.85 (note that these data were from one experimental measurement only, Fig. 14 C left panel). We reasoned that the characteristic decrement in initial rate of free $[Ca^{2+}]_i$ rise measured at the highest $[Na^+]$ tested (150 mM in both Fig. 12 E and F, and Fig. 14 C left panel) with D548E and N572C were in fact indicative of Na^+/Ca^{2+} competition at the exofacial configuration of NCKX2, and asked whether the decrement may be abrogated in magnitude by increasing the $[Ca^{2+}]_o$ further. Fig. 14 C right panel illustrates two separate experimental measurements of Na^+-affinity of D548E, one made in the presence of 3.2 mM $[Ca^{2+}]_o$ and the other in the presence of 5 mM $[Ca^{2+}]_o$. The initial rates derived from the experiment carried out in the presence of 3.2 mM $[Ca^{2+}]_o$ were exceptionally higher than initial rates typically obtained with D548E (see Fig. 12 E and 14 C left panel), but the data in this case were not normalized to a value of 1.0 as in Fig. 14 C left panel. With the highest $[Ca^{2+}]_o$ tested (5 mM), the initial rate of free

$[Ca^{2+}]_i$ rise obtained with 150 mM Na^+ was at the same level as that obtained with lower $[Na^+]$ of 55-75 mM, while in the example shown with 3.2 mM $[Ca^{2+}]_o$, the rate at 150 mM Na^+ was still substantially less than the rate at 75 mM Na^+. The Hill plots fitted to the D548E data obtained in the presence of 3.2 mM and 5 mM $[Ca^{2+}]_o$ gave K_m values of ~23 mM Na^+, and ~36 mM Na^+ respectively (Hill coefficients of 3.1). Note that even at the very high $[Ca^{2+}]_o$ of 5 mM, the apparent K_m of D548E for $[Na^+]_i$ (~36 mM) remained substantially lower than that of wild-type NCKX2 (~55 mM Na^+ at 250 μM $[Ca^{2+}]_o$ and ~90 mM Na^+ at 2 mM $[Ca^{2+}]_o$).

As a final methodological issue, we investigated whether our assay was sensitive to shifts in apparent affinities for Na^+ towards higher concentrations, as might be expected for substitution of amino acid residues critical for liganding Na^+. In our initial screening of the single amino acid substitution constructs with fluo-3, we found that L549A displayed a prominent decrease in apparent affinity for Na^+, while its functional activity level was not greatly diminished as in many other single amino acid substitution constructs (Fig. 5 D); its level of activity when measured with fluo-4FF was comparable to that of D548E (see Fig. 12 B). We assayed HEK293 cells transiently transfected with L549A for Na^+-affinity with $[Ca^{2+}]_o$ of 250 μM and 2 mM (Fig. 14 D). We found that indeed the apparent affinity of L549A for Na^+ was significantly shifted to higher $[Na^+]$; the K_m obtained from the Hill plot fitted to the mean of initial rates of $[Ca^{2+}]_i$ rise for L549A (normalized to highest $[Na^+]$ of 200 mM) was 95 mM Na^+ (± SEM of 8 mM; Hill coefficient 2.7, Fig. 14 D left panel). Even when L549A was assayed in the presence of 2 mM $[Ca^{2+}]_o$, where wild-type NCKX2 displayed an apparent K_m for Na^+ of around 90 mM, the data points of L549A appeared to be far right-shifted with respect to the curve obtained with wild-type NCKX2, and could not be fit reliably with a Hill plot since V_{max} was predicted to be at a much higher $[Na^+]$ range (Fig. 14 D right panel).

CHAPTER FOUR: DISCUSSION

In this study, I had set out to modify a fluorescence based assay previously established in the lab of Dr. Paul Schnetkamp, so as to allow for the efficient screening of single amino acid substitution constructs of human NCKX2 for shifts in Na^+-affinity. The hypothesis we were addressing was that the amino acid residues previously found to confer sensitivity to Ca^{2+} and K^+ in NCKX2 would be the same ones found to affect the apparent affinity of NCKX2 for Na^+. This is in line with the accepted alternating access model for operation of secondary active transporters, where it is hypothesized that the amino acids found to be critical for defining apparent Ca^{2+} and K^+ affinities of NCKX2 line a binding pocket, or aqueous channel for the conduction of these ions, and it follows that these same residues would also be involved in liganding Na^+. In the process of devising an assay for screening NCKX2 mutants for Na^+-affinity (which relied on measurements of the Ca^{2+} influx mode of NCKX2), we additionally carried out a number of experiments aimed at examining the Ca^{2+} extrusion mode of NCKX2. An early observation of the Ca^{2+} extrusion mode of NCKX2 heterologously expressed in HEK293 cells suggested that Ca^{2+} fluxes mediated by NCKX2 were not completely reversible (see Fig. 6); this was reminiscent of observations made *in situ* in bovine retinal rod outer segments (Schnetkamp *et al*. 1991c; Schnetkamp and Szerencsei 1993; Schnetkamp 1995b). We decided to examine this apparent inactivation of Ca^{2+} clearance more closely, and in the following I will discuss those results, before returning to the original hypothesis to comment on the validity of the assay devised in this thesis for screening NCKX2 mutants for shifts in Na^+-affinity.

4. 1. NCKX2-mediated Ca^{2+} fluxes are not completely reversible due to inactivation

Early experiments investigating free $[Ca^{2+}]_i$ regulation by NCKX1 in bovine retinal rod outer segments indicated that although NCKX1 can be used to effectively load rod outer segments with Ca^{2+}, even at very low $[Ca^{2+}]_o$ of 20 nM, when the $[Ca^{2+}]$ gradient across the plasma membrane was reversed, NCKX1 was not competent in lowering $[Ca^{2+}]_i$ to below 100 nM (Schnetkamp *et al*. 1991c). Instead, NCKX1 operated in short bursts (< 20 s) of high $[Ca^{2+}]_i$ extrusion activity, followed by an abrupt decrease in the $[Ca^{2+}]_i$

extrusion rate, with final steady-state $[Ca^{2+}]_i$ levels considerably higher than would otherwise be predicted by thermodynamic considerations. It was later discovered that the internal disks of bovine retinal rod outer segments acted as a major membrane-bounded store for Ca^{2+} fluxes mediated by NCKX1, effectively sequestering Ca^{2+} transported to the cytoplasm (Schnetkamp and Szerencsei 1993). But, even when Ca^{2+} sequestration in rod outer segment internal disks was prevented by the use of low doses of the Ca^{2+} ionophore A23187, it was found that NCKX1 was nevertheless inactivated and did not lower $[Ca^{2+}]_i$ to the predicted level of less than 10 nM. The results shown in Fig. 6 A and B appeared remarkably similar to those obtained *in situ* with bovine rod outer segments. Hence, we first sought to define the cellular Ca^{2+} handling mechanisms that were operational and relevant to our free $[Ca^{2+}]_i$ measurements in NCKX2-transfected HEK293 cells. The results of Fig. 6 and 8, indicated that several Ca^{2+} handling mechanisms in HEK293 cells were competing with Ca^{2+} fluxes mediated by NCKX2, and the major contributing mechanism was mitochondrial Ca^{2+} sequestration. Specifically, it appeared that mitochondria were accumulating Ca^{2+} when free $[Ca^{2+}]_i$ reached relatively high levels in the μM range; this can be estimated by the use of the two probes – fluo-3 with sub-μM affinity for Ca^{2+} and fluo-4FF with μM affinity for Ca^{2+}. Also note that at low free $[Ca^{2+}]_i$ levels attained by the application of low $[Na^+]$ to NCKX2-transfected HEK293 cells, there was no apparent increase in the level of $[Ca^{2+}]_i$ reached with FCCP treatment (compare 10 mM Na^+ traces in Fig. 6 B and Fig. 6 C), whereas there was a marked difference in the level of $[Ca^{2+}]_i$ plateau reached when higher $[Na^+]$ was used to induce Ca^{2+} influx (compare 75 mM Na^+ traces in Fig. 6 B and Fig. 6 C). Hence, in subsequent experimentation, we ensured that we isolate, as best as practically possible, the activity of NCKX2 in mediating changes in free $[Ca^{2+}]_i$, by the use of the combination of Tg and FCCP to eliminate endoplasmic reticulum and mitochondrial Ca^{2+} sequestration respectively.

Next we defined the major condition under which the apparent inactivation of NCKX2 occurred. In Fig. 6, it was apparent that inactivation became more prominent as the $[Na^+]$ used was increased. This led us to conclude that inactivation was related to exposure to high $[Na^+]_i$, as had been well characterized in members of the NCX family

(Hilgemann *et al*. 1992a). However, since our measurements were based on the use of free $[Ca^{2+}]_i$ probes, and made use of the monovalent cation ionophore gramicidin to clamp alkali cations across the membrane, two potential issues had to be addressed – saturation of the Ca^{2+} probe, and competitive interactions between Na^+ and Ca^{2+}.

4. 2. Apparent inactivation is not due to saturation of Ca^{2+} probe

With respect to the issue of saturation of the intracellular Ca^{2+} probe, it was clear that with the use of fluo-3, and especially when NCKX2 activity was isolated by eliminating mitochondria, the free $[Ca^{2+}]_i$ measurements were subject to saturation effects. Therefore, fluo-4FF was used to make most of the experimental measurements where free $[Ca^{2+}]_i$ was driven to high levels, and we believe that this probe was most ideal and least susceptible to saturation for the range of free $[Ca^{2+}]_i$ measurements presented herein. To further substantiate that the apparent slowing of the $[Ca^{2+}]_i$ extrusion rate by NCKX2 when $[Ca^{2+}]_i$ loading was high and prolonged was not reflective of saturation of fluo-4FF, we used the yet lower Ca^{2+}-affinity probe fluo-5N, and still found a discernible difference in $[Ca^{2+}]_i$ extrusion kinetics when comparing short (40 s) and long (150 s) intracellular Na^+ exposure times (Fig. 9 C). The experiments carried out with the mutant constructs D548E and N572C also argue strongly against saturation of the dye being the cause of the diminishment of the $[Ca^{2+}]_i$ extrusion rate. In Fig. 13 A, there appeared a marked flattening of the $[Ca^{2+}]_i$ extrusion rate for D548E when the $[Ca^{2+}]_i$ level at the time of engaging of Ca^{2+} extrusion was comparable to the $[Ca^{2+}]_i$ attained with wild-type NCKX transfected HEK293 cells, and in the case of N572C the $[Ca^{2+}]_i$ was even substantially lower than those attained by wild-type NCKX2 transfected HEK293 cells, yet it was clear that fluo-4FF was responsive at that $[Ca^{2+}]_i$ level as illustrated by the traces for wild-type NCKX2 and E166D. Likewise, the experiment illustrated in Fig. 10 A argues strongly against saturation of the $[Ca^{2+}]_i$ probe; note that this experiment was actually carried out with fluo-3 which has a higher affinity for $[Ca^{2+}]_i$ and yet in the case where the assay was carried out in 150 mM KCl-EDTA medium and the Ca^{2+} loading was induced in wild-type NCKX2 transfected HEK293 cells with use of 250 μM free $[Ca^{2+}]_o$ and 20 mM Na^+, there were dynamic fluxes in $[Ca^{2+}]_i$ (both influx and efflux), but when the assay was carried out in

150 mM NaCl-EDTA medium (high $[Na^+]$ of 150 mM), there was marked inactivation of the Ca^{2+} extrusion rate from a $[Ca^{2+}]_i$ plateau that was lower than the $[Ca^{2+}]_i$ plateau for the measurement carried out in 150 mM KCl-EDTA medium.

4. 3. Apparent inactivation is not due to competitive Na^+-Ca^{2+} interactions

Secondly, with respect to potential Na^+/Ca^{2+} competitive interactions, we carried out a number of experiments to assess whether in fact competition between Na^+ and Ca^{2+} at the ion liganding sites of NCKX2 were influencing either our estimates of K_m for intracellular Na^+, or the apparent diminishment of $[Ca^{2+}]_i$ extrusion which we had termed Na^+_i-dependent inactivation. Firstly, the experiment illustrated in Fig. 9 A proved that Na^+_i-dependent inactivation occurred after exposure of NCKX2 to high cytoplasmic Na^+ for substantial periods of time (> 40 s), but not at earlier time points when, if anything, $[Ca^{2+}]_i$ extrusion rates might be expected to be slower since $[Ca^{2+}]_i$ levels had not reached the steady-state high plateau attained at later time points tested (80, 150, and 300 s following the addition of Na^+). Comparing the $[Ca^{2+}]_i$ clearance rates at the 110 s time point (80 s following the addition of 75 mM Na^+), and at the 180 s time point (150 s following the addition of 75 mM Na^+) would reveal that the $[Ca^{2+}]_i$ extrusion rate was slower at the later time point, despite that under both conditions $[Ca^{2+}]_i$ levels were similar (see also Fig. 9 C) and intracellular Na^+ applied in both cases was 75 mM. Another experiment that argued against competition between Na^+ and Ca^{2+} at the cytoplasmic configuration ion transport sites of NCKX2 is that illustrated in Fig. 10 B. When free $[Ca^{2+}]_o$ added was 10 μM, NCKX2 surprisingly did not appear to inactivate, despite being exposed to high intracellular Na^+ (75 mM) for 150 s. NCKX2 was in fact competent in rapidly extruding (the relatively low level) $[Ca^{2+}]_i$ back to baseline very rapidly, when if competitive interactions between Na^+ and Ca^{2+} were evident at the cytoplasmic configuration ion transport sites of NCKX2, we would have expected these to be more prominent in such a case. This result was also reminiscent of results reported by Hilgemann *et al*. (1992a) for the cardiac Na^+/Ca^{2+} exchanger, where it was found that inactivation not only required exposure of giant excised sarcolemma patches to high cytoplasmic Na^+ (> 100 mM), but also to high exoplasmic Ca^{2+} (2 mM; whereas 0.4 mM

Ca^{2+} substantially reduced the extent of Na^+_i-dependent inactivation). The argument presented therein was that reduction of exoplasmic $[Ca^{2+}]$ would be expected to shift a larger fraction of Na^+/Ca^{2+} exchangers in the membrane to the exofacial configuration, whereas Na^+_i-dependent inactivation is so called because it requires the binding of Na^+ to the cytoplasmic configuration transport sites, hence when $[Ca^{2+}]_o$ was reduced a smaller fraction of Na^+/Ca^{2+} exchangers was exposed to inactivating conditions.

We also carried out experiments that demonstrated that Na^+_i-dependent inactivation could be relieved, in a time-dependent manner, by reducing $[Na^+]$ (Fig. 11). Fig. 11 B shows that although the four different experimental traces commenced at relatively similar $[Ca^{2+}]_i$ levels, each trace, reflecting different ionic and timing conditions, assumed markedly different kinetics in $[Ca^{2+}]_i$ clearance. Only when $[Na^+]$ was reduced 4-fold (from 100 mM to 25 mM) was the $[Ca^{2+}]_i$ extruded effectively through NCKX; in the case where the $[Na^+]$ dilution was carried out after 150 s of $[Ca^{2+}]_i$ loading (i.e. after development of strong inactivation), the relief of inactivation was prolonged in comparison to the case where $[Na^+]$ dilution was carried out 40 s following $[Ca^{2+}]_i$ loading. In the two traces where $[Na^+]$ was not diluted, there was also a clear time-dependent difference in kinetics of $[Ca^{2+}]_i$ clearance. In the case where Ca^{2+} extrusion mode of NCKX2 was engaged at the earlier time point of 40 s following Ca^{2+} loading, $[Ca^{2+}]_i$ was cleared to a substantially lower level than when Ca^{2+} extrusion mode of NCKX2 was engaged 150 s following exposure to high $[Na^+]_i$ (Fig. 11 B).

4. 4. Comparison of NCKX2 Na^+_i-dependent inactivation with NCX I_1 inactivation, and retinal rod NCKX1 inactivation

The process of Na^+_i-dependent inactivation described herein for NCKX2 shares several features, as aforementioned, with the well-established process of Na^+_i-dependent inactivation characterized in the cardiac Na^+/Ca^{2+} exchanger NCX1, as well as in heterologously expressed NCX1. These features include the requirement for cytoplasmic configuration transport sites of NCKX2 or NCX1 to be saturated with relatively high $[Na^+]$, in our case 75 mM or higher $[Na^+]$ was required to observe strong inactivation, and in addition the observation that lowering $[Ca^{2+}]_o$ abrogated Na^+_i-dependent inactivation. It

must be pointed out though that Na^+_i-dependent inactivation has been characterized using very different methodology, namely electrophysiology in giant excised sarcolemma patches, whereas we have relied on measurements of changes in free $[Ca^{2+}]_i$ in intact cells (Hilgemann *et al*. 1992a). Hence there are also clear differences, as is the case for the $[Ca^{2+}]_o$ required to observe inactivation with NCX and NCKX. In the Hilgemann *et al*. (1992a) study, Na^+_i-dependent inactivation was typically observed with exoplasmic $[Ca^{2+}]$ of 2-8 mM, whereas it was abrogated when exoplasmic $[Ca^{2+}]$ was 0.4 mM. In our case we observed Na^+_i-dependent inactivation when free $[Ca^{2+}]_o$ was only 0.25 mM, whereas 0.01 mM was insufficient to produce inactivation. This may be related to the markedly different $[Ca^{2+}]_o$ affinities of NCX and NCKX; NCKX has a relatively high affinity for $[Ca^{2+}]_o$ with K_m values in the range 1-3 μM, as opposed to K_m values of 100-300 μM reported for NCX, with some studies citing even lower $[Ca^{2+}]_o$ affinities for NCX (Miura and Kimura 1989; Matsuoka and Hilgemann 1992; Linck *et al*. 1998; Blaustein and Lederer 1999; Iwamoto *et al*. 2000; Sheng *et al*. 2000; Szerencsei *et al*. 2001; Kang *et al*. 2005a; Ottolia *et al*. 2005; Visser *et al*. 2007). Hence, in our experiments we were confident that the exofacial configuration transport site(s) of NCKX2 were saturated with 250 μM $[Ca^{2+}]_o$, whereas 10 μM would not have been sufficient, and in the case of NCX 2 mM $[Ca^{2+}]_o$, but not 400 μM $[Ca^{2+}]_o$, would be sufficient to saturate the exofacial configuration Ca^{2+} transport site(s) (Hilgemann *et al*. 1992a).

The other distinction between our observations herein and those of Hilgemann *et al*. (1992a), is while in the latter Na^+_i-dependent inactivation was applicable to both the Ca^{2+} influx, as well as the Ca^{2+} efflux mode of NCX1, in our experiments, we could not distinguish whether Na^+_i-dependent inactivation affected the Ca^{2+} influx mode as it did for the Ca^{2+} extrusion mode of NCKX2. In fact, it appeared that despite prolonged exposure to high intracellular Na^+ levels, NCKX2 was continually engaged in Ca^{2+} influx, as evidenced by the experiment illustrated in Fig. 9 D, where the mitochondrial Ca^{2+} pool appeared to grow larger over time as a result of continual sequestration of cytoplasmic Ca^{2+} transported from the extracellular medium by NCKX2. In this respect NCKX2 inactivation reported herein resembles the inactivation process described earlier for NCKX1 *in situ* in retinal rod outer segments, where it appeared to affect the Ca^{2+} extrusion mode specifically; although

a difference is that under most experimental conditions used herein, we did not observe brief "bursts" of high activity Na^+/Ca^{2+} exchange preceding abrupt inactivation (Schnetkamp *et al*. 1991c; Schnetkamp and Szerencsei 1993; Schnetkamp 1995b). Our observations herein warrant future investigations to address whether Na^+_i-dependent inactivation indeed only affects the Ca^{2+} extrusion mode – electrophysiological patch clamp methods may prove useful in this regard to allow for more precise control over ionic conditions on both sides of the plasma membrane. It is also pertinent to investigate whether the large cytoplasmic loop of NCKX, which is a common structural feature shared with NCX – albeit with little to no amino acid sequence similarity, may be involved in Na^+_i-dependent inactivation as has been demonstrated with NCX (Hilgemann *et al*. 1992a; Matsuoka *et al*. 1993).

4. 5. Physiological conditions under which NCKX2 Na^+_i-dependent inactivation may be operational

Schnetkamp *et al*. (1993) argued that the process of inactivation of NCKX1 in retinal rod outer segments (where NCKX1 is the only Ca^{2+} transport mechanism aside from cyclic nucleotide gated channels) may serve to prevent unregulated extrusion of $[Ca^{2+}]_i$, that would otherwise lower $[Ca^{2+}]_i$ to unfavourably low levels (< 10 nM as predicted thermodynamically by the coupling ratio of 4 Na^+:1 Ca^{2+} + 1 K^+). Our measurements herein were made in intact whole cells where NCKX2 was not the only Ca^{2+} handling mechanism (Fig. 6 and Fig. 8), so it is not clear what functional purpose this regulatory feature might serve in a physiological context. Nevertheless, the condition of prolonged exposure to high levels of intracellular Na^+ are met in physiological settings where NCKX2 is found, namely in neuronal synaptic terminals. NCKX2 has been reported to be highly expressed at the mRNA transcript level in many regions of the mammalian brain, and two studies have reported antibody staining indicating that NCKX2 is preferentially targeted to plasma membrane of both pre- and post-synaptic neuronal compartments (Tsoi *et al*. 1998; Lee *et al*. 2002; Li and Lytton 2002; Lytton *et al*. 2002; Kim *et al*. 2003; Li *et al*. 2006). In small volume, restricted diffusion compartments such as axon terminals, high frequency stimulation is expected to result in substantial elevations in local concentrations of Na^+ and

Ca^{2+} through the opening of voltage-gated Na^+ and Ca^{2+} channels, and this may be prolonged (on the time scale of several seconds to a few minutes) depending on the duration and frequency of presynaptic nerve firing. For example, peaks of up to 80 mM $[Na^+]_i$ have been recorded (using fluorescent Na^+ indicator) in axon terminals of crayfish during tetanic stimulation (Zhong *et al*. 2001). A well documented observation in neuronal synaptic terminals is that Ca^{2+} transients induced by neuronal stimulation exceed temporally the duration of the stimulation itself (Regehr *et al*. 1994; Habets and Borst 2005). Among the explanations put forth for this observation were Na^+/Ca^{2+} exchangers operating in the Ca^{2+} influx mode (due to the depolarized membrane and compromised Na^+ gradient), as well as delayed release of sequestered Ca^{2+} from mitochondria (Zhong *et al*. 2001; Tang and Zucker 1997; García-Chacón *et al*. 2006). Since NCKX2 appears to be a major Ca^{2+} clearance mechanism in mammalian neuronal synaptic terminals, Na^+_i-dependent inactivation of Ca^{2+} extrusion may be another contributor to the depression of Ca^{2+} clearance in synaptic terminals that is related to elevation of intracellular Na^+ (Scheuss *et al*. 2006).

4. 6. Validity of assay developed to measure Na^+-affinity of NCKX2

The measurements made herein for the apparent affinity of NCKX2 for cytoplasmic Na^+ yielded K_m values of between 50-56 mM (Hill coefficients 2.6-2.9; Fig. 12 and Fig. 14). These values can be compared with previously reported values of 30-40 mM cytoplasmic Na^+ measured for NCKX1 using similar method (use of alkali cation ionophores) in bovine retinal rod outer segments (Schnetkamp *et al*. 1995). The other measurement made on NCKX2 heterologously expressed in the High Five insect cell line yielded a relationship of $[Ca^{2+}]_o$ influx to cytoplasmic Na^+ that did not appear to saturate (K_m>100 mM Na^+); the reason for the discrepancy is not clear at this time, but may be related to the use of the insect (High Five cells) as opposed to the mammalian heterologous expression system used herein (Winkfein *et al*. 2003). The rationale for selecting the assay conditions used herein, specifically the choice of 150 mM KCl as the base medium is based on earlier studies where it was found that high $[K^+]$ favoured Ca^{2+} influx mode of NCKX1 in rod outer segments by minimizing inhibitory interactions between Na^+ and Ca^{2+} at the

exofacial configuration transport sites of NCKX (Schnetkamp *et al*. 1991b). The use of gramicidin by necessity also resulted in the introduction of K^+ on the cytoplasmic side of the membrane, which is also expected to result in competition with cytoplasmic Na^+. However we believe that this method is the best available compromise to achieve our goal of efficient screening through a large (> 100) number of single amino acid substitution constructs for relative shifts (with respect to the value we obtain for wild-type NCKX2) in cytoplasmic Na^+-affinity. With respect to the $[Ca^{2+}]_o$ selected for carrying out our assay, the rationale behind selecting a concentration of 250 μM is that firstly, from our previous knowledge, it is sufficient to saturate the exofacial configuration transport sites of NCKX2 (K_m of 1-3 μM), and secondly, to minimize potential interfering Ca^{2+} fluxes – mainly store-operated Ca^{2+} entry. Most of our measurements were made after treating NCKX2 transfected HEK293 cells with Tg in a medium that was Ca^{2+} free (100 μM EDTA) to control external Ca^{2+}, since NCKX2 has a high affinity for $[Ca^{2+}]_o$ and is capable of transporting external Ca^{2+} even at sub-micromolar concentrations (Schnetkamp *et al*. 1991b). However, these precise conditions – prolonged incubation in Ca^{2+} free media, and the use of Tg – are known to activate store-operated Ca^{2+} entry, which is a ubiquitous cellular mechanism for replenishing intracellular Ca^{2+} stores (Hoth *et al*. 1997; Prakriya and Lewis 2003). Hence we chose 250 μM $[Ca^{2+}]_o$, since significant contaminating Ca^{2+} fluxes through store-operated Ca^{2+} channels typically require $[Ca^{2+}]$ in the millimolar range (Hoth and Penner 1993; Tanneur *et al*. 2002; Bogeski *et al*. 2006). As previously stated, NCKX2 K_m values for internal Na^+ reported in our measurements herein are in line with those measured under similar conditions for NCKX1 *in situ* in retinal rod outer segments, so the apparent right-ward shift in the K_m value when the internal Na^+-dependence assay was carried out in the presence of 2 mM $[Ca^{2+}]_o$ was surprising. One interpretation is that we have under estimated the K_m for cytoplasmic Na^+ in the condition with 250 μM $[Ca^{2+}]_o$, because 250 μM $[Ca^{2+}]$ is too low to overcome potential competitive interactions with the $[Na^+]$ added to the cuvette (where Na^+ is present not only on the cytoplasmic side to drive Ca^{2+} influx through NCKX2, but also on the extracellular side). Another plausible interpretation is that the use of 2 mM $[Ca^{2+}]_o$ introduced contaminating Ca^{2+} fluxes, likely from store-operated Ca^{2+} channels, in the short period (10-30 s) before engaging the Ca^{2+}

influx mode of NCKX2 by the addition of Na^+. Such extraneous Ca^{2+} fluxes have been observed in some experimental measurements, and are observable with the use of the high affinity Ca^{2+} probes fluo-3 or fluo-4. An example of this extraneous run up of intracellular Ca^{2+} (before the addition of Na^+) is illustrated in the traces of Fig. 10 A, where the probe used was fluo-3 (see also Fig. 6 C). The run up of intracellular Ca^{2+}, when observed with high affinity fluo-3 or fluo-4, was always larger in magnitude when 2 mM Ca^{2+} was added to the cuvette (instead of 250 μM; not shown), corroborating that a channel-like mechanism was driving the $[Ca^{2+}]_i$ build-up. This cytoplasmic Ca^{2+} may in turn influence NCKX2 by some, as of yet, unidentified mechanism. To this end, it is interesting to note that previous measurements of heterologously expressed NCKX2-mediated, Na^+-driven, outward currents in whole-cell patch-clamped HEK293 cells increased by 50% when free Ca^{2+} in the patch pipette was elevated from zero to 1 μM (Dong *et al*. 2001). Thus it may be that the presence of elevated cytoplasmic $[Ca^{2+}]$ after the addition of 2 mM $[Ca^{2+}]_o$ in our assay had an influence on NCKX2 mediated changes in free cytoplasmic $[Ca^{2+}]$ and secondarily our estimate of apparent K_m for internal Na^+. This warrants further future investigation.

When our assay herein was tested with a residue that was expected to show a shift in affinity for Na^+ – D548E, indeed we were able to detect a substantial shift from the value obtained for wild-type NCKX2 (Fig. 12 and Fig. 14). D548E in fact, along with N572C, displayed characteristic decrease in the initial rate of activity when $[Na^+]$ was elevated beyond their apparent V_{max}, and it is this observation, we believe, that reflects the appearance of competitive interactions between Na^+ and Ca^{2+}. Since we did not observe such a pattern with wild-type NCKX2 under either assay condition (250 μM or 2 mM $[Ca^{2+}]_o$), we dismiss the interpretation of the apparent right-shift in the K_m value for Na^+ obtained for wild-type NCKX2 under 2 mM $[Ca^{2+}]_o$ being resultant of Na^+ competing with Ca^{2+} at the exofacial configuration transport sites of NCKX2. This is based on well-established observations that, unlike in NCX, ion affinities for NCKX are symmetric with respect to the membrane configuration of the transport sites (Schnetkamp *et al*. 1989; Schnetkamp *et al*. 1991b; Schnetkamp 1991; Schnetkamp *et al*. 1995). Regardless, the aim of this thesis was to develop the assay so as to allow for efficient screening of the large number of single amino acid substitution constructs of NCKX2 to be assayed for relative

shifts in Na^+-affinity, and as illustrated in Fig. 12 and Fig. 14, the relative shift for D548E and N572C toward lower K_m values for cytoplasmic Na^+ with respect to wild-type NCKX2 were internally consistent whether the assay was carried out in the presence of 250 μM or 2 mM $[Ca^{2+}]_o$. The results obtained with D548E and N572C also support the proposal that Na^+_i-dependent inactivation characterized in this thesis is related to, and dependent on saturation of the cytoplasmic configuration transport sites of NCKX2 with Na^+. Hence both these constructs, D548E and N572C, displayed prominent inactivation at substantially lower $[Na^+]_i$ than for wild-type NCKX2 (Fig. 13 A).

Another residue, adjacent to the critical acidic residue Asp^{548}, Leu^{549} was also tested to confirm whether the assay would be suitable to detect shifts in the opposite direction, i.e. toward higher K_m values for cytoplasmic Na^+; again this proved to be the case whether the assay was carried out with 250 μM or 2 mM $[Ca^{2+}]_o$ (Fig. 14 D). At this point, insufficient data have been accumulated to fully substantiate or refute the main hypothesis proposed in this thesis, that amino acid residues found to influence the apparent affinity of NCKX2 for Ca^{2+} and K^+ would also prove to be influential on the apparent affinity for Na^+. Nevertheless the results presented herein for Na^+-affinity with D548E and L549A, taken together with earlier results for Ca^{2+} and K^+, seem to suggest that at least this critical region of NCKX2 does display shifts for all transported ions when mutated (Kang *et al*. 2005a; Visser *et al*. 2007). The observation that when assaying for shifts in Na^+-affinity, mutation of nearby residues can have opposite effects on the direction of shift (where D548E shifts Na^+-affinity toward higher $[Na^+]$, but the adjacent L549A shifts Na^+-affinity in the opposite direction), has also been reported in the results of Ottolia *et al*. (2005) when assaying NCX1 for shifts in Na^+-affinity.

4. 7. Concluding remarks

In conclusion, the results presented in this thesis have demonstrated an effective assay to test mutant constructs of NCKX2 for shifts in apparent Na^+-affinity, and indicated that shifts do occur for three amino acid residue substitutions in functionally critical domains. Future experimentation will resume to accumulate information on other residues and domains of NCKX2 that are thought to be important for liganding and transporting

Na^+. Moreover, this thesis has re-examined the process of inactivation of NCKX2, and has defined the conditions under which inactivation of NCKX2 transport occurs. More specifically, we now know that it shares certain features with inactivation of NCKX1 *in situ* (prominent inactivation of Ca^{2+} extrusion mode), as well as inactivation of the distantly related cardiac exchanger NCX1 (requirement for saturating cytoplasmic Na^+, and saturating exoplasmic Ca^{2+}). Future experimentation will be aimed at investigating the structural elements of NCKX2 responsible for mediating Na^+_i-dependent inactivation.

REFERENCES

Altimimi, H. F., and Schnetkamp, P. P. M. 2007. Na^+-dependent inactivation of the retinal cone/brain Na^+/Ca^{2+}-K^+ exchanger NCKX2. J. Biol. Chem. **282**: 3720-3729.

Artigas, P., and Gadsby, D. C. 2003. Na^+/K^+-pump ligands modulate gating of palytoxin-induced ion channels. Proc. Natl. Acad. Sci. U. S. A. **100**: 501-505.

Baker, P. F., Blaustein, M. P., Hodgkin, A. L., and Steinhardt, R. A. 1969. The influence of calcium on sodium efflux in squid axons. J. Physiol. **200**: 431-458.

Blaustein, M. P., and Lederer, W. J. 1999. Sodium/calcium exchange: its physiological implications. Physiol. Rev. **79**: 763-854.

Bogeski, I., Bozem, M., Sternfeld, L., Hofer, H. W., and Schulz, I. 2006. Inhibition of protein tyrosine phosphatase 1B by reactive oxygen species leads to maintenance of Ca^{2+} influx following store depletion in HEK 293 cells. Cell Calcium **40**: 1-10.

Bruns, D., Engert, F., and Lux, H. D. 1993. A fast activating presynaptic reuptake current during serotonergic transmission in identified neurons of Hirudo. Neuron **10**: 559-572.

Cai, X., and Lytton, J. 2004. The cation/Ca^{2+} exchanger superfamily: phylogenetic analysis and structural implications. Mol. Biol. Evol. **21**: 1692-1703.

Carafoli, E. 1991. Calcium pump of the plasma membrane. Physiol. Rev. **71**: 129-153.

Cervetto, L., Lagnado, L., Perry, R. J., Robinson, D. W., and McNaughton, P. A. 1989. Extrusion of calcium from rod outer segments is driven by both sodium and potassium gradients. Nature **337**: 740-743.

Chen, L., Koh, D. S., and Hille, B. 2003. Dynamics of calcium clearance in mouse pancreatic β-cells. Diabetes **52**: 1723-1731.

Cooper, C. B., Szerencsei, R. T., and Schnetkamp, P. P. M. 2000. Spectrofluorometric detection of Na^+/Ca^{2+}-K^+ exchange. Methods Enzymol. **315**: 847-864.

Dahan, D., Spanier, R., and Rahamimoff, H. 1991. The modulation of rat brain Na^+-Ca^{2+} exchange by K^+. J. Biol. Chem. **266**: 2067-2075.

David, G., and Barrett, E. F. 2000. Stimulation-evoked increases in cytosolic [Ca^{2+}] in mouse motor nerve terminals are limited by mitochondrial uptake and are temperature-dependent. J. Neurosci. **20**: 7290-7296.

DeFelice, L. J. and Goswami, T. 2007. Transporters as channels. Annu. Rev. Physiol. **69**: 87-112.

Dong, H., Light, P. E., French, R. J., and Lytton, J. 2001. Electrophysiological characterization and ionic stoichiometry of the rat brain K^+-dependent Na^+/Ca^{2+} exchanger, NCKX2. J. Biol. Chem. **276**: 25919-25928.

Dong, H., Dunn, J., and Lytton, J. 2002. Stoichiometry of the Cardiac Na^+/Ca^{2+} exchanger NCX1.1 measured in transfected HEK cells. Biophys. J. **82**: 1943-1952.

Dong, H., Jiang, Y., Triggle, C. R., Li, X., and Lytton, J. 2006. Novel role for K^+-dependent Na^+/Ca^{2+} exchangers in regulation of cytoplasmic free Ca^{2+} and contractility in arterial smooth muscle. Am. J. Physiol. Heart Circ. Physiol. **291**: H1226-H1235.

Duchen, M. R. 2000. Mitochondria and Ca^{2+} in cell physiology and pathophysiology. Cell Calcium **28**: 339-348.

Duman, J. G., Chen, L., and Hille, B. 2008. Calcium transport mechanisms of PC12 cells. J. Gen. Physiol. **131**: 307-323.

Fujioka, Y., Komeda, M., and Matsuoka, S. 2000. Stoichiometry of Na^+-Ca^{2+} exchange in inside-out patches excised from guinea-pig ventricular myocytes. J. Physiol. **523**: 339-351.

García-Chacón, L. E., Nguyen, K. T., David, G., and Barrett, E. F. 2006. Extrusion of Ca^{2+} from mouse motor terminal mitochondria via a Na^+-Ca^{2+} exchanger increases post-tetanic evoked release. J. Physiol. **574**: 663-675.

Ginger, R. S., Askew, S. E., Ogborne, R. M., Wilson, S., Ferdinando, D., Dadd, T., Smith, A. M., Kazi, S., Szerencsei, R. T., Winkfein, R. J., Schnetkamp, P. P., and Green, M. R. 2008. SLC24A5 encodes a *trans*-Golgi network protein with potassium-dependent sodium-calcium exchange activity that regulates human epidermal melanogenesis. J. Biol. Chem. **283**: 5486-5495.

Habermann, E. 1989. Palytoxin acts through Na^+,K^+-ATPase. Toxicon **27**: 1171-1187.

Habets, R. L. and Borst, J. G. 2005. Post-tetanic potentiation in the rat calyx of Held synapse. J. Physiol. **564**: 173-187.

Hilgemann, D. W., and Ball, R. 1996. Regulation of cardiac Na^+,Ca^{2+} exchange and K_{ATP} potassium channels by PIP_2. Science **273**: 956-959.

Hilgemann, D. W., Matsuoka, S., Nagel, G. A., and Collins, A. 1992a. Steady-state and dynamic properties of cardiac sodium-calcium exchange. Sodium-dependent inactivation. J. Gen. Physiol. **100**: 905-932.

Hilgemann, D. W., Collins, A., and Matsuoka, S. 1992b. Steady-state and dynamic properties of cardiac sodium-calcium exchange. Secondary modulation by cytoplasmic calcium and ATP. J. Gen. Physiol. **100**: 933-961.

Hoth, M., and Penner, R. 1993. Calcium release-activated calcium current in rat mast cells. J. Physiol. **465**: 359-386.

Hoth, M., Fanger, C. M., and Lewis, R. S. 1997. Mitochondrial regulation of store-operated calcium signaling in T lymphocytes. J. Cell Biol. **137**: 633-648.

Iwamoto, T., Watano, T., and Shigekawa, M. 1996. A novel isothiourea derivative selectively inhibits the reverse mode of Na^+/Ca^{2+} exchange in cells expressing NCX1. J. Biol. Chem. **271**: 22391-7.

Iwamoto, T., Uehara, A., Imanaga, I., and Shigekawa, M. 2000. The Na^+/Ca^{2+} exchanger NCX1 has oppositely oriented reentrant loop domains that contain conserved aspartic acids whose mutation alters its apparent Ca^{2+} affinity. J. Biol. Chem. **275**: 38571-38580.

Jardetzky, O. 1966. Simple allosteric model for membrane pumps. Nature **211**: 969-970.

Jeon, D., Yang, Y.M., Jeong, M.J., Philipson, K.D., Rhim, H., and Shin, H.S. 2003. Enhanced learning and memory in mice lacking Na^+/Ca^{2+} exchanger 2. Neuron **38**: 965-976.

Kang, K., and Schnetkamp, P. P. M. 2003. Signal sequence cleavage and plasma membrane targeting of the retinal rod NCKX1 and cone NCKX2 Na^+/Ca^{2+}-K^+ exchangers. Biochemistry **42**: 9438-9445.

Kang, K. J., Kinjo, T. G., Szerencsei, R. T., and Schnetkamp, P. P. M. 2005a. Residues contributing to the Ca^{2+} and K^+ binding pocket of the NCKX2 Na^+/Ca^{2+}-K^+ exchanger. J. Biol. Chem. **280**: 6823-6833.

Kang, K. J., Shibukawa, Y., Szerencsei, R. T., and Schnetkamp, P. P. M. 2005b. Substitution of a single residue, Asp^{575}, renders the NCKX2 K^+-dependent Na^+/Ca^{2+} exchanger independent of K^+. J. Biol. Chem. **280**: 6834-6839.

Kang, T. M., and Hilgemann, D. W. 2004. Multiple transport modes of the cardiac Na^+/Ca^{2+} exchanger. Nature **427**: 544-548.

Kim, M. H., Lee, S. H., Park, K. H., Ho, W. K., and Lee, S. H. 2003. Distribution of K^+-dependent Na^+/Ca^{2+} exchangers in the rat supraoptic magnocellular neuron is polarized to axon terminals. J. Neurosci. **23**: 11673-11680.

Kim, M. H., Korogod, N., Schneggenburger, R., Ho, W. K., and Lee, S. H. 2005. Interplay between Na^+/Ca^{2+} exchangers and mitochondria in Ca^{2+} clearance at the calyx of Held. J. Neurosci. **25**: 6057-6065.

Kim, T. S., Reid, D. M., and Molday, R. S. 1998. Structure-function relationships and localization of the Na/Ca-K exchanger in rod photoreceptors. J. Biol. Chem. **273**: 16561-16567.

Kimura, M., Aviv, A., and Reeves, J. P. 1993. K^+-dependent Na^+/Ca^{2+} exchange in human platelets. J. Biol. Chem. **268**: 6874-6877.

Kimura, M., Jeanclos, E. M., Donnelly, R. J., Lytton, J., Reeves, J. P., and Aviv, A. 1999. Physiological and molecular characterization of the Na^+/Ca^{2+} exchanger in human platelets. Am. J. Physiol. **277**: H911-H917.

Kinjo, T. G., Szerencsei, R. T., Winkfein, R. J., Kang, K., and Schnetkamp, P. P. M. 2003. Topology of the retinal cone NCKX2 Na/Ca-K exchanger. Biochemistry **42**: 2485-2491.

Kinjo, T. G., Kang, K., Szerencsei, R. T., Winkfein, R. J., and Schnetkamp, P. P. M. 2005. Site-directed disulfide mapping of residues contributing to the Ca^{2+} and K^+ binding pocket of the NCKX2 Na^+/Ca^{2+}-K^+ exchanger. Biochemistry **44**: 7787-7795.

Kraev, A., Quednau, B. D., Leach, S., Li, X. F., Dong, H., Winkfein, R., Perizzolo, M., Cai, X., Yang, R., Philipson, K. D., and Lytton, J. 2001. Molecular cloning of a third member of the potassium-dependent sodium-calcium exchanger gene family, NCKX3. J. Biol. Chem. **276**: 23161-23172.

Lagnado, L., Cervetto, L., and McNaughton, P. A. 1988. Ion transport by the Na-Ca exchange in isolated rod outer segments. Proc. Natl. Acad. Sci. U. S. A. **85**: 4548-4552.

Lamason, R. L., Mohideen, M. A., Mest, J. R., Wong, A. C., Norton, H. L., Aros, M. C., Jurynec, M. J., Mao, X., Humphreville, V. R., Humbert, J. E., Sinha, S., Moore, J. L., Jagadeeswaran, P., Zhao, W., Ning, G., Makalowska, I., McKeigue, P. M., O'donnell, D., Kittles, R., Parra, E. J., Mangini, N. J., Grunwald, D. J., Shriver, M. D., Canfield, V. A., and Cheng, K. C. 2005. SLC24A5, a putative cation exchanger, affects pigmentation in zebrafish and humans. Science **310**: 1782-1786.

Lee, J. Y., Visser, F., Lee, J. S., Lee, K. H., Soh, J. W., Ho, W. K., Lytton, J., and Lee, S. H. 2006. Protein kinase C-dependent enhancement of activity of rat brain NCKX2 heterologously expressed in HEK293 cells. J. Biol. Chem. **281**: 39205-39216.

Lee, S. H., Kim, M. H., Park, K. H., Earm, Y. E., and Ho, W. K. 2002. K^+-dependent Na^+/Ca^{2+} exchange is a major Ca^{2+} clearance mechanism in axon terminals of rat neurohypophysis. J. Neurosci. **22**: 6891-6899.

Lee, S. L., Yu, A. S., and Lytton, J. 1994. Tissue-specific expression of Na^+-Ca^{2+} exchanger isoforms. J. Biol. Chem. **269**: 14849-14852.

Li, X. F., and Lytton, J. 2002. Differential expression of Na/Ca exchanger and Na/Ca + K exchanger transcripts in rat brain. Ann. N. Y. Acad. Sci. **976**: 64-66.

Li, X. F., Kraev, A. S., and Lytton, J. 2002. Molecular cloning of a fourth member of the potassium-dependent sodium-calcium exchanger gene family, NCKX4. J. Biol. Chem. **277**: 48410-48417.

Li, X. F., Kiedrowski, L., Tremblay, F., Fernandez, F. R., Perizzolo, M., Winkfein, R. J., Turner, R. W., Bains, J. S., Rancourt, D. E., and Lytton, J. 2006. Importance of K^+-dependent Na^+/Ca^{2+}-exchanger 2, NCKX2, in motor learning and memory. J. Biol. Chem. **281**: 6273-6282.

Li, Z., Nicoll, D. A., Collins, A., Hilgemann, D. W., Filoteo, A. G., Penniston, J. T., Weiss, J. N., Tomich, J. M., and Philipson, K. D. 1991. Identification of a peptide inhibitor of the cardiac sarcolemmal Na^+-Ca^{2+} exchanger. J. Biol. Chem. **266**: 1014-1020.

Li, Z., Matsuoka, S., Hryshko, L. V., Nicoll, D. A., Bersohn, M. M., Burke, E. P., Lifton, R. P., and Philipson, K. D. 1994. Cloning of the NCX2 isoform of the plasma membrane Na^+-Ca^{2+} exchanger. J. Biol. Chem. **269**: 17434-17439.

Linck, B., Qiu, Z., He, Z., Tong, Q., Hilgemann, D. W., and Philipson, K. D. 1998. Functional comparison of the three isoforms of the Na^+/Ca^{2+} exchanger (NCX1, NCX2, NCX3). Am. J. Physiol. **274**: C415-C423.

Lytton, J. 2007. Na^+/Ca^{2+} exchangers: three mammalian gene families control Ca^{2+} transport. Biochem. J. **406**: 365-382.

Lytton, J., Li, X. F., Dong, H., and Kraev, A. 2002. K^+-dependent Na^+/Ca^{2+} exchangers in the brain. Ann. N. Y. Acad. Sci. **976**: 382-393.

Matsuoka, S., and Hilgemann, D. W. 1992. Steady-state and dynamic properties of cardiac sodium-calcium exchange. Ion and voltage dependencies of the transport cycle. J. Gen. Physiol. **100**: 963-1001.

Matsuoka, S., Nicoll, D. A., Reilly, R. F., Hilgemann, D. W., and Philipson, K. D. 1993. Initial localization of regulatory regions of the cardiac sarcolemmal Na^+-Ca^{2+} exchanger. Proc. Natl. Acad. Sci. U. S. A. **90**: 3870-3874.

Matsuoka, S., Nicoll, D. A., Hryshko, L. V., Levitsky, D. O., Weiss, J. N., and Philipson, K. D. 1995. Regulation of the cardiac Na^+-Ca^{2+} exchanger by Ca^{2+}. Mutational analysis of the Ca^{2+}-binding domain. J. Gen. Physiol. **105**: 403-420.

Matsuoka, S., Nicoll, D. A., He, Z., and Philipson, K. D. 1997. Regulation of cardiac Na^+-Ca^{2+} exchanger by the endogenous XIP region. J. Gen. Physiol. **109**: 273-286.

Miura, Y., and Kimura, J. 1989. Sodium-calcium exchange current. Dependence on internal Ca and Na and competitive binding of external Na and Ca. J. Gen. Physiol. **93**: 1129-1145.

Nicoll, D. A., Longoni, S., and Philipson, K. D. 1990. Molecular cloning and functional expression of the cardiac sarcolemmal Na^+-Ca^{2+} exchanger. Science **250**: 562-565.

Nicoll, D. A., Quednau, B. D., Qui, Z., Xia, Y. R., Lusis, A. J., and Philipson, K. D. 1996. Cloning of a third mammalian Na^+-Ca^{2+} exchanger, NCX3. J. Biol. Chem. **271**: 24914-24921.

Nicoll, D. A., Ottolia, M., Lu, L., Lu, Y., and Philipson, K. D. 1999. A new topological model of the cardiac sarcolemmal Na^+-Ca^{2+} exchanger. J. Biol. Chem. **274**: 910-917.

Niedergerke, R. 1963. Movements of Ca in frog heart ventricles at rest and during contractures. J. Physiol. **167**: 515-550.

Ottolia, M., Nicoll, D. A., and Philipson, K. D. 2005. Mutational analysis of the α-1 repeat of the cardiac Na^+-Ca^{2+} exchanger. J. Biol. Chem. **280**: 1061-1069.

Paillart, C., Winkfein, R. J., Schnetkamp, P. P., and Korenbrot, J. I. 2007. Functional characterization and molecular cloning of the K^+-dependent Na^+/Ca^{2+} exchanger in intact retinal cone photoreceptors. J. Gen. Physiol. **129**: 1-16.

Prakriya, M., and Lewis, R. S. 2003. CRAC channels: activation, permeation, and the search for a molecular identity. Cell Calcium **33**: 311-321.

Prasad, V., Okunade, G. W., Miller, M. L., and Shull, G. E. 2004. Phenotypes of SERCA and PMCA knockout mice. Biochem. Biophys. Res. Commun. **322**: 1192-1203.

Prinsen, C. F., Szerencsei, R. T., and Schnetkamp, P. P. M. 2000. Molecular cloning and functional expression of the potassium-dependent sodium-calcium exchanger from human and chicken retinal cone photoreceptors. J. Neurosci. **20**: 1424-1434.

Pyrski, M., Koo, J. H., Polumuri, S. K., Ruknudin, A. M., Margolis, J. W., Schulze, D. H., and Margolis, F. L. 2007. Sodium/calcium exchanger expression in the mouse and rat olfactory systems. J. Comp. Neurol. **501**: 944-958.

Quednau, B. D., Nicoll, D. A., and Philipson, K. D. 2004. The sodium/calcium exchanger family–SLC8. Pflügers Arch. **447**: 543-548.

Reeves, J. P., and Hale, C. C. 1984. The stoichiometry of the cardiac sodium-calcium exchange system. J. Biol. Chem. **259**: 7733-7739.

Regehr, W. G., Delaney, K. R., and Tank, D. W. 1994. The role of presynaptic calcium in short-term enhancement at the hippocampal mossy fiber synapse. J. Neurosci. **14**: 523-537.

Reiländer, H., Achilles, A., Friedel, U., Maul, G., Lottspeich, F., and Cook, N. J. 1992. Primary structure and functional expression of the Na/Ca,K-exchanger from bovine rod photoreceptors. EMBO J. **11**: 1689-1695.

Reuter, H., and Seitz, N. 1968. The dependence of calcium efflux from cardiac muscle on temperature and external ion composition. J. Physiol. **195**: 451-470.

Ruknudin, A. M., Wei, S. K., Haigney, M. C., Lederer, W. J., and Schulze, D. H. 2007. Phosphorylation and other conundrums of Na/Ca exchanger, NCX1. Ann. N. Y. Acad. Sci. **1099**: 103-118.

Sampath, A. P., Matthews, H. R., Cornwall, M. C., and Fain, G. L. 1998. Bleached pigment produces a maintained decrease in outer segment Ca^{2+} in salamander rods. J. Gen. Physiol. **111**: 53-64.

Scheuss, V., Yasuda, R., Sobczyk, A., and Svoboda, K. 2006. Nonlinear [Ca^{2+}] signaling in dendrites and spines caused by activity-dependent depression of Ca^{2+} extrusion. J. Neurosci. **26**: 8183-8194.

Schnetkamp, P. P. M. 1986. Sodium-calcium exchange in the outer segments of bovine rod photoreceptors. J. Physiol. **373**: 25-45.

Schnetkamp, P. P. M. 1989. Na-Ca or Na-Ca-K exchange in rod photoreceptors. Prog. Biophys. Mol. Biol. **54**: 1-29.

Schnetkamp, P. P. M. 1991. Optical measurements of Na-Ca-K exchange currents in intact outer segments isolated from bovine retinal rods. J. Gen. Physiol. **98**: 555-573.

Schnetkamp, P. P. M. 1995a. Chelating properties of the Ca^{2+} transport site of the retinal rod Na-Ca+K exchanger: evidence for a common Ca^{2+} and Na^{+} binding site. Biochemistry **34**: 7282-7287.

Schnetkamp, P. P. M. 1995b. How does the retinal rod Na-Ca+K exchanger regulate cytosolic free Ca^{2+}? J. Biol. Chem. **270**: 13231-13239.

Schnetkamp, P. P. M. 1995c. Calcium homeostasis in vertebrate retinal rod outer segments. Cell Calcium **18**: 322-30.

Schnetkamp, P. P. M. 2004. The *SLC24* Na^+/Ca^{2+}-K^+ exchanger family: vision and beyond. Pflügers Arch. **447**: 683-688.

Schnetkamp, P. P. M., and Szerencsei, R. T. 1991. Effect of potassium ions and membrane potential on the Na-Ca-K exchanger in isolated intact bovine rod outer segments. J. Biol. Chem. **266**: 189-197.

Schnetkamp, P. P. M., and Szerencsei, R. T. 1993. Intracellular Ca^{2+} sequestration and release in intact bovine retinal rod outer segments. Role in inactivation of Na-Ca+K exchange. J. Biol. Chem. **268**: 12449-12457.

Schnetkamp, P. P. M., Basu, D. K., and Szerencsei, R. T. 1989. Na^+-Ca^{2+} exchange in bovine rod outer segments requires and transports K^+. Am. J. Physiol. **257**: C153-C157.

Schnetkamp, P. P. M., Szerencsei, R. T., and Basu, D. K. 1991a. Unidirectional Na^+, Ca^{2+}, and K^+ fluxes through the bovine rod outer segment Na-Ca-K exchanger. J. Biol. Chem. **266**: 198-206.

Schnetkamp, P. P. M., Li, X. B., Basu, D. K., and Szerencsei, R. T. 1991b. Regulation of free cytosolic Ca^{2+} concentration in the outer segments of bovine retinal rods by Na-Ca-K exchange measured with fluo-3. I. Efficiency of transport and interactions between cations. J. Biol. Chem. **266**: 22975-22982.

Schnetkamp, P. P. M., Basu, D. K., Li, X. B., and Szerencsei, R. T. 1991c. Regulation of intracellular free Ca^{2+} concentration in the outer segments of bovine retinal rods by Na-Ca-K exchange measured with fluo-3. II. Thermodynamic competence of transmembrane Na^+ and K^+ gradients and inactivation of Na^+-dependent Ca^{2+} extrusion. J. Biol. Chem. **266**: 22983-22990.

Schnetkamp, P. P. M., Tucker, J. E., and Szerencsei, R. T. 1995. Ca^{2+} influx into bovine retinal rod outer segments mediated by $Na^+/Ca^{2+}/K^+$ exchange. Am. J. Physiol. **269**: C1153-C1159.

Schwarz, E. M., and Benzer, S. 1997. *Calx*, a Na-Ca exchanger gene of *Drosophila melanogaster*. Proc. Natl. Acad. Sci. U. S. A. **94**: 10249-10254.

Sheng, J. Z., Prinsen, C. F., Clark, R. B., Giles, W. R., and Schnetkamp, P. P. M. 2000. Na^+-Ca^{2+}-K^+ currents measured in insect cells transfected with the retinal cone or rod Na^+-Ca^{2+}-K^+ exchanger cDNA. Biophys. J. **79**: 1945-1953.

Strehler, E. E., and Zacharias, D. A. 2001. Role of alternative splicing in generating isoform diversity among plasma membrane calcium pumps. Physiol. Rev. **81**: 21-50.

Sokolow, S., Manto, M., Gailly, P., Molgó, J., Vandebrouck, C., Vanderwinden, J.M., Herchuelz, A., and Schurmans, S. 2004. Impaired neuromuscular transmission and skeletal muscle fiber necrosis in mice lacking Na/Ca exchanger 3. J. Clin. Invest. **113**: 265-273.

Szerencsei, R. T., Tucker, J. E., Cooper, C. B., Winkfein, R. J., Farrell, P. J., Iatrou, K., and Schnetkamp, P. P. M. 2000. Minimal domain requirement for cation transport by the potassium-dependent Na/Ca-K exchanger. Comparison with an NCKX paralog from *Caenorhabditis elegans*. J. Biol. Chem. **275**: 669-676.

Szerencsei, R. T., Prinsen, C. F., and Schnetkamp, P. P. M. 2001. Stoichiometry of the retinal cone Na/Ca-K exchanger heterologously expressed in insect cells: comparison with the bovine heart Na/Ca exchanger. Biochemistry **40**: 6009-6015.

Tang, Y., and Zucker, R. S. 1997. Mitochondrial involvement in post-tetanic potentiation of synaptic transmission. Neuron **18**: 483-491.

Tanneur, V., Ilgaz, D., Duranton, C., Fillon, S., Gamper, N., Huber, S. M., and Lang, F. 2002. Time-dependent regulation of capacitative Ca^{2+} entry by IGF-1 in human embryonic kidney cells. Pflügers Arch. **445**: 74-79.

Tsoi, M., Rhee, K. H., Bungard, D., Li, X. F., Lee, S. L., Auer, R. N., and Lytton, J. 1998. Molecular cloning of a novel potassium-dependent sodium-calcium exchanger from rat brain. J. Biol. Chem. **273**: 4155-4162.

Visser, F., Valsecchi, V., Annunziato, L., and Lytton, J. 2007. Analysis of ion interactions with the K^+-dependent Na^+/Ca^+ exchangers NCKX2, NCKX3, and NCKX4: Identification of Thr-551 as a key residue in defining the apparent K^+ affinity of NCKX2. J. Biol. Chem. **282**: 4453-4462.

Vogel, P., Read, R.W., Vance, R.B., Platt, K.A., Troughton, K., and Rice, D.S. 2008. Ocular albinism and hypopigmentation defects in Slc24a5-/- mice. Vet. Pathol. **45**: 264-279.

Wakimoto, K., Kobayashi, K., Kuro-o, M., Yao, A., Iwamoto, T., Yanaka, N., Kita, S., Nishida, A., Azuma, S., Toyoda, Y., Omori, K., Imahie, H., Oka, T., Kudoh, S., Kohmoto, O., Yazaki, Y., Shigekawa, M., Imai, Y., Nabeshima, Y., and Komuro, I. 2000. Targeted disruption of Na^+/Ca^{2+} exchanger gene leads to cardiomyocyte apoptosis and defects in heartbeat. J. Biol. Chem. **275**: 36991-36998.

Wennemuth, G., Babcock, D. F., and Hille, B. 2003. Calcium clearance mechanisms of mouse sperm. J. Gen. Physiol. **122**: 115-128.

West, I. C. 1997. Ligand conduction and the gated-pore mechanism of transmembrane transport. Biochim. Biophys. Acta **1331**: 213-234.

Winkfein, R. J., Szerencsei, R. T., Kinjo, T. G., Kang, K., Perizzolo, M., Eisner, L., and Schnetkamp, P. P. M. 2003. Scanning mutagenesis of the alpha repeats and of the transmembrane acidic residues of the human retinal cone Na/Ca-K exchanger. Biochemistry **42**: 543-552.

Woodruff, M. L., Sampath, A. P., Matthews, H. R., Krasnoperova, N. V., Lem, J., and Fain, G. L. 2002. Measurement of cytoplasmic calcium concentration in the rods of wild-type and transducin knock-out mice. J. Physiol. **542**: 843-854.

Xiang, M., Mohamalawari, D., and Rao, R. 2005. A novel isoform of the secretory pathway Ca^{2+},Mn^{2+}-ATPase, hSPCA2, has unusual properties and is expressed in the brain. J. Biol. Chem. **280**: 11608-11614.

Xu, W., Wilson, B. J., Huang, L., Parkinson, E. L., Hill, B. J., and Milanick, M. A. 2000. Probing the extracellular release site of the plasma membrane calcium pump. Am. J. Physiol. Cell Physiol. **278**: C965-C972.

Zhong, N., Beaumont, V., and Zucker, R. S. 2001. Roles for mitochondrial and reverse mode Na^{+}/Ca^{2+} exchange and the plasmalemma Ca^{2+} ATPase in post-tetanic potentiation at crayfish neuromuscular junctions. J. Neurosci. **21**: 9598-9607.